A METHOD OF PIPING FLEXIBILITY ANALYSIS BY DEFLECTION MEASUREMENTS IN SCALE MODELS

CHARLES F. RAUCH, JR.

A METHOD OF PIPING FLEXIBILITY ANALYSIS BY DEFLECTION MEASUREMENTS IN SCALE MODELS

* * * * * * * * * *

Charles F. Rauch, Jr.

A METHOD OF PIPING FLEXIBILITY ANALYSIS BY DEFLECTION MEASUREMENTS IN SCALE MODELS

by

Charles F. Rauch, Jr.

Lieutenant, United States Navy

Submitted in partial fulfillment of
the requirements for the degree of

MASTER OF SCIENCE
IN
MECHANICAL ENGINEERING

United States Naval Postgraduate School
Monterey, California

1957

A METHOD OF PIPING FLEXIBILITY ANALYSIS BY DEFLECTION MEASUREMENTS IN SCALE MODELS

by

Charles F. Rauch, Jr.

This work is accepted as fulfilling
the thesis requirements for the degree of
MASTER OF SCIENCE
IN
MECHANICAL ENGINEERING

from the
United States Naval Postgraduate School

ABSTRACT

Until the advent of the high-speed computer, engineers have spent untold hours with monotonous and lengthy computations when they have attempted analytical solutions of piping flexibility for even moderately simple configurations. Therefore, due to the complexity of this problem, several companies in both the United States and Europe are using model tests today as both an accepted independent method of piping flexibility analysis and as a check on analytical results. Heretofore, model test systems have utilized direct force-measuring instruments at the extremities of the branches. This thesis describes a method by which translational and angular deflection measurements are made a distance from the anchored ends so that with these displacements, reaction forces and moments may be computed at the extremities by use of simple statics and cantilever beam deflection formulas. The thesis also describes a practical and simple device to accomplish this purpose, reports on actual tests of several typical configurations, and compares the results so obtained with those given by analytical solution.

The writer wishes to express his appreciation to the following people at the United States Naval Postgraduate School for their assistance in this investigation: Professor John E. Brock for his encouragement and assistance and for his untiring work in providing analytical solutions to all the problems described herein; Professor S. H. Kalmbach, for his assistance with the optics problems encountered; and to the personnel of the Engineering School Machine Shop for their eager cooperation. The writer also wishes to thank Professor Robert E. Newton for his suggestions and encouragement to pursue the investigation discussed in the last several pages of Appendix IV.

TABLE OF CONTENTS

Section Title Page

1. Introduction 1

2. Basic Principles 3

3. Description of Apparatus 6

4. Operating Technique 35

5. Development of Theory 44

6. Analysis of Data 51

7. Results 55

8. Conclusions 57

9. Bibliography 60

APPENDIX I Calibration of Optics System 61

APPENDIX II Development of Basic Formula Relating Reactions to Deflections 68

APPENDIX III Tests Conducted on Simple Cantilevers With Standard Weights 73

APPENDIX IV Solution of Two-dimensional Z Bend Problem, Example 1 79

APPENDIX V Solution of Three-dimensional Hovgaard Bend Problem, Example 2 98

APPENDIX VI Analysis of Typical Piping System, Example 3 106

APPENDIX VII List of Commercially Available Equipment Used in Model Test Apparatus 117

LIST OF ILLUSTRATIONS

Figure		Page
1.	A Typical Pipe Model Showing Coordinate Sets Used in This Paper	4
2.	Drawing of Mirror Mounting Barrel	10
3.	Deflection Method Model Testing Apparatus Showing Framework and All Accessories Mounted For Analysis of the Z-Bend Problem, Example 1	14
4.	Apparatus Set Up For Typical Piping System Described in Appendix VI, Example 3	15
5.	Deformation Assembly Consisting of Lathe Milling Attachment Mounted on a Compound Feed	17
6.	View of Model Clamped in Anchor Assembly	21
7.	Instrument Mounting Frame	23
8.	Knife Edge Contact Assembly and Schematic of Associated Electrical Circuits	26
9.	Translation Measuring Instrument Assembly	29
10.	Rotation Measuring Instrument Assembly	31
11.	Operation of Rotation Measuring Apparatus	33
12.	Instrument Panel	36
13.	Instruments and Model Installed for Z-Bend Analysis Showing Relationship of the Translational and Rotational Measuring Systems	41
14.	Static Relationship Between Reactions at Point P and Those at Point of Anchor	48
15.	Typical Three-dimensional Model	50
16.	Paths of Reflected Point of Light for Three Cases of Rotation Measurement	62
17.	Calibration Curves for Rotation Measuring Apparatus for the Three Cases of Figure 16	67
18.	Drawing Showing Displacement Measurements on Simple End-Loaded Cantilever	74

Page

19. Drawing Showing Displacement Measurement for Simple Cantilever With End Moment About the Axis of the Model 74

20. Curve Showing Percentage Error in M_x, Versus Length L 78

21. Z-Bend Problem; Example 1 80

22. Curve Showing Percentage Error in F_y, Versus Length L for Example 1 86

23. Curve Showing Percentage Error of M_z, Versus Length L for Example 1 88

24. Hovgaard Bend Problem; Example 2 99

25. Orientation of Coordinates of Example 2 With Model Inverted 99

26. Typical Piping System; Example 3 107

27. Orientation of Coordinates for Example 3 With Model Inverted 109

TABLE OF SYMBOLS

A	Extremity of pipe or model OPPOSITE the extremity at the origin of the stated problem
~~B~~	Linear thermal expansion, inches/100 feet
C d, do t,	Point at center of four-inch double convex lens
D_2	Translation (inches) in y'' direction with origin at point of measurement, point P
D_3	Translation (inches) in z'' direction with origin at point P
D_4	Angular displacement (radians) about x'' axis measured at point P
D_5	Angular displacement (radians) about y'' axis measured at point P
D_6	Angular displacement (radians) about z'' axis measured at point P
E	Modulus of Elasticity, pounds per square inch
F	Force (pounds) acting a [illegible]; used with subscript to denote component and coordinate system, and model or pipe. For use with numerical subscripts see below.
$\bar{F}$	Resultant force (pounds) that anchor (boiler, turbine, etc.) applies on pipe
F_2	Shear force (pounds) at point of measurement, point P, of model in y'' direction
F_3	Shear force (pounds) at point P of model in z'' direction
F_4	Twisting moment (pound inches) at point of measurement, point P, about x'' axis
F_5	Bending moment (pound inches) at point P about y'' axis
F_6	Bending moment (pound inches) at point P about z'' axis
g G	Modulus of elasticity in shear, pounds/square inch
I	Moment of inertia of cross section with respect to neutral axis, inches to the fourth power
J	Polar moment of inertia of cross section, inches to fourth power

k	Bend flexibility factor
L	Linear distance (inches) from point of anchor to point of measurement
M	Moments (pound inches or pound feet); used with subscripts to denote components and coordinate systems, and model or pipe
$\bar{M}$	Resultant moment (pound inches or pound feet) that anchoring equipment applies to pipe
O	Point of origin of problem as originally stated, and origin of the unprimed system of coordinates. Fixed in the model or pipe
P	Point of measurement; found at longitudinal center of mirror mounting barrel
S_F	Force scale factor; force in piping system divided by corresponding force in the model
S_M	Moment scale factor; moment in piping system divided by corresponding moment in the model
X, Y, Z	x, y, and z coordinates of point A
x, y, z	Coordinates of a general point taken with respect to origin at point 0 as stated in the original problem
x', y', z'	Coordinates with origin at anchor with directions the same as for x'', y'', and z'', respectively
x''	Coordinate with origin at point P in direction parallel to model and positive going from P to anchor
y''	Coordinate with origin at point P in a direction parallel to the pipes of the instrument assembly primary support, and positive going from the knife edge to the model at point of measurement, P ; (See Fig. 1)
z''	Coordinate with origin at point P in a direction parallel to the straight pipe of the instrument assembly secondary support, and positive in a direction consistent with x'' and y'' for forming a right hand coordinate system; (See Fig. 1)
Δ	Deformation, inches
λ_p / λ_m	Ratio of linear dimensions of pipe to that of model
ξ, η, ζ	Coordinates of reflected point of light on rotation measurement crosssection paper such that $\xi_2 - \xi_1$, $\eta_2 - \eta_1$, and $\zeta_2 - \zeta_1$ indicate angular displacements about x'', y'',

and z'' axes, respectively

ν Poisson's Ratio

SUBSCRIPTS

A	Refers to point A
m	Refers to model system
O	Refers to point O
p	Refers to actual piping system to be analyzed
x, y, z	Refer to components in directions x, y, and z, respectively
x', y', z'	Refer to components in directions x', y', and z', respectively
1	Pertains to set of data taken with system deformed in negative direction (This does not apply to use of number subscripts with D or F ; see D_2 , F_2 , etc. for their special use)
2	Pertains to set of data taken with system deformed in positive direction (Not applicable to D and F ; see 1 above)

A METHOD OF PIPING FLEXIBILITY ANALYSIS BY DEFLECTION MEASUREMENTS IN SCALE MODELS

1. Introduction.

The increased importance of piping flexibility analysis is well recognized. While the use of high-speed digital computers has made the solution of these problems by analytical methods more practical than heretofore, model test methods are still of considerable interest and value.

This paper, therefore, will be devoted entirely to the scale model as a means of solution to piping flexibility problems. In this approach, a scale model of the piping system to be studied is constructed of tubing or rod. The system is deformed an amount proportional to the thermal expansion of the pipe and supporting equipment. Reaction forces and moments are then usually measured by some force-measuring device mounted at the extremities of the model, and these results are scaled up to values for the piping system by use of suitable formulas. A report by the Commission of Research for the Study of Steam Piping Systems [8][1] working for the "Institute for the Encouragement of Scientific Research in Industry and Agriculture" in Brussels, Belgium, (the organization hereafter is referred to as the Belgian I. R. S. I. A. Commission) compares their model test system with those of three other European organizations and with three companies of the United States. These various types of apparatus vary mainly in (1) the type of force measuring device employed, and (2) the method of support of a rigid six-branch cross located at one extremity of the model. For example, the Belgian I. R. S. I. A. Commission uses 12 needles to support this cross and they obtain their force and moment measurements by compen-

---

[1] Numbers in brackets refer to bibliography on page 60 .

sating weights acting on six of these needles to return the measured extremity to a zero location and orientation. On the other hand the M. W. Kellogg Company of New York supports its rigid six-branch cross by 12 flexible supporting struts within the measuring head, and their loads are measured by paired electrical strain gages. [9] Thus, in both of these methods the forces and moments are measured directly at the extremities of the model by rather complex devices.

This paper presents the development of another type of model test in which the forces and moments at an extremity are inferred from actual measurements of translational and rotational displacements at a point some distance away from the anchor. There seems to be considerable virtue in developing such a system. Although much of the preparations involved are the same as for the direct-force-measuring types, the actual measuring device can be relatively simple since the somewhat complex force measuring devices are not used. This eliminates the system of strain gages or counter weights and the six-branch cross and its intricate means of support. Furthermore, since it is possible to fabricate a deflection-measurement model test device practically entirely from commercially available components, it should be possible to hold the cost of the apparatus to a minimum.

As a matter of fact, the apparatus described in this paper was designed with two specifications in mind: (1) attempt to keep the apparatus itself as simple as possible consistent with a certain degree of accuracy, and (2) use as many components as possible from available manufactured equipment in order to eliminate both high costs and the need for a great amount of machine work.

2. Basic Principle.

Before proceeding with the development of the basic theory used, a few definitions of terms as used in this paper should be noted. When speaking collectively of the reaction forces and moments at any point, the term REACTIONS will be used. Similarly, when referring to both the angular and translational displacements of any particular section, the term DISPLACEMENTS or DEFLECTIONS will be employed. However, TRANSLATION will indicate linear displacement and ROTATION will mean angular displacement; moreover, the term DEFORMATION will be used when discussing displacement applied at one extremity for the purpose of deforming the system in a prescribed manner. In addition, when referring to values of reactions obtained by first measuring displacements and then computing reactions from these measurements, reference will be made to the MEASURED reactions.

Further, the origin of the originally stated problem will invariably be at one extremity which will be labeled point O . The opposite end will be known as point A . (See Fig. 1) These points will remain fixed to the wire model regardless of how the model is shifted about. In the deflection method of model testing one extremity will be embedded in a rigid anchor and the other will be clamped in an adjustable device that can be deformed in any of three dimensions. The end that is in the rigid anchor will be known as the POINT OF ANCHOR while the other end will be the DEFORMABLE END or DEFORMABLE POINT. Note that either point O or point A may be at the point of anchor depending on how the model is mounted. The point where displacements are measured will be known as point P , and the distance from the point of anchor to point P is the length, L . A set of rectangular coordinates with origin at point of anchor will be designated with a single prime (x', y', and z') ,

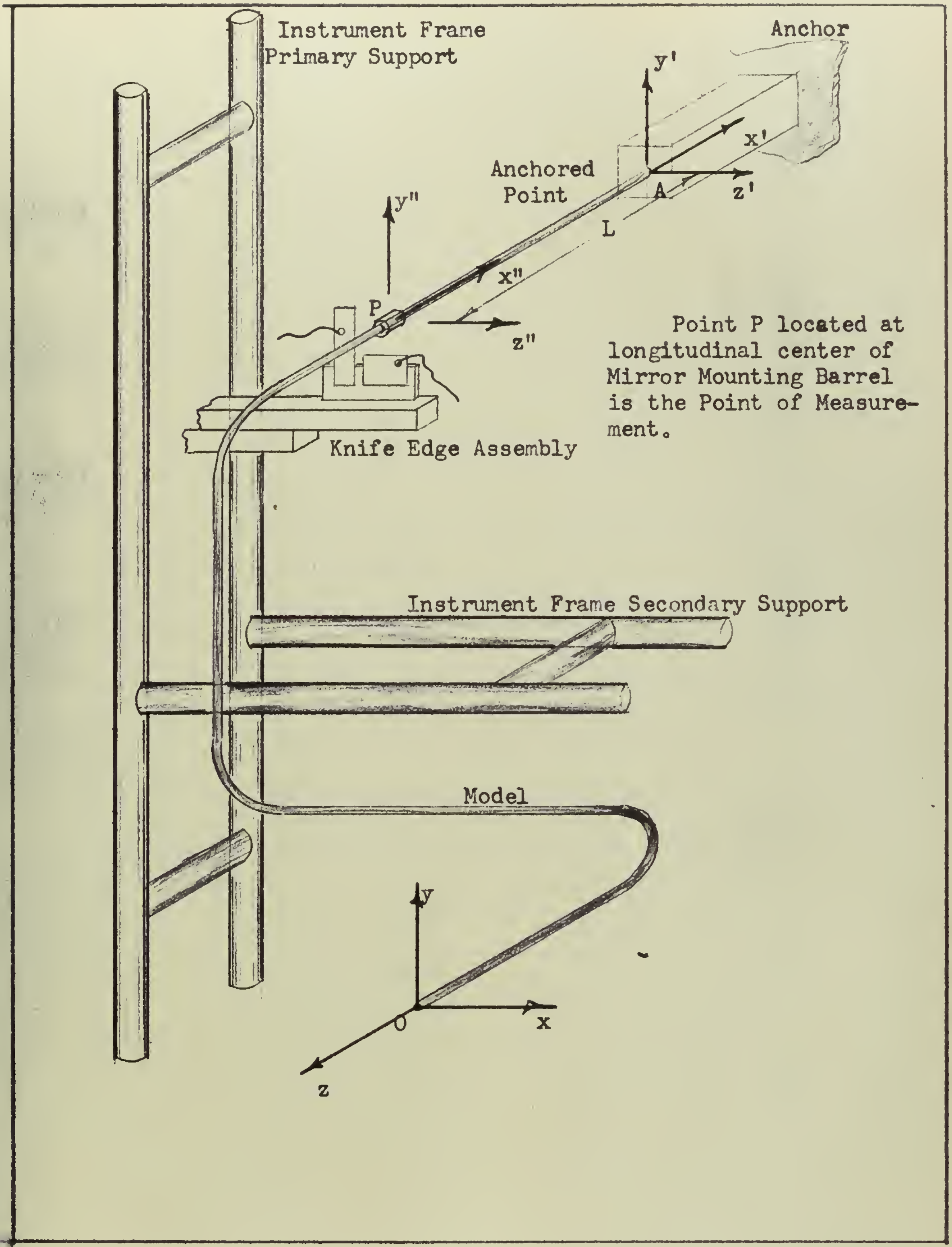

Figure 1 A Typical Pipe Model Showing Coordinate Sets Used in This Paper

and another set parallel to these but with origin at point P are labeled with double primes. In the first part of this paper no reference will be made to the unprimed set of coordinates; therefore, they will not be discussed until Section 4.

In studying the basic theory used in this type of apparatus, we see that the first steps are practically the same as those for any piping flexibility model test system. A scale model of the configuration to be studied is fabricated from wire, or rod or tubing, and mounted with one end anchored and the other clamped in the deformation apparatus. The deformable end is displaced by an amount representative of thermal expansion of the piping and any thermal displacements of terminal points. The next steps are peculiar to the deflection model test method and they consist of measuring the displacements at point P and applying equations (based on structural properties of simple cantilevers with various types of end loading) derived in Section 5 to convert these displacements to the reactions at point P (imposed by one portion of the pipe on the other through the cross section at P). Then by extremely simple statics the P-reactions can be used to obtain reactions at point of anchor and at other points if desired.

The above measurement yields five of the six unknown reaction components at the point of anchor. Obviously, there will be no measurable displacement in the x'' direction, and it results that it is not possible to determine $F_{x'}$ from these data alone. This presents no problem when the two extreme legs are not parallel; because when the model is "reversed" and the forces at the opposite end are measured, the unknown force will be determined.

However, if the extreme ends are parallel, five of the six reactions

will be obtained at one end, say at point A; and then the model will be inverted as before and five of the six reactions at point O will also be found. The missing reaction will be the same for both cases, and by use of simple static relationships, this unknown force can then be computed.

Once any of the reactions are obtained on the model, they can be scaled up to the piping system by use of scale factors expressed as simple ratios of dimensional and elastic properties and which can be computed as shown in Section 5. This is true because both the pipe and model obey the same laws of structures.

3. Description of apparatus.

Much of the following description deals with the apparatus as specifically designed for the experiments reported in this paper. In most cases there are many ways of accomplishing the same results, and therefore, all the variations feasible for performing the tasks described can not possibly be discussed here but must be left to the imagination of the reader. There are, in fact, several instances below in which it is pointed out that a more versatile design of particular components is mandatory for increased capacity in terms of the type of system it is possible to analyze.

(a) The model.

In order to visualize the requirements of the testing apparatus it is necessary first to take a look at the model itself. In the interest of economy and simplicity it was decided to use standard one-eighth-inch diameter mild steel or aluminum rod for the model. In addition to the ready availability of standard rod, this material also lends itself to cold bending by hand, thus eliminating heat treatment of any

kind. However, a discussion of the limitations of rod as a model material is pertinent.

Piping components other than straight pipe, principally bends and elbows, show unusual flexural properties which generally result in an increased flexibility over that predicted from ordinary beam theory and an intensification of stresses. The reason for this will not be treated here, but it is covered clearly by Den Hartog [5] in a discussion of the phenomenon first explained by von Karman in 1911. The amplification of stresses may be taken into account by multiplying the calculated or experimentally determined bending moments by an appropriate stress intensification factor. However, the increased flexibility of the bends or elbows in a piping structure clearly indicates that a model of such a system must have bends and elbows whose flexibility is proportionally higher than that of the straight portions of the structure.

In analytical calculations, this increased flexibility of elbows and bends is taken into account by use of a flexibility factor, which can be computed by the following formula given in the ASA Code for Pressure Piping [3]:

$$k = 1.65 \frac{r^2}{tR} \quad \text{or} \quad k = 1 \text{ , whichever is greater,}$$

where t = wall thickness of pipe; r = mean radius of pipe; R = bend radius of elbow or bend; and k = bend flexibility factor. This factor is applied as a divisor of its nominal moment of inertia or of the modulus of elasticity. There is no corresponding decrease in torsional rigidity. The formula above is a reduction to simple

valid terms of several theoretical results which have been given by various authors; for example, see the bibliography accompanying a recent paper by H. H. George and E. C. Rodabaugh [6].

While theoretically it would be possible to simulate in the model the precise conditions of the prototype simply by preserving all geometrical ratios, in practice this is not feasible because tubing having all the ratios of wall thickness to outside diameter encountered in piping practice simply is not available. Moreover, it would be extremely difficult to reproduce bends and short radius elbows in small tubing.

For many configurations, the effect of increased bend flexibility is such as to invalidate the results of an analysis which does not take the flexibility factor into account or an experimental treatment in which the flexibility of the elbows in the model is not appropriately increased. On the other hand, there are many configurations in which the bend flexibility factor is unity and the results of a model test are perfectly valid.

Obviously serious difficulties are involved in properly simulating, in a model, the increased flexibility of pipe bends and elbows. Since this problem is of considerable magnitude and since it is separable from the problem of determining, by the displacement method described herein, the forces at the ends of a deformed elastic filament, the decision was made to omit this complication completely and to leave it as a problem to be dealt with by others.

The problems analyzed in Appendices IV and V and referred to frequently in the text, (the standard Z-Bend and the Hovgaard Bend), are cases in which the bend flexibility factor is substantially larger

than unity. Accordingly the results of the tests reported herein differ appreciably from solutions given elsewhere. However, we have compared our results with an analytical solution which artificially used a unit value for the bend flexibility factor so as to provide a standard by which the accuracy of the present model method with its present limitation could be evaluated.

For the most part steel rod was used in the experiments reported herein, but example 3 was conducted with both the steel rod described and also with one-eighth-inch aluminum rod. Steel was used primarily because of the identical Poisson's ratio between pipe and model, but the small difference between this value for aluminum and for steel does not produce much error.

Before leaving a discussion of the model it is advisable to mention the morror mounting barrel, the purpose of which will be further treated in a description of the measuring instruments. Let it suffice here to say that the optics systems, by which rotation measurements are made, require two mirrors, perpendicular to each other and both parallel to the rod, to be mounted on the model at the point of measurement. To accomplish this, a small barrel-type assembly was designed according to dimensions shown in Fig. 2. It consists of a 3/16-inch long, hollow cylinder of one-quarter-inch outside diameter and an inside diameter equal to 0.126 inches so that the barrel will just slide along the one-eighth-inch rod model. Two mutually perpendicular plane surfaces were produced parallel to the axis of the cylinder by milling the outside of the cylinder. An 0-80 setscrew was provided in order to attach the barrel firmly to the rod at any desired point. Two small front-surface mirrors

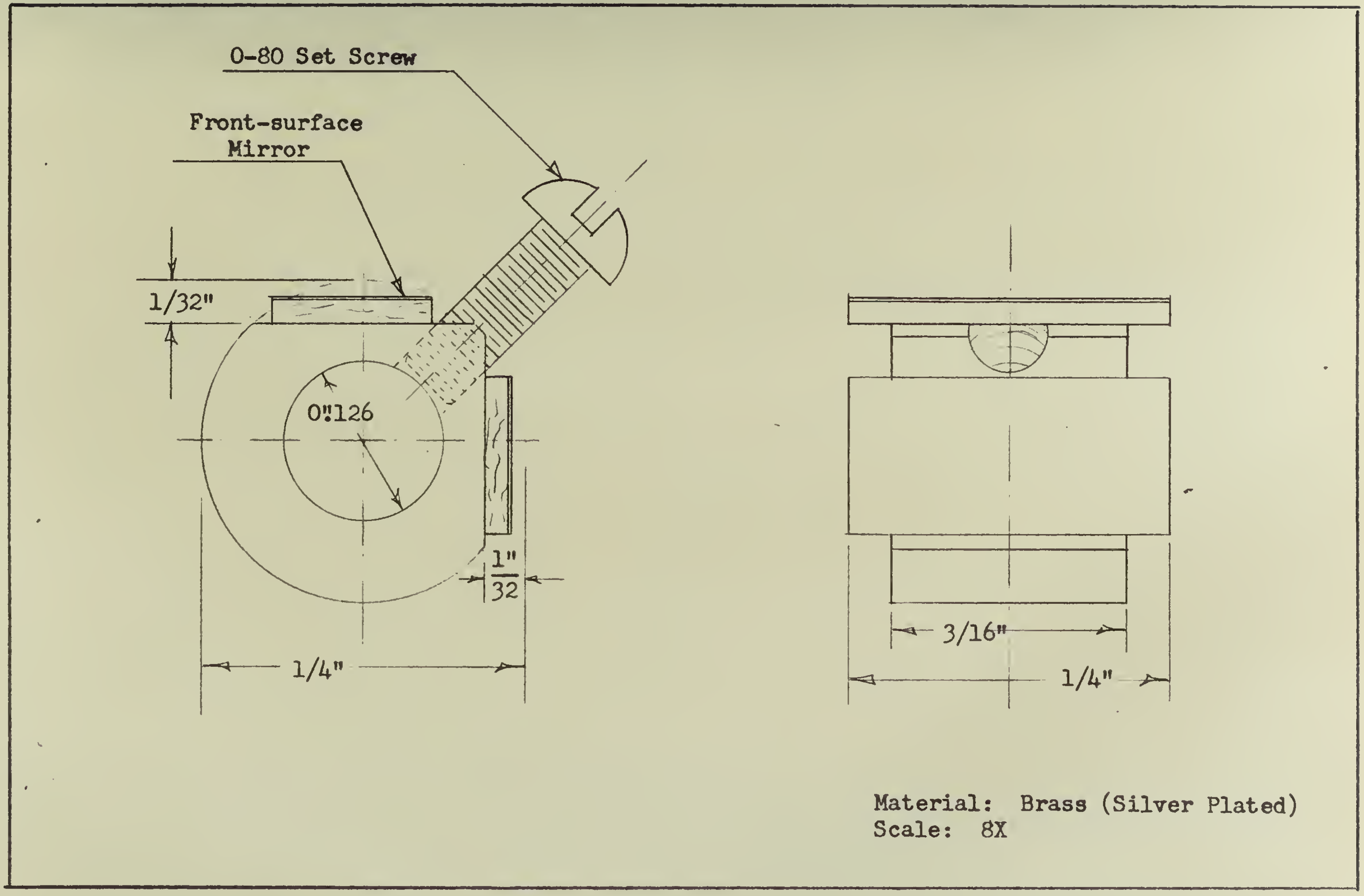

Figure 2 Drawing of Mirror Mounting Barrel

approximately one-quarter inch by one-eighth inch were cemented each to one of the plane surfaces, with the long dimension parallel to the cylinder axis. Front surface mirrors have the disadvantage of being more susceptible to marring and scratching, but they adhere to the surfaces of the mirror mounting barrel extremely well. When back surface mirrors were tried, the cement had to be applied to the back of the silver, thus enabling the glass to strip loose from the silver and fall off the assembly. When front surface mirrors are used, the glue forms a bond directly between the surface of the barrel and the glass of the mirror. Moreover, if damage should occur to the surface of either of the mirrors it is a simple matter to replace it as dozens of these mirrors can be cut from one silvered microscope slide glass. In fact, the entire mirror mounting assembly can easily be replaced since it is quite as simple to machine four or five cylinders as it is one.

The first mirror mounting barrel used was fabricated from aluminum, but since the translation measuring device depends on making an electrical contact at the point of measurement, aluminum proved unsatisfactory because it readily forms an oxide coating of high electrical resistance. Therefore, the barrel was fabricated from brass and was subsequently silver plated.

(b) Main framework.

A skeleton or platform from which the model and measuring equipment may be suspended is an obvious necessity. Such a system has three important specifications: (1) rigidity, (2) adjustability, and (3) accessibility of equipment. Implicit in any model test apparatus is the prime requirement that the elastic properties of the

framework be so rigid as compared to that of the model material that any displacement of the framework during testing is infinitesimally small and therefore negligible.

At the same time, paradoxically, the framework must be sufficiently temporary in nature that it readily lends itself to fairly rapid modifications, alterations, and adjustments. The capacity of the system in terms of variety of types of problems it can accomodate is a function of this versatility and capability of the framework to be assembled and disassembled with a minimum of effort. The third requirement, but one of almost equal importance to rigidity and adjustability, is the complete accessibility of all equipment used in the tests.

There are a variety of methods possible that will satisfy the three requirements listed above. Two basic concepts come to mind. The most variable perhaps is the use of mounting fixtures that can be built right into an existing room of a building so that any piece of apparatus could be welded in virtually any attitude at any position in the room. When it comes time to change the configuration it would simply be a case of burning the equipment off at one place and welding it on at another. A more convenient method considering laboratory facilities and services readily available at this institution, however, appeared to be the use of a skeleton framework constructed of iron pipe and scaffold fittings. This skeleton may be made in such a manner that its own dimensions can be easily changed. Any cross struts or sub-assemblies made of pipe may be placed in practically any position desired as foundations for measuring or anchoring equipment.

This variability in the latter case is provided by use of scaffold fittings, various spare lengths of pipe, and other accessories. (See Appendix VII).

The main purpose of this investigation is to ascertain the feasibility of developing a deflection measuring technique of model testing. Furthermore, it was decided to test this system by analyzing the three problems solved in Appendices IV, V, and VI (Examples 1, 2, and 3). Reasons for these selections will become apparent later. To conduct this investigation the framework was designed specifically to handle these three problems. Therefore, the main framework used (See Figs. 3 and 4) was designed to be of a more permanent nature than a larger capacity would dictate. However, it is only fair to point out that even this permanent type of framework lends itself to sufficient modification to allow the analysis of infinitely more problems than the three solved for this paper.

This framework was fabricated from standard 1-1/2-inch (1.9" O. D.) black iron pipe welded together in the form of the frames of a 51" x 51" x 38" rectangular solid sitting on four six-inch legs. This makes possible the use of ordinary scaffold fittings for rigidly attaching any pipe frame subassemblies at any point desired. These fittings usually are available with right angles or with adjustable angles to provide for use of any stiffening diagonals. Joints provided by the right angle fittings are exceptionally rigid and should be used whenever possible. However, adjustable fittings are by nature flexible and require some modification to increase their rigidity. Because of this the adjustable fittings were avoided entirely in this investigation. If a configuration demanded their use, though,

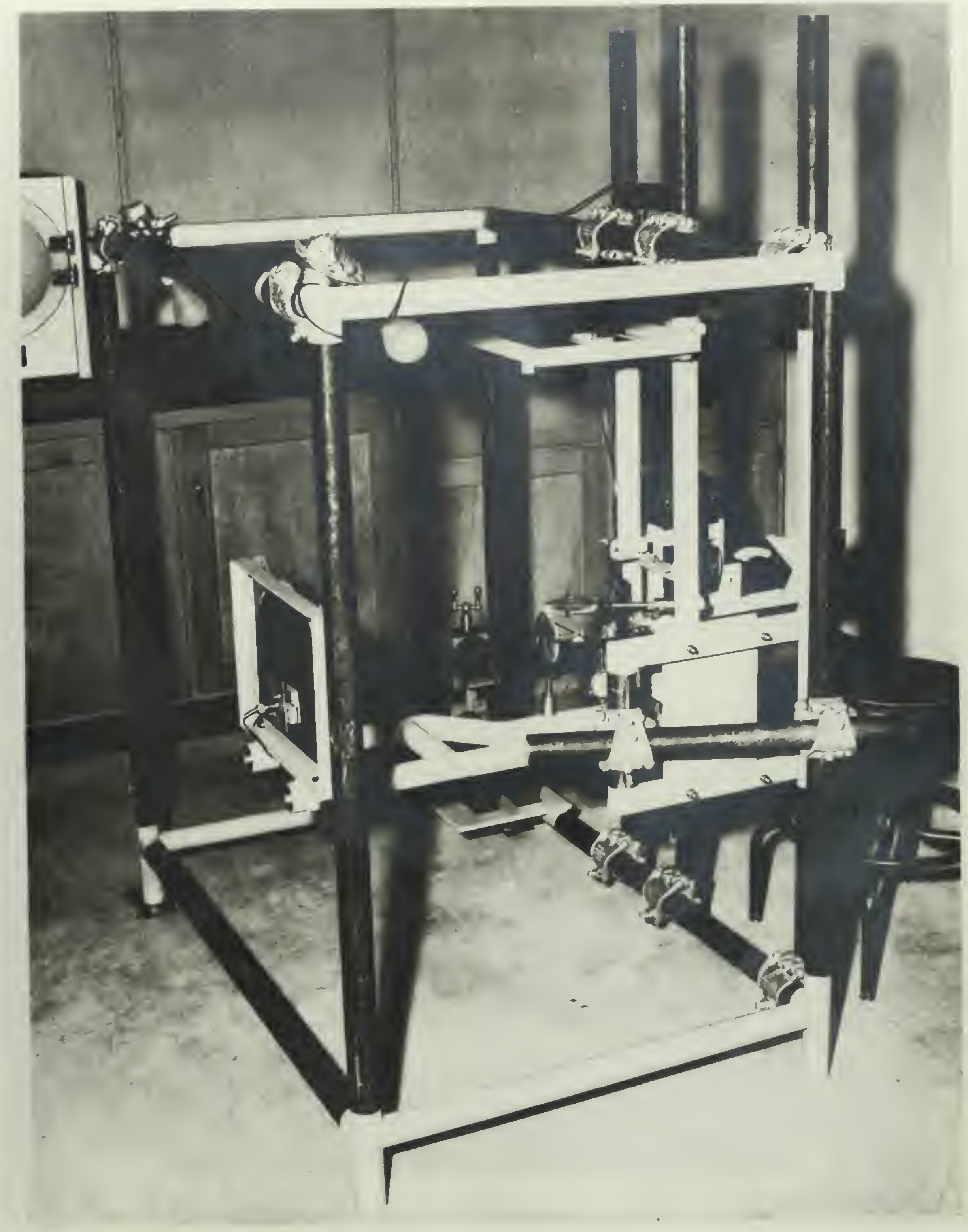

Figure 3 Deflection Method Model Testing Apparatus Showing Framework and All Accessories Mounted for Analysis of the Z-bend Problem, Example 1

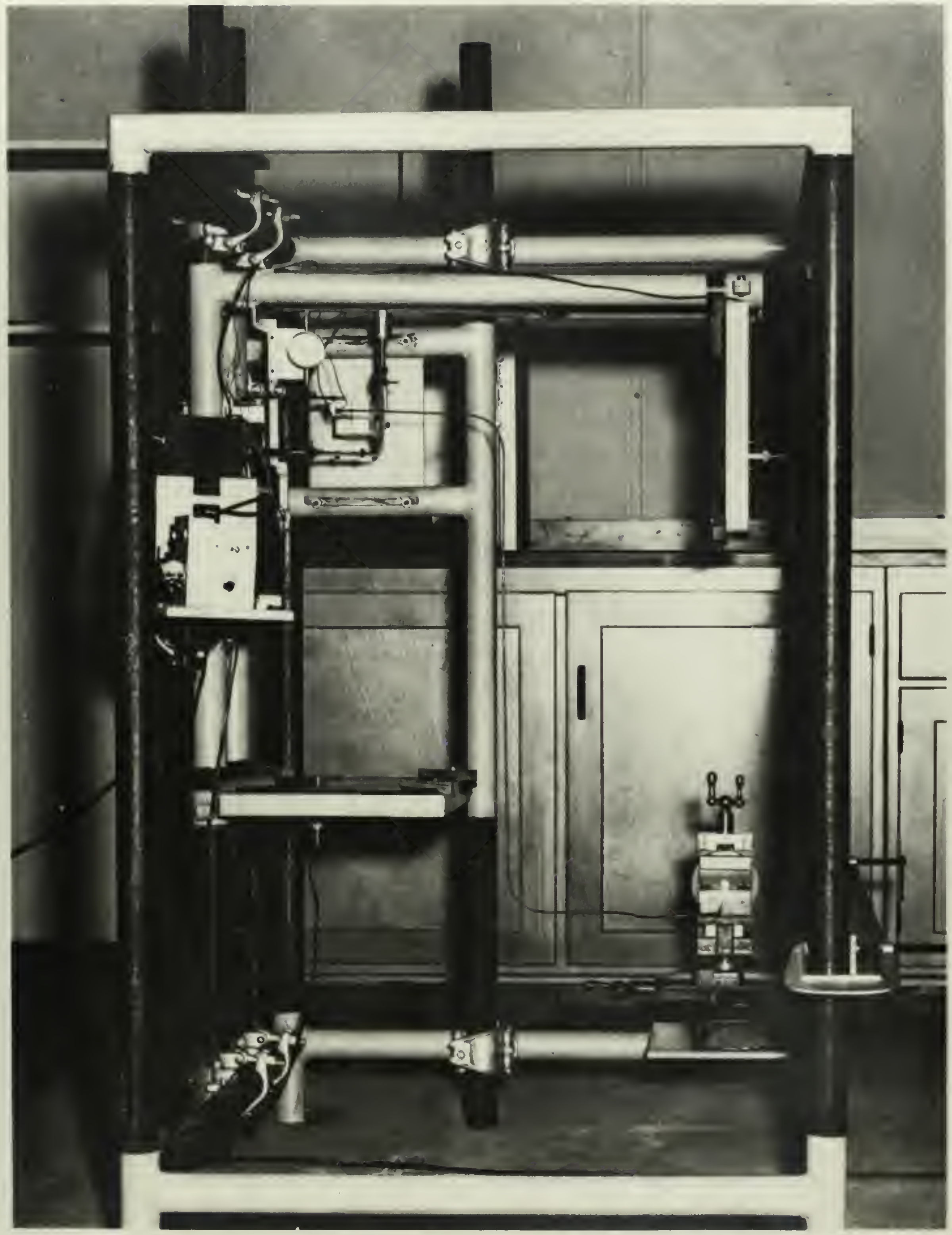

Figure 4 Apparatus Set Up for Typical Piping System Described in Appendix VI, Example 3

the necessary rigidity could be obtained with a little ingenuity.

(c) Deformation assembly.

As pointed out in Section 2, page 4 , the model is first mounted within the framework and then deformed an amount consistent with thermal expansion of pipe and external equipment. Thus, after the displacements in three directions are computed, from a knowledge of prototype dimensions, temperature change, coefficient of thermal expansion, and terminal displacements, they must be applied at one extremity of the model. For purposes of this test, a system should be provided to introduce these known deformations correct to the nearest one-thousandth of an inch in each of three orthogonal directions. The device must contain a method of firmly clamping one end of the model. Furthermore, it should be possible to place this assembly in any orientation desirable for maximum versatility of the system as a whole.

Again there are many systems that could be visualized to accomplish the above requirements. Any orthogonal combination of devices designed to transmit and measure linear motion with precision and yet be rigid in comparison with the rod model will work nicely. For the purposes of this investigation, an attempt was again made to employ equipment available. (See Appendix VII). This resulted in the use of compound feed for a lathe, that provided motion in the two directions in a horizontal plane, on which was mounted a lathe milling attachment to provide vertical motion. (See Fig. 5) This whole assembly was bolted to a 3/8-inch steel plate which in turn was welded to one of the lower corners of the main frame work. Ranges of motion provided by the two pieces of equip-

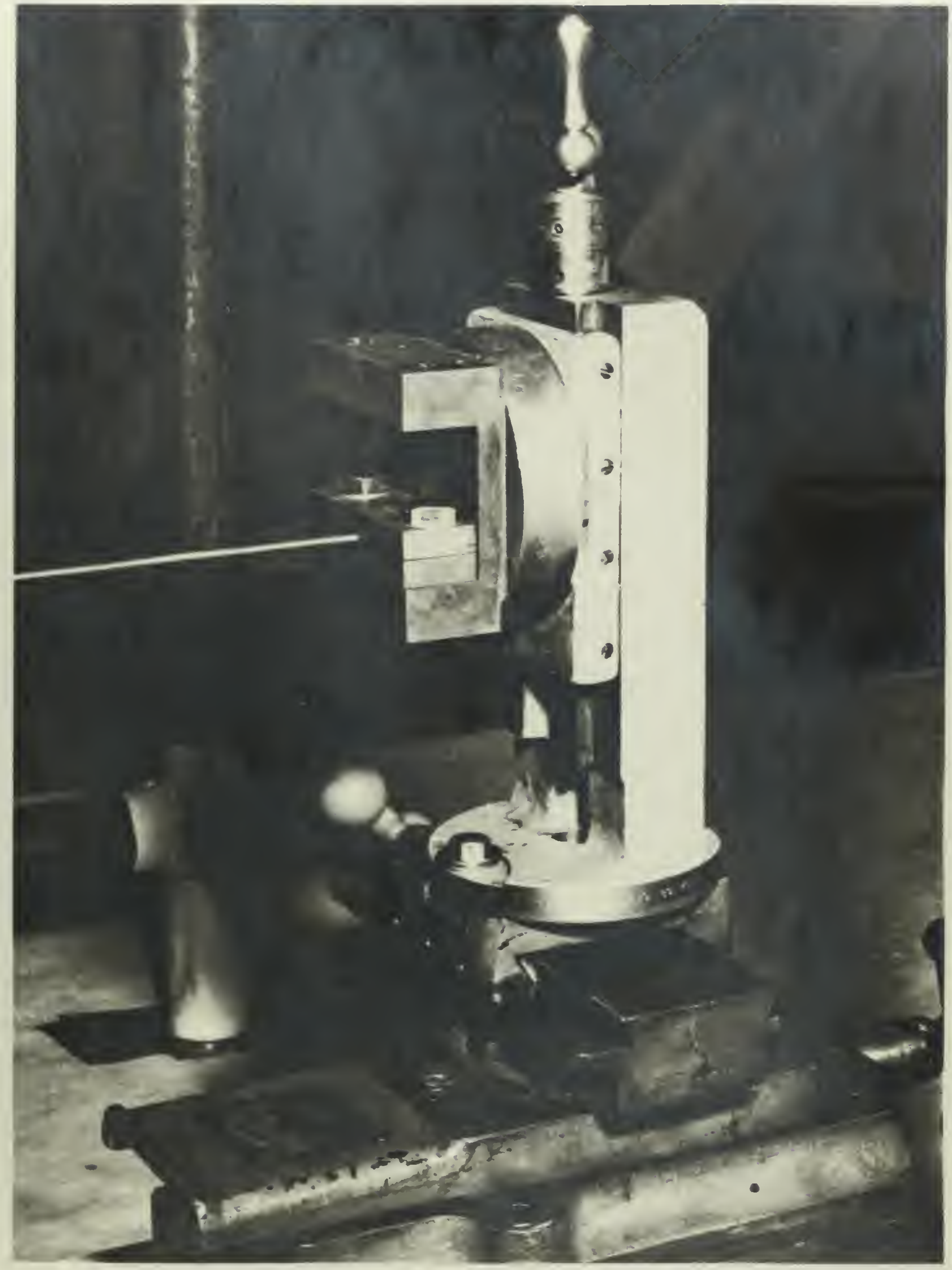

Figure 5 Deformation Assembly Consisting of a Lathe Milling Attachment Mounted on a Compound Feed

ment are as follows: compound feed, five inches in one direction and four and one-half inches in the other: millingattachment, three and one-half inches.

It is imperative that this apparatus be rigidly attached to the main framework, and for the treatment of the three problems of the Appendix, it was not necessary to change its orientation. As a result the 3/8-inch plate to which the vise is bolted was welded in position. As stated before, the versatility of the system as described in this paper is sufficient to conduct analysis of a considerable variety of configurations; however, the provision of a greater variety of mounting capabilities for the deformation assembly would mean an even greater capacity for the system.

A device for clamping the extremity of the model rod was simply made on a principle similar to that described in the next section on the anchor assembly. Briefly, the two three inch by one inch vise plates provided with the milling attachment were placed together with a 1/32-inch shim between them, and a one-eighth-inch hole was drilled through the shim and plates so that a circular groove of 1/16-inch radius, but of something less than a semi-circle, was produced across the facing surfaces of the two vise plates. Thus, the rod could be inserted in the grooves and the two plates then bolted together and to the vise attached to the milling attachment. This provided a tenacious grip over one inch of the rod.

(d) Anchor assembly.

The design of the anchor assembly ultimately became quite elementary, and will be described presently. However, certain mention must be made of the disposition of an early concept of this

portion of the apparatus. One of the very basic problems encountered in the development of this system was the question of how $F_{x'}$ should be found. It seemed plausible that with any success at all the deflection measurements obtained would yield the other five reactions to some degree of accuracy. However, it was obvious from the onset that a solution of $F_{x'}$ was non-existent for this set-up. Therefore, the following design was considered and the equipment was actually fabricated.

The so-called anchored end of the model rod would be embedded in the center of a five-inch long, one-inch diameter piston. The rod was so clamped that its axis coincided with that of the piston. This piston was lap-fitted into a cylinder two inches in outside diameter and six inches in length with a flange at one end to allow rigid mounting on a 3/8-inch steel plate. The plate in turn was bolted to a pipe frame that could be mounted anywhere on the main framework by pipe couplers. The end of the piston attached to the model was fitted with a collar to which could be bolted a device that would allow freedom of motion in the axial direction but would prevent any rotation about the main axis. It was felt that if an adequate oil film could be maintained between piston and cylinder it would accomplish two mandatory purposes. First it would eliminate any undesirable degree of freedom of translation in the direction perpendicular to the axis of the piston and of rotation about coordinates perpendicular to the piston axis. And second, while eliminating the above four degrees of freedom, it would provide complete freedom of motion in the direction of the axis. If the above phenomena could be achieved an $F_{x'}$-measuring device would be provided, possibly in the form of

a calibrated coil spring incorporated in the x-axis rotation-preventing-mechanism. Experiments with the piston and cylinder above demonstrated that a sufficient oil film could in fact be set up momentarily if the piston was rotated in the cylinder several times. However, the film was immediately broken down when the cylinder was not absolutely horizontal, and it collapsed within a few seconds even when the cylinder was held level. It is believed that pressurizing the lubrication system might indeed give favorable results, but the use of the piston and cylinder already rendered the system more complex than the original philosophy of the deflection model test method would allow. Thus, the piston and cylinder was completely abandoned and another means of obtaining $F_{x'}$ was sought.

The decision was finally made to forget about $F_{x'}$ entirely and to merely infer it directly or indirectly from measurements made at the other extremity. Having decided on this tack the anchoring problem at this end was tremendously simplified. Fig. 6 shows the anchor assembly itself, and Figs. 3 and 4 show two different ways of orienting and clamping the anchor pipe frame to the main framework. The anchor itself is nothing more than a six-inch long piece of two-inch square steel bar welded to a 3/8-inch steel plate, which is mounted as described above for the piston and cylinder design. The steel bar was split longitudinally a distance of an inch, and then a cut was made half way across the section at the base of the longitudinal cut thus separating a rectangular solid block from the end of the bar. The block (henceforth known as the clamping block) thus provided was drilled and the bar was drilled and tapped so that the block could be bolted back in the place from which it was

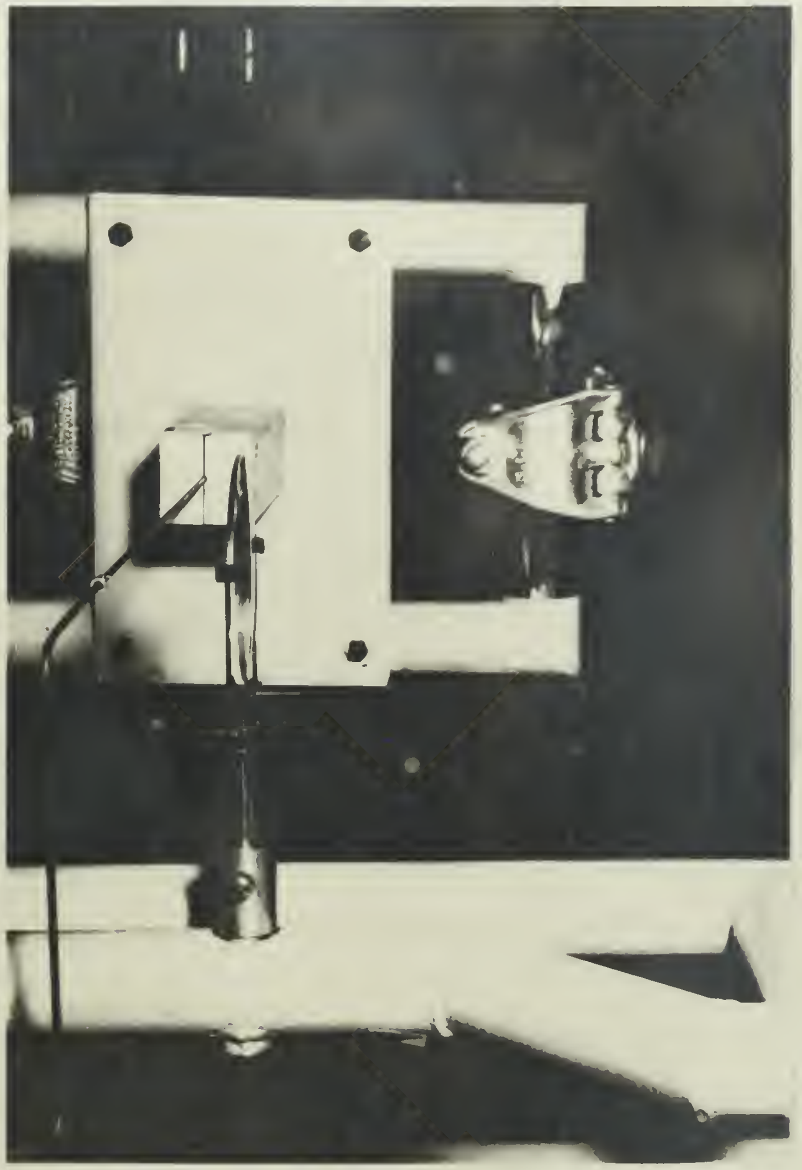

Figure 6 View of Model Clamped in Anchor Assembly

removed. A 1/32-inch shim was placed between the clamping block and the bar, and a one-eighth-inch hole was drilled along the longitudinal axis of the laminated apparatus thus formed. Removal of the 1/32-inch shim made it possible to insert the one-eighth-inch model rod between the clamping block and bar so that setting up on the clamping bolts firmly gripped the rod over a length of one inch.

The pipe framework to which the 3/8-inch steel anchor mounting plate was attached consists of a single 68-inch straight length of pipe to which were welded the free ends of a U-shaped pipe layout that carries the steel plate. (See Fig. 3) The anchor assembly frame can be adequately attached to the main framework by scaffold fittings at opposite ends of the 68-inch pipe and by extra lengths of pipe clamped at the base of the U and to another position of the main framework wherever convenient.

(e) Instrument assembly - main frame

With a main framework of the type constructed for the purposes of these experiments, the measuring instruments envisioned could be mounted a number of ways. However, it was decided that any alignment and calibration of the instruments would be simplified if all the instrumentation could be mounted on one pipe frame. This frame was designed as follows. The basic structure was composed of two parallel 68-inch pipes (all pipe used in the entire equipment is standard 1-1/2-inch black iron pipe) held firmly 6-1/2 inches apart by two short pipe struts welded one near each end. (See Fig. 7) This basic framework will henceforth be referred to as the INSTRUMENT FRAME PRIMARY SUPPORT. Another pipe skeleton was welded to the primary support such that the plane of the

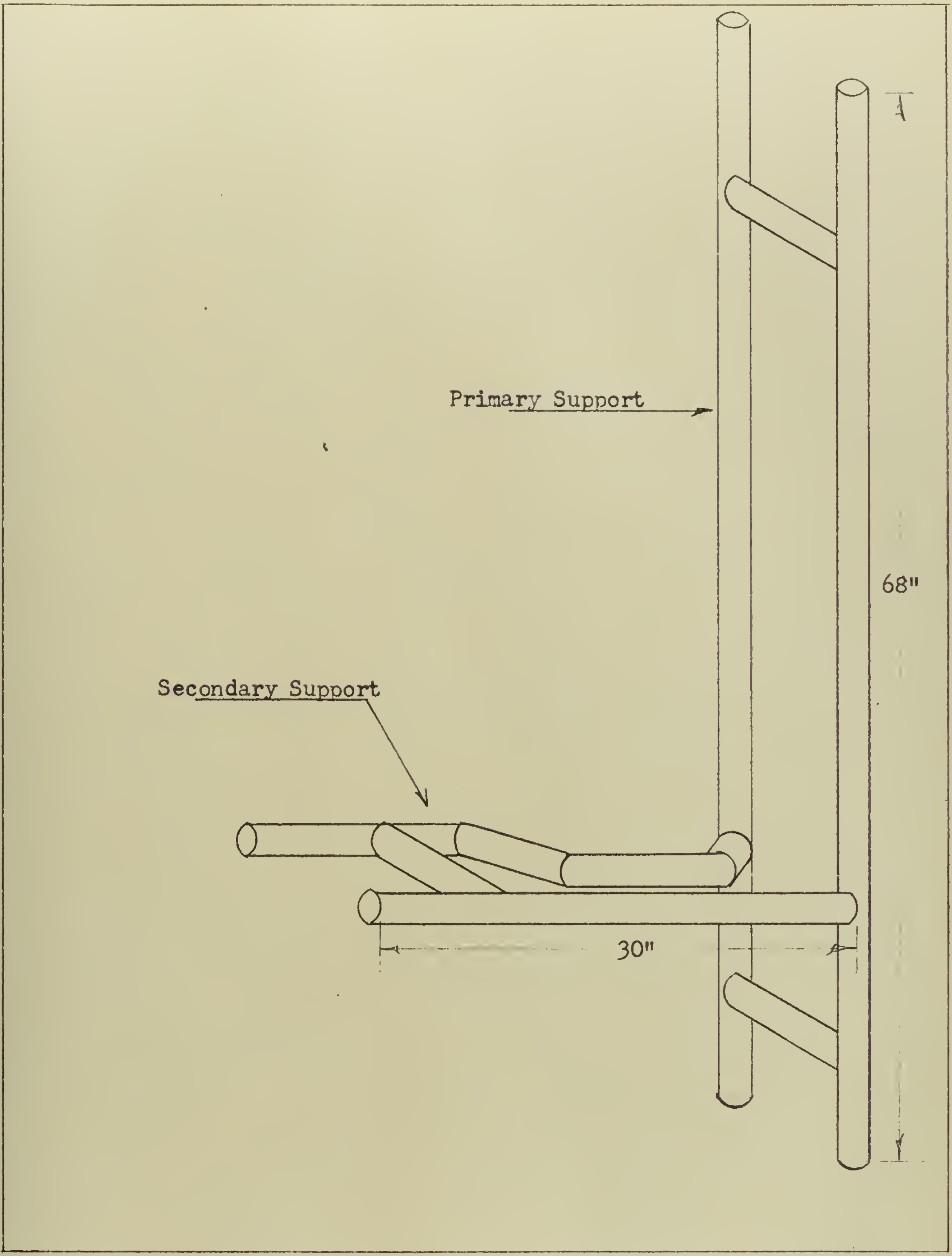

Figure 7 Instrument Mounting Frame

attached pipe was perpendicular to the plane of the primary support. This attached framework will correspondingly be designated as the INSTRUMENT FRAME SECONDARY SUPPORT. Four pipe couplers, placed one near each end of each pipe of the primary support were sufficient to attach the instrument frame rigidly to the main framework: The secondary support was also constructed of pipe so that, if necessary, additional lengths of pipe could be clamped to the support at any location and then to a portion of the main framework. It turned out in practice, however, that the four fittings on the primary support were quite adequate.

The degree of variability achieved by this particular system is due largely to the several possibilities of orientation and adjustment of the anchor assembly frame and of the instrument assembly frame. Through the use of the scaffold fittings both frames can be mounted at any position along any two sets of adjacent parallel pipes of the main framework. As an example it will be noted that in Fig. 3, the instrument frame primary supports are vertical and are located on one side of the main framework while in Fig. 4 although still vertical they are completely inverted and mounted on the opposite side of the framework. Furthermore, for the configuration of example 2 (Appendix V), the orientation of the primary supports was horizontal.

(f) Instrument assembly - translation measurement

The translation measuring device designed for this equipment incorporates the principle employed by the Belgian I. R. S. I. A. Commission in some preliminary calibration tests of a two-dimen-

sional model. [8] It consists essentially of providing a micrometer type linear measuring device that is advanced until an electrical contact is just made with the model at the point measurement is desired. For the purposes of this investigation two orthogonal translations must be measured: $y_2' - y_1'$, and $z_2' - z_1'$. Here again it seemed expedient to stick to the basic philosophy of using available equipment. Thus, a Bausch and Lomb mechanical stage for microscopes was borrowed for a basis of the translation measuring equipment. The mechanical stage as normally used consists of a stationary arm to be clamped to the existing microscope stage. By use of two rack and pinion sets a microscope slide can be moved in directions parallel to and perpendicular to this stationary arm. The operator can position the slide by adjustment of two knobs which directly control the two pinions. The mechanical stage incorporates scales and verniers calibrated in tenths of millimeters for linear measurement in each direction.

To adapt this mechanical stage to measure translations of the model rod, the microscope slide holders were removed, and in the place of a portion of the slide holder, the knife edge contact assembly shown in Fig. 8 was installed. The knife edge contact assembly consists of two separate contacts bolted to a small rectangular piece of insulating material; the piece of insulation was in turn screwed to the mechanical stage. The knife edges of the two contacts are perpendicular, respectively, to each of the sliding arms of the stage. An electrical wire soldered to each contact terminates in a circuit containing a flashlight battery in parallel with a 1.1 volt lamp and a small potentiometer. The center lead from the potentiometer was

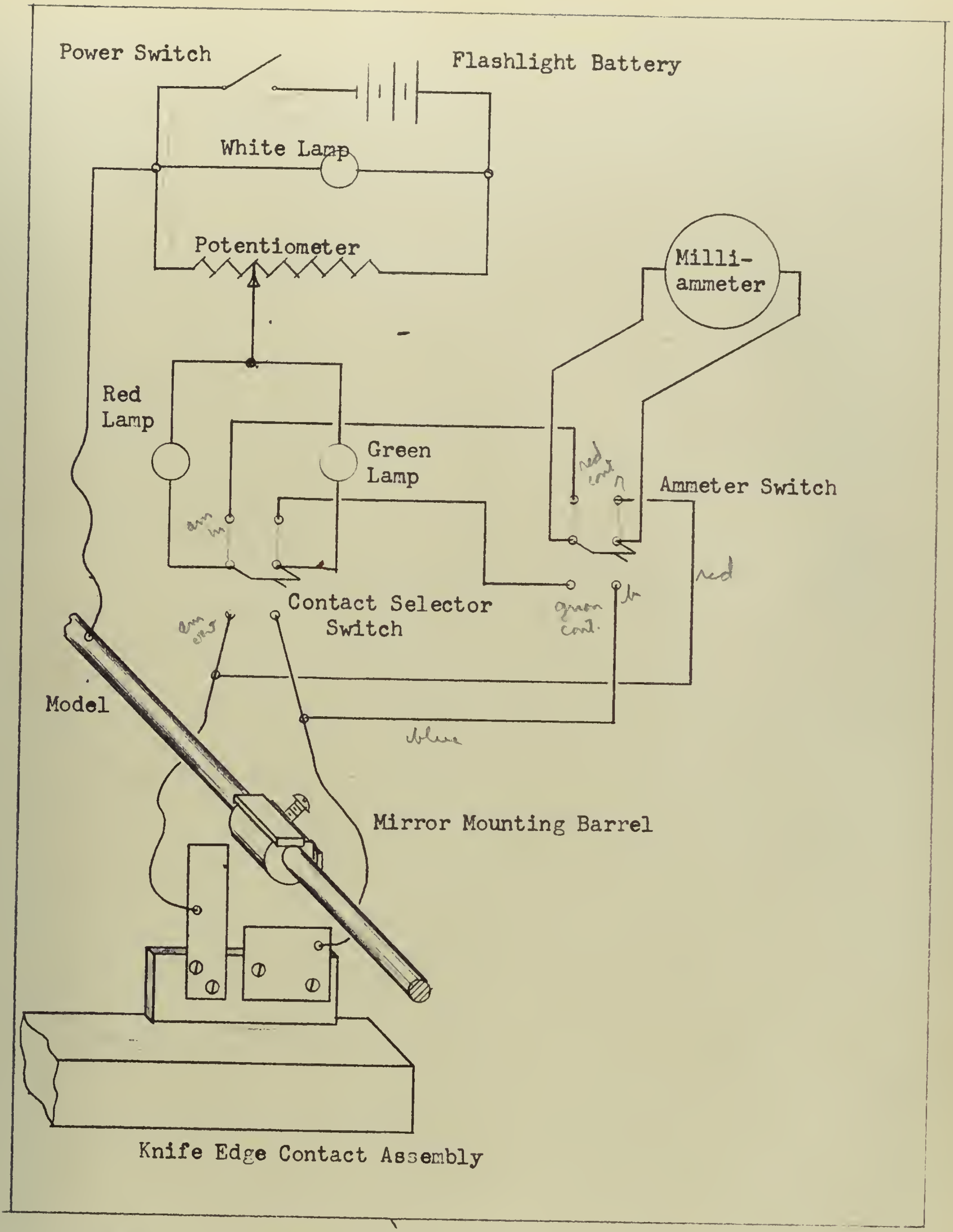

Figure 8 Knife Edge Contact Assembly and Schematic of Associated Electrical Circuits

led to a milliammeter and thence to ground on some point of the framework. Various switches provide for cutting the battery in and out of the circuit, selecting the knife edge contact desired, and cutting the ammeter in or out. Two other lamps were provided to indicate flow of current through the contact if the milliammeter is not used. However, best results have been obtained by cutting the potentiometer down till about 10 milliamps flow through the circuit when one of the knife edges is in contact with the model rod. With this current flowing the voltage across the contact circuit is approximately 20 millivolts.

Since the translation and rotation measurements must be made at precisely the same point, the actual electrical contact is made between the knife edges and the longitudinal center of the mirror mounting barrel. This is the reason mentioned earlier for fabricating the mirror mounting barrel from brass and then silver plating it. By also using silver plated knife edges, a good electrical contact is made the instant the knife edge touches the barrel. With this design measurements were possible approximately to the nearest 0.1 mm (or 0.004 inches), which, as it developed was not sufficiently precise for a deflection method of model testing.

An experiment was therefore conducted to ascertain the feasibility of using two height gages, whose verniers give readings to the nearest 0.001 inch. A duplicate knife edge assembly was mounted on the slide of an 18-inch height gage, and several measurements were attempted. This introduced the complication of trying to mount two height gages at right angles to each other, which could probably have been done had the increased precision warranted it. However,

the difficulty in getting the light in the correct position for reading the very fine graduations on the vernier rendered it cumbersome to say the least. And besides, better precision than 0.001 inch was desired; thus, the height gages were abandoned.

The answer to both the reading and precision problem seemed to lie in the possible utilization of dial indicators, but it was impossible to use a dial indicator acting on the rod itself. Thus evolved the system now used. The mechanical stage is used as before; but instead of measuring the motion of its arms by its own vernier scales, two dial indicators are mounted in such a way as to measure motion of the arms of the stage. Two aluminum blocks were designed to allow mounting of the two 0.001-inch graduation, one-inch range dial indicators so that motion of the two sliding arms of the mechanical stage could be estimated to the nearest 0.0001 inch. Inasmuch as the ranges of the mechanical stage are 40 mm (1.51 inches) in one direction and 80 mm (3.15 inches) in the other, the range of the dial indicators would not be adequate to cover the entire range of the stage. To provide for this deficiency, the aluminum mounting blocks were drilled and tapped so each of the dial indicators could be clamped at any one of four positions along its mounting block by use of an Allen screw.

This ultimate translation measuring device was mounted midway between the two primary support pipes with the mechanical stage stationary arm parallel to these pipes. Fig. 9 is a picture of the translation instrument measuring device in position to measure the motion of the model of example 1 .

(g) Instrument assembly - rotation measurement.

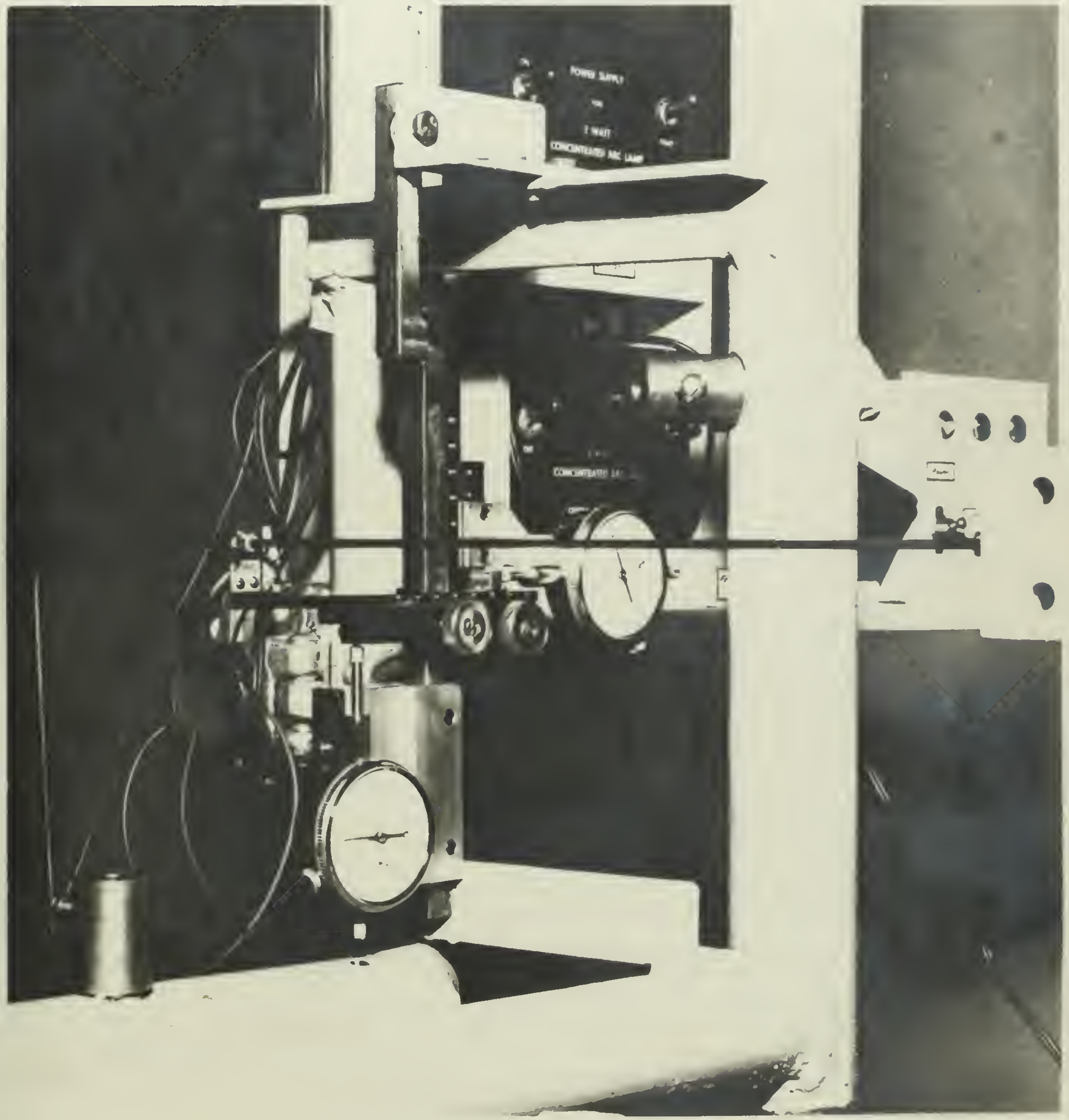

Figure 9 Translation Measuring Instrument Assembly

The rotation measuring equipment used is really a three-dimension modification of a simplified version of the optics system of a sensitive wall galvanometer[1]. It is based on the principle that the angle of reflection from a mirror placed behind a collimating lens will be essentially unchanged by any translational motion of the mirror, but the change in angle of reflection will be proportional to any rotational motion of the mirror. Perhaps the best way to elaborate on this explanation is to describe the system used and discuss its operation. Two identical optical systems were actually employed to be used with the two mirrors mounted on the barrel described earlier; thus, a complete description of only one set of components is necessary.

The optics system employed is quite simply constructed as follows. The only moving component of the apparatus is, of course, the mirror which is fixed to the model by tightening the setscrew of the mirror mounting barrel. As pointed out, these small mirrors (1/2" x 1/8") are cemented to the barrel so the long dimension is parrallel to the rod. A four-inch diameter, double convex, 500 mm focal length lens is clamped in position by a mounted laboratory lens holder. Mirror and lens are designed to be about 2-1/4 inches apart. A 15-inch diameter sheet of Masonite is located 19.7 inches (500 mm) on the other side of the lens from the mirror. This carries a large piece of cross-section paper (small division spacing of 1 mm) and contains a two-watt concentrated arc lamp mounted about an inch from the center of the board. Fig. 10 shows this apparatus. Descriptions and costs of the above equipment are contained in Appendix VII.

---

[1] The Belgian I. R. S. I. A. Commission [8] used a system very similar to the optics of a wall galvanometer for measurement of a single rotation in one of their early calibration tests.

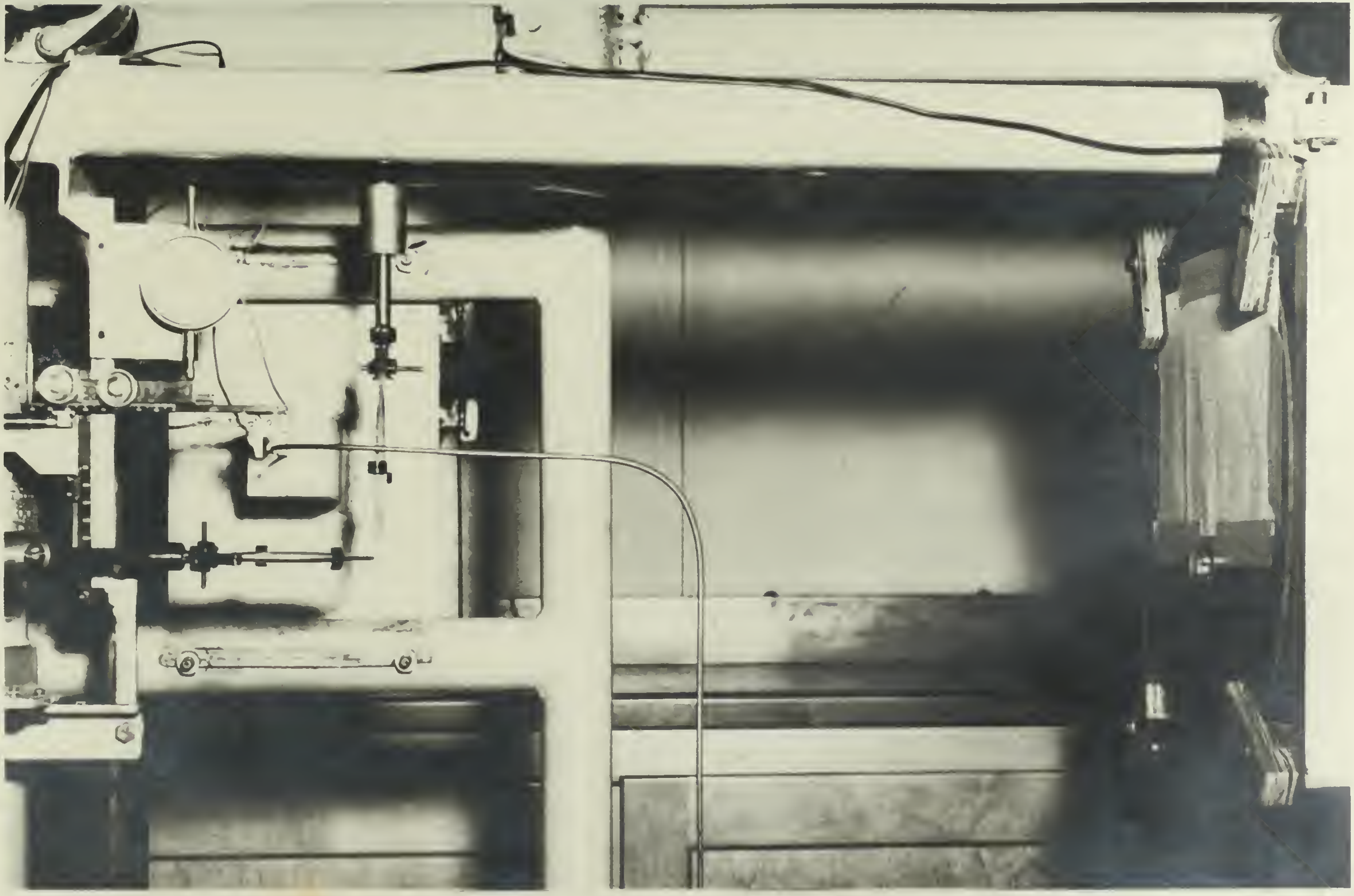

Figure 10 Rotation Measuring Instrument Assembly

The concentrated arc provides a point source of light at the focal point of the lens. All light rays from this point source falling on the lens are therefore collimated; that is, they are so refracted by the lens that they emerge on the other side as parallel rays of light. Some of these parallel rays strike the mirror and are all reflected back as parallel rays at a constant angle of reflection. The reflected parallel rays are refracted by the collimating lens to focus at a point on the rotation measuring scale (cross-section paper). (See Fig. 11) Thus far we have discussed the phenomenon causing a small dot of light to be shown at a point marked ξ_1 . Now regardless of any translational motion in any direction, if the ? mirror rotates an angle of D_4 , then the point of reflected light moves along the scale such that the angle $\xi_1 C \xi_2$ is equal to $2D_4$. Therefore, assuming small geometry, D_4 in radians can be computed by the simple relationship:

$$2 D_4 = \frac{(\xi_2 - \xi_1)}{500} \; ; \text{ or } \; D_4 = (\xi_2 - \xi_1) \times 10^{-3} \quad (1)$$

Now theoretically, D_4 should be readily obtained by use of equation (1) . However, initial tests on simple cantilevers similar to tests described in Appendix III suggested that the rotations thus measured were between one and two percent too small, a phenomenon probably due to abberations of the lens. Furthermore, it was realized that since the angle $\xi_1 C \xi_2$ was twice as big as the lens rotation, the assumption of small geometry might introduce errors sooner than realized. For these reasons rotation-measuring calibrations were made in the optics laboratory by comparing actual

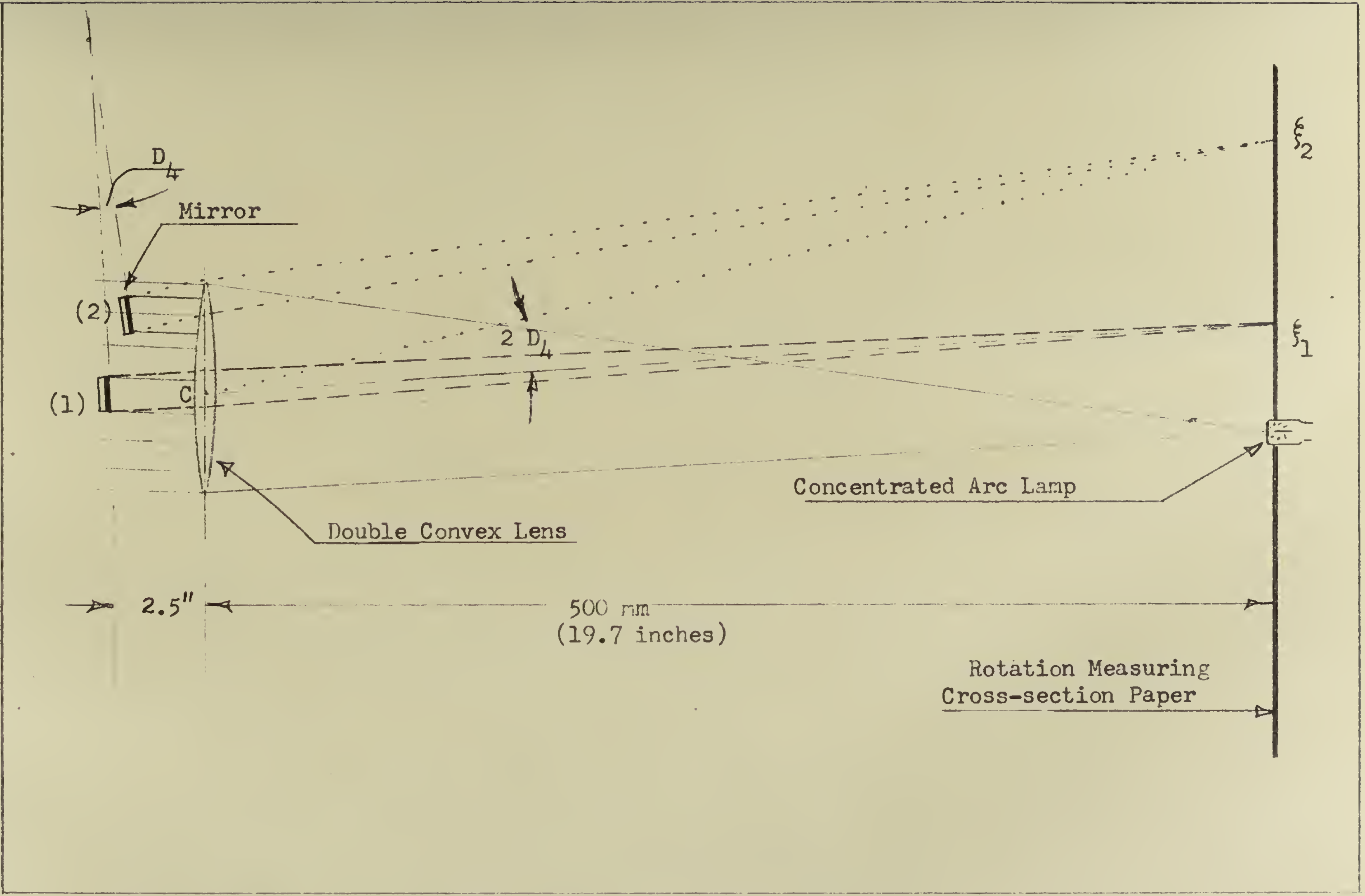

Figure 11 Operation of Rotation Measuring Apparatus

rotations measured on a spectrometer table with those measured by our apparatus. Appendix I describes these experiments and the results obtained. The calibration curves (Fig. 17) obtained were used in the analysis of all examples reported in the Appendix of this paper. Two calibrations were deemed necessary inasmuch as the geometry of the methods of measuring D_4 differed somewhat from that of D_5 and D_6 . (D_4 , D_5 , and D_6 represent rotations in radians about the x'' , y'' , and z'' axes, respectively , and ξ, η, and ζ are coordinates on the rotation measuring scale corresponding to D_4 , D_5 , and D_6 , respectively.) A glance at Fig. 16 shows this difference. The path traced by the reflected dot in going from η_1 to η_2 was a straight line crossing generally through the center of the graph and coming no closer than one or two inches from the light source. The path from ξ_1 to ξ_2 moved over a portion of the radial line from the light source. It is realized that the effect of compound rotations actually observed causes an interaction that introduces errors for which we have not calibrated. However, these are not large and therefore, no further calibration was made. By estimating the coordinates of the reflected points on the rotation measuring cross-section paper to the nearest 0.1 millimeter we obtain precision in the order of 0.1×10^{-3} or 0.0001 radians, which is consistent with that of the translation measurements.

The two optics systems are identical. One is mounted on the secondary supports in such fashion that a line drawn through the center of the mirror, lens, and measuring scale, is parallel to the straight pipe of the secondary support and in a plane midway between the two pipes of the primary support. The other optics set has its

component center line parallel to the pipes of the primary support and also lies in their bisecting plane.

(e) Miscellaneous accessories.

The intensity of the reflected dot described above is not enough for the point to be seen in the presence of bright overhead lights. As a result, it was convenient to place an off-on or dimming switch for the overhead lights in the vicinity of the apparatus. Since it is also convenient to have power supplies for the concentrated arc lamps and switches for the translation measurement electrical circuitry easily accessible, the small instrument panel pictured in Fig. 12 was fabricated to bring these various switches and the translation milliammeter together.

(f) Cost of Construction.

As pointed out throughout the above sections, every attempt was made to utilize commercially available material in the assembly of all components used. Appendix VII is a list of the main purchasable items together with their approximate present day prices. The total cost of the entire system described herein is approximately $1,000 at commercial rates. Included in this price are costs of purchasable equipment and materials in addition to 13 man days of machine shop labor; however, this does not include alignment and adjustments of components by the investigator.

4. Operating technique.

The use of the system just described in analyzing the three examples produced some definite techniques in installing model and equipment and

Figure 12 Instrument Panel

in effecting the desired measurements. Some of these are worth discussion and are therefore reported below.

(a) Preparation and mounting of model

In setting up the apparatus described above it is first necessary to prepare the model to be tested. A scale is picked to permit as large a model as the framework will allow. The configuration is laid out to scale on large sheets of cross-section paper. A piece of rod is cut at least two inches longer than the total length needed for the model. (One-eighth-inch rod comes in 12-foot lengths, which should always be ample.) The rod is then placed on the layouts and starting at one end it can be shaped by bending it by hand. Aluminum bends quite easily; but even with steel, very good models can be fabricated by hand so that the variation from the layout is never more than 1/16 inch . This turns out to be quite adequate, and it is again in keeping with our basic philosophy of simplicity. Any further accuracy in model fabrication would require annealing, bending over templates, and subsequent heat treating, a complication that is not considered warranted. Care must be taken to allow an extra inch at each end to permit anchoring the model.

After the model is formed, the mirror mounting barrel is slipped over the end of the model to be measured. This barrel may be roughly placed at this time, and it should be as far away from the end as the rest of the configuration will allow. At least four inches away is mandatory, and eight or ten inches is preferred. Experiments (Appendix IV) demonstrate that accuracy is a function of this distance of point of measurement from the anchored end, distance L.

Before continuing we must define the unprimed set of coordinates, to which brief reference was made previously. (See Fig. 1) Axes x , y , and z are those of the original coordinates as stated in the problem. They will have origin at point O , which is also assigned when first making up the problem. It is important to remember that while the primed and double primed coordinate sets are always at the anchored end and a function of the orientation of the anchor and instrument assemblies, the UNPRIMED COORDINATES AND POINTS O AND A ARE FIXED WITH THE MODEL. That is, any inversion of the model results in moving and inverting the unprimed coordinate system. One more group of symbols we should know at this time is X , Y , and Z , which are merely the coordinates of point A in the unprimed system.

Now assuming that we first want to measure reactions at point A , we must compute X , Y , and Z from the model dimensions. The deformation assembly is set in approximately the middle of its range in all three directions. Then the end of the anchor block is spotted as accurately as possible so that it lies roughly distances of X , Y , and Z from the clamping vise of the deformation assembly. The anchor assembly framework is then clamped into place by use of the pipe couplers. Once this is spotted, slight adjustments can be made to the deformation assembly until the distances X , Y , and Z are established between the anchor point and the deformation clamping point.

Before mounting the model a final check is made for parallelism and correct positioning of equipment. This final adjustment is accomplished by use of a flexible steel rule calibrated to the near-

est 0.01 inches, a large carpenter's square, a level, and a square-level combination. Using the floor and the framework side opposite the instrument assembly as working surfaces, the various components of measuring and mounting equipment can be aligned. A straight, rigid piece of angle iron can be clamped to the two pipes of the working side of the framework by three-inch C-clamps. (See Fig. 4) This angle can be moved up and down the side and is a great alignment aid. The above-mentioned alignment should be made with the instrument assembly frame in its approximate location. With the completion of this adjustment, the model can be inserted into both the anchor and the clamping vise of the deformation assembly. Tightening bolts on both of these devices rigidly supports the model. No further support has been used in any of the examples worked thus far, and in keeping with the notion of maximum simplicity none is envisioned. It is true that the weight of the model causes it to sag somewhat, but this does not change the configuration appreciably, and thus far has not exhibited a large effect.

(b) Deformation and measurement.

Under the topic of development of theory in Section 5 there is a discussion of the method of computing deformations to be applied at the deformable end. In order to utilize a moderately large total displacement without introducing errors due to geometric distortion of the deformed configuration, a technique described by T. M. Charlton [2] is used. It consists simply of displacing the deformable end, first one-half the desired total amount in a negative direction, and then one-half in the positive sense.

How this is done with this apparatus can best be seen by using a simple example. Assume that, for the present orientation, point O is at the deformable end and the only deformation desired is one of $\Delta x = +1.000$ inch. We first turn the x-crank to move the assembly 0.500 inches in a negative x direction. It is necessary to use the usual precaution of always coming up on the reading from the same direction to avoid backlash error. After taking one set of displacement measurements, the assembly is then cranked 1.000 inch in the positive x direction, and another set of displacements read. For a good check it is advisable to move the assembly back again 1.000 inch in the negative x direction (remembering to avoid backlash error) and ascertain if the original readings are duplicated. It is pointed out with satisfaction that in this system they have always been in good agreement.

Before the first deformation is made, the instrument assembly frame should be slid into the exact position desired and firmly clamped in place. Position is determined by insuring: (1) that knife edges are a distance from the anchor equal to the L length desired, and (2) that with model undeformed the rod passes the lenses at a distance of approximately two and one-half inches from the center of each one. (See Fig. 13) Once the instrument frame is set, the mirror mounting barrel must be finally adjusted so that (1) knife edges will strike it at its longitudinal center, and (2) with concentrated arc lamps on, the point is reflected back to cross-section paper approximately in the center of the board. When it is adjusted properly the barrel should be firmly fixed on the model rod by the set screw. Now that all apparatus is tight and in position,

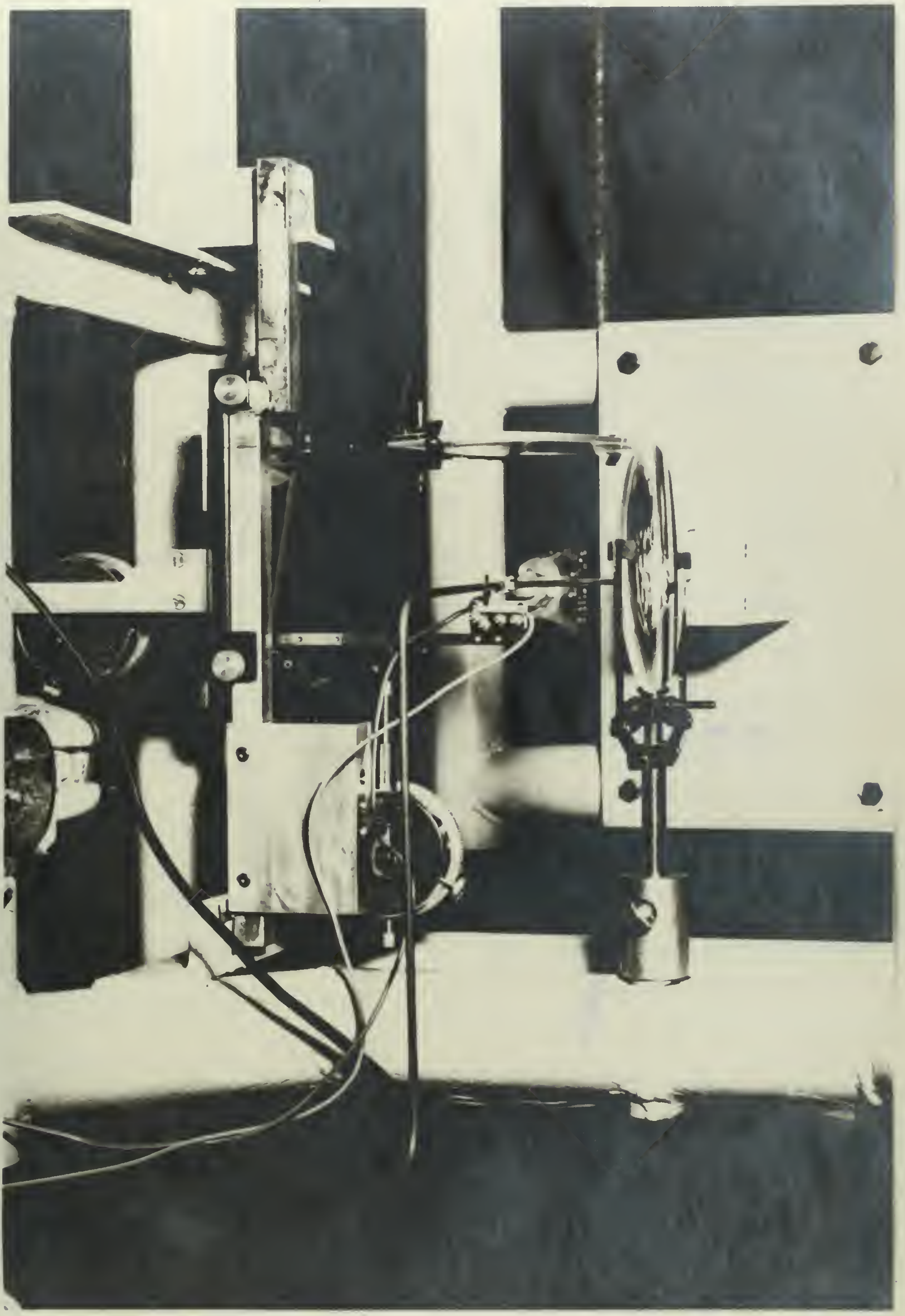

Figure 13 Instruments and Model Installed for Z-bend Analysis Showing Relationship Between Translational and Rotational Measuring Systems

the distance L , between end of the anchor bar and the knife edge contacts, can be measured to the nearest 0.01 inches with a precision flexible steel rule.

As pointed out by cantilever experiments of Appendix III, a very small error in either rotation or translation measurements will cause a considerable error in reactions computed from this data due to the nature of the equations used. (See equations 31 to 35) Thus, care must be taken to realize the best precision possible.

The best method of taking dial indicator readings for the translation measurements is as follows: set the temporarily unused knife edge a certain predetermined distance from the barrel (to insure always measuring at the same point on the knife being used), then advance the knife edge assembly towards the barrel by twisting the proper mechanical stage knob until a deflection is received on the milliammeter. Note the dial indicator reading and then turn the knob in the other direction till the milliammeter needle abruptly falls off to zero. The correct reading has now been bracketed, and the precise point of contact can be found by adjusting the knife edge in as small motions as is possible while watching the dial indicator. After each slight motion the operator should glance at the milliammeter. Ultimately, the motion of another one or two ten-thousandths of an inch will cause a deflection; this point of threshold of contact is where the dial indicator is read and recorded. After the reading is made by the y'' knife, it should be set at a prescribed distance from the barrel and the same procedure as listed above carried through for the z'' knife. The easily read dial indicators render this procedure a quick and precise means of obtaining the transla-

tional displacement readings. Of course, another set of readings is taken after the positive deformation and the differences between the two sets gives the translations D_2 and D_3 directly.

The rotations can be as readily found as the translations. After the first (negative) deformations are applied, two sets of coordinate axes are arbitrarily drawn on the rotation measuring graphs of each system on some convenient bold lines in the vicinity of the reflected points. Then the two coordinates of the reflected point are recorded for each system. On one graph, ξ_1 and η_1 will be obtained and on the other ξ_1 again and ζ_1 will be recorded. After deformation of the system, it is simply a case of recording ξ_2 and η_2 and ξ_2 and ζ_2, respectively. A quick check of the two $\Delta\xi$'s will indicate any error in reading or misalignment of the system.

There is one more observation which should be made and that is the closest point of approach of the reflected point to the concentrated arc lamp. This information is used in selecting the proper calibration curve from Fig. 17.

One other item that bears mentioning under the title of technique is the model inversion problem. For two dimension problems with parallel ends this is no problem; the model is simply rotated 180° about the axis out of the model plane and reinstalled. In practically all other cases, however, a slight respotting of anchor and instrument frame will be necessary. Suffice to say here that there are several ways of inverting the model in each case, but almost always, one method causes a minimum of instrument modification, and naturally such an inversion is to be sought.

5. Development of theory.

The basic principles for the type of model test used herein were described briefly in Section 2; however, a more specific discussion of actual equations used is covered in this section. Common to all model test systems is the method of scaling from model results to actual pipe reactions. The following is quoted from a description of the M. W. Kellogg Model Test [9]:

> As the end and intermediate restraints for the model and the piping system which it represents are assumed to be the same, and since both are structures obeying the conventional load-deflection relationship, their mutual force and moment relationships can be expressed as a simple ratio of their respective dimensional and elastic properties and corresponding load-deflection relationships.

Therefore, as pointed out in the same section, the following equations are pertinent:

$$\frac{F_p}{F_m} = \frac{E_p}{E_m} \quad \frac{I_p}{I_m} \quad \frac{\Delta_p}{\Delta_m} \quad \frac{\lambda_m^3}{\lambda_p^3} \quad , \text{ and} \qquad (2)$$

$$\frac{M_p}{M_m} = \frac{E_p}{E_m} \quad \frac{I_p}{I_m} \quad \frac{\Delta_p}{\Delta_m} \quad \frac{\lambda_m^2}{\lambda_{\cancel{m}p}^2} \quad , \qquad (3)$$

where subscripts p and m refer to piping system and model, respectively. E = modulus of elasticity, I = moment of enertia, Δ_p / Δ_m = ratio of end deformations (ratio of total deformation computed for prototype to deformation applied to the model), and λ_m / λ_p = linear dimensional scale of the model.

Before any analysis of piping flexibility can be undertaken by any method, model or analytical, it is necessary to compute end deformations Δx , $\Delta \overset{y}{m}$, and Δz . These consist of contributions from the thermal expansion of the pipe as well as from thermal displacements of

equipment to which the pipe is fastened. These contributions can be intuitively unscrambled, but the following table is a helpful device for keeping algebraic signs straight in computing the various deformations: assume that we desire deformation Δx for the model mounted with point O at the deformable end, and we know the linear thermal expansion = B inches/100 feet; we know X, the coordinate of point A in feet; Δx_O = external motion of point O and Δx_A = external motion of point A. Then by use of the table (equation 4) we see that $\Delta x_p = XB + \Delta x_O - \Delta x_A$.

	Pipe Expansion Alone	Equipment Expansion Alone		
	Motion of A due to thermal expansion for O stationary and A unrestrained	Motion of point O	Reverse of motion of point A	Total
Δx_p	X B	Δx_O	$- \Delta x_A$	$(XB + \Delta x_O$ $- \Delta x_A)$

Equation (4)

Once Δx_p is obtained, multiplication of this result by the deformation ratio, Δ_m/Δ_p, yields Δx_m, the deformation to be applied to the model. The question arises of how to choose the deformation ratio. Experiments to date have produced no definitive method of arriving at this ratio; obviously it depends on how large we desire the largest component of deformation to be. Appendix IV reports the results of an experiment in which the accuracy of one of the force components were observed for various values of the deformation ratio. It is clear from this experiment that the deformation ratio has no effect on the accuracy of the system except in the cases where it produces such extremely small dis-

placements at point P to cause potentially large errors for small mistakes in measuring. As an order-of-magnitude estimate only, a maximum deformation of two inches in any one direction is suggested as something that would normally produce satisfactory results with this equipment.

At this time it is worthwhile to review the coordinate systems being used. First of all the double-primed coordinate set has its origin in the plane of the mechanical stage and point of measurement and is controlled only by the position of the instrument and anchor assemblies. For example, x'' is always measured from point P along the model positive in the direction towards the anchored end. And similarly, y'' is always parallel to the 68-inch pipes of the instrument frame primary support, and positive going from the knife edge towards the model. Therefore, z'' is always parallel to the straight pipe of the instrument frame secondary support and is positive in a direction to be consistent with x'' and y'' for a right hand system. Displacements in this double primed system are labelled D_2 , D_3 , D_4 , D_5 , and D_6 to indicate translations in y'' and z'' directions, and rotations about the x'' , y'' , and z'' axes, respectively. Similarly, reactions F_2 and F_3 are forces in y'' and z'' directions while F_4 , F_5 , and F_6 are moments about the x'' , y'' , and z'' axes, respectively.

It will be remembered that the single primed set of coordinates, x' , y' , and z' , are parallel and in the same direction as the double primed set, but with origin ALWAYS AT THE POINT OF ANCHOR; and the unprimed set of coordinates, x , y , and z , are FIXED IN THE MODEL with origin at point O , and are supplied in the original statement of the problem.

The heart of the deflection measurement method of model testing is contained in equations 31 through 35 derived in Appendix II. The equations are repeated below for emphasis:

$$F_2 = \frac{6\,E\,I}{L^2}\left(\frac{2\,D_2}{L} + D_6\right) \qquad (31)$$

$$F_3 = \frac{6\,E\,I}{L^2}\left(\frac{2\,D_3}{L} - D_5\right) \qquad (32)$$

$$F_4 = \frac{J\,G}{L}\left(D_4\right) \qquad (33)$$

$$F_5 = \frac{6\,E\,I}{L^2}\left(\frac{2\,L\,D_5}{3} - D_3\right) \qquad (34)$$

$$F_6 = \frac{6\,E\,I}{L^2}\left(\frac{2\,L\,D_6}{3} + D_2\right) \qquad (35)$$

Appendix II is a matrix derivation of these equations based on relationships listed by Timoshenko and McCullough [10]. Once F_2 through F_6 are obtained, it then becomes necessary to use simple static relationships to find the reactions at the anchored point. The following relations follow immediately from static equations: $\sum F_i = 0$ and $\sum (M_i)_n = 0$: (See Fig. 14)

$$F_{y'} = -F_2 \qquad (5)$$

$$F_{z'} = -F_3 \qquad (6)$$

$$M_{x'} = -F_4 \qquad (7)$$

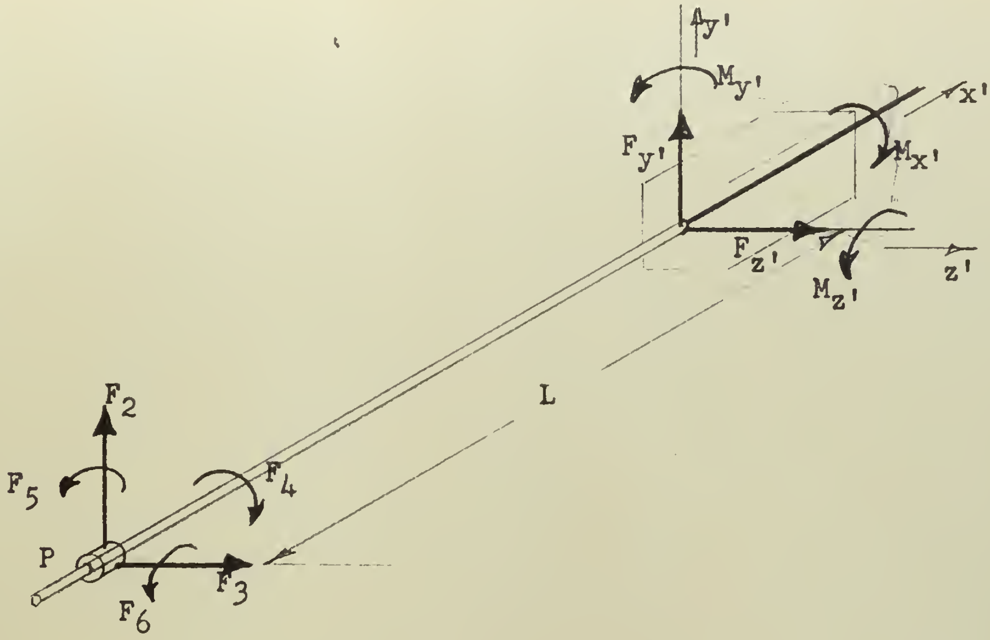

$$\Sigma F_y = 0; \quad F_2 + F_{y'} = 0; \quad F_{y'} = -F_2$$

$$\Sigma F_z = 0; \quad F_3 + F_{z'} = 0; \quad F_{z'} = -F_3$$

$$\Sigma (M_x)_P = 0; \quad F_4 + M_{x'} = 0; \quad M_{x'} = -F_4$$

$$\Sigma (M_y)_P = 0; \quad F_5 + M_{y'} - F_{z'}L = 0; \quad \begin{aligned} M_{y'} &= F_{z'}L - F_5 \\ M_{y'} &= -F_3L - F_5 \end{aligned}$$

$$\Sigma (M_{z_P}) = 0; \quad F_6 + M_{z'} + F_{y'}L = 0; \quad \begin{aligned} M_{z'} &= -F_6 - F_{y'}L \\ M_{z'} &= -F_6 + F_2L \end{aligned}$$

Figure 14 Static Relationship Between Reactions at Point P and Those at Point of Anchor

$$M_{y'} = -F_3 L - F_5 \tag{8}$$

$$M_{z'} = F_2 L - F_6 \tag{9}$$

We now have the reactions at the anchored point in the primed coordinate system. The next step is to convert these reactions to the coordinates of the problem, the unprimed set. The following matrix equation described by J. E. Brock [1] is a general solution:

$$F_0 = L_{01} \chi \; F_1 , \tag{10}$$

where F_0 and F_1 are column matrices of reactions in the unprimed and primed systems, respectively, and L_{01} is a 6 x 6 matrix based on direction cosines between the two systems. In many cases, however, the two coordinate systems have parallel axes, and in such problems the conversion is an elementary consideration of merely changing algebraic signs and labels. This is the case in examples 1 though 3 in the Appendix.

It will be remembered that the measurements at one end do not reveal the force $F_{x'}$. For this reason measurements are taken at the other end of the model, again failing to provide the new $F_{x'}$ at that end. Now if the two end legs are not parallel, conversion to the basic coordinates of the problem will reveal all unknown reactions. However, for cases where the end legs are parallel and in cases where a check is desired on known data, it is necessary to have equations linking the two ends from which it is possible to solve for the as yet undetermined components. Conversion to the coordinates of the problem results in reactions in the unprimed system at both point O and point A. (Subscripts O and A will differentiate between the reactions at these

two points). It will be remembered that X , Y , and Z are coordinates of point A.

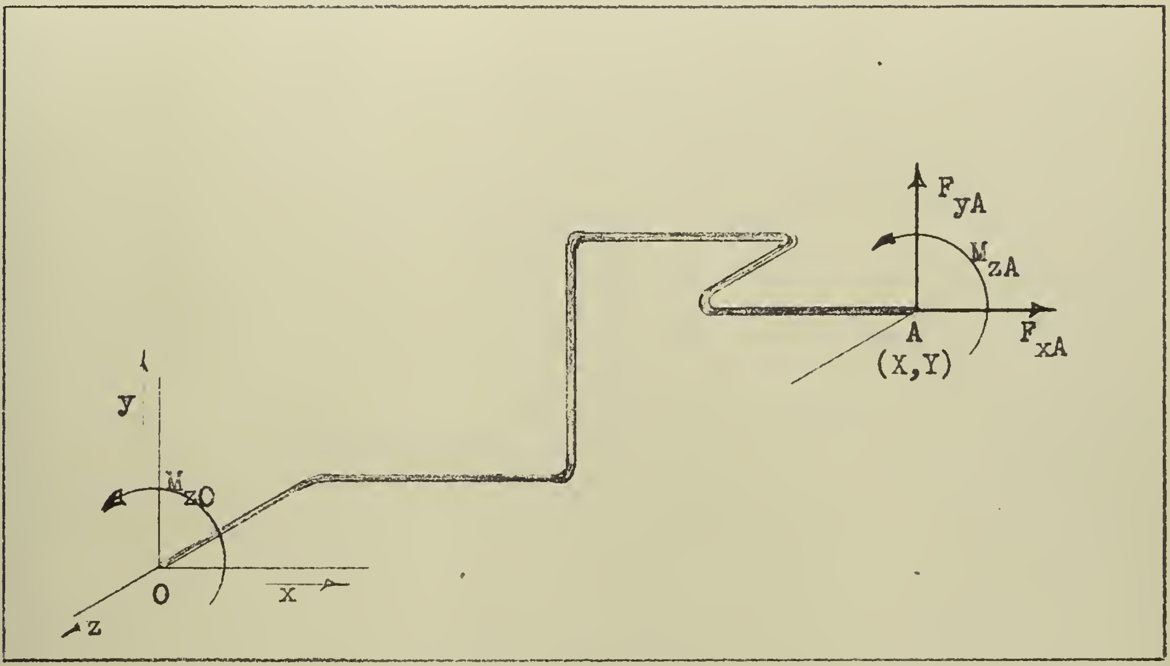

Figure 15 Typical Three-dimensional Model

Fig. 15 shows a typical three-dimension pipe system. Summing moments about point O , we have:

$$M_{zO} + M_{zA} + F_{yA} X - F_{xA} Y = 0 \tag{11}$$

and solving for F_{xA} :

$$F_{xA} = \frac{(M_{zO} + M_{zA}) + F_{yA} X}{Y} \tag{12}$$

Duplicating the above for the other two planes, and solving for both forces in each equation leads us to the following equations:

$$F_{xA} = \frac{F_{zA} X - (M_{zO} + M_{zA})}{Z} \tag{13}$$

$$F_{yA} = \frac{(M_{xO} + M_{xA}) + F_{zA} Y}{Z} \qquad (14)$$

$$F_{yA} = \frac{F_{xA} Y - (M_{zO} + M_{zA})}{X} \qquad (15)$$

$$F_{zA} = \frac{(M_{yO} + M_{yA} + F_{xA} Z}{X} \qquad (16)$$

$$F_{zA} = \frac{F_{yA} Z - (M_{xO} + M_{xA})}{Y} \qquad (17)$$

Equations (12) through (17) have considerable utility since (1) for parallel end legs two equations can be used to find the unmeasured force and four others are available for checks, and (2) for non-parallel end legs all six equations may be used for various checks.

6. Analysis of data.

As soon as it is decided to what scale the model will be built and what deformation ratio will be used, the scale factors, $S_F = \frac{F_p}{F_m}$ and $S_M = \frac{M_p}{M_m}$, can be computed from equations (2) and (3). In the examples of the Appendix, these computations are made on data sheet I, provided as a convenience for this purpose. It will be noted, however, that S_M contains a factor of 12 in the denominator to give results in pound feet.

In converting from measured displacements at point P to reactions at A and O, many factors are common to several of the individual calculations. Therefore, it was also convenient to devise an orderly method of using these common factors and of recording results. As a result, data sheet II has evolved. Thus, as soon as L is known, we can solve for $2/L$, $2/3\,L$, L^2, $6\,EI/L^2$, and JG/L immediately, for use in later computations. $6\,E_m I_m = 2155$ lb. in.^{2} and

$J_m G_m$ = 287.5 lb. in.^{2} are values for an one-eighth-inch diameter steel rod.

The translation section of the sheet provides space for recording the dial indicator readings after negative and positive deformations and a place for their differences, D_2 and D_3 . The rotation section similarly provides spaces for recording coordinates of the reflected dot after negative and positive deformations and a place for their differences. In addition, room is available for recording and applying the conversion factor obtainable from the calibration chart of Fig. 17 .

For the force computations two sections are available for step by step use of equations (31) and (32) to solve for F_m's , and for recording and applying the force scale factors. By changing algebraic sign when applying S_F , we can not only scale the answer to the piping system, but also apply equations (5) and (6) to give final results of $F_{y'}$ and $F_{z'}$. The section for $M_{x'}$ computation allows for multiplying D_4 by $J\,G/L$ and an application of the moment scale factor with a change of sign to account for equation (7) .

The other two moment sections of data sheet II , were devised for step by step use of equations (34) and (35) . However, here multiplication by $(-6EI/L^2)$ is effected to produce negative values of F_{5m} and F_{6m} . These are used to compute $M_{y'm}$ and $M_{z'm}$ by equations (8) and (9) . Therefore, in this case a multiplication by the positive moment scale factor yields $M_{y'}$ and $M_{z'}$.

At the foot of data sheet II there is space for the reactions in the unprimed or original coordinate system. Having filled out two data sheets, one for each end of the model, we will have at our disposal two forces and three moments at both O and A . As the forces at A are

the same as the negatives of those at O , the unknowns of the problem consist of three forces, three moments at O , and three moments at A. Now, we have all the unknown moments at both O and A.

Let us consider the case where the A leg is not parallel to the leg at O but it is parallel to one of the unprimed axes. Here we have available two forces at A and a repeat of one of these forces plus one new one at O . Therefore, all unknowns have been measured.

Now in the case where the A leg is neither parallel to the leg at O nor parallel to any of the unprimed axes, the conversion from primed coordinate reactions to unprimed reactions at A , will involve the use of equation (10) . The matrix multiplication in this case will produce three unprimed forces at A , all containing the unknown $F_{x'}$. Since information at O will contain three other forces also containing $F_{x'}$ (or else two known forces) , equating any of the corresponding pairs of forces will give an equation in $F_{x'}$. Having solved for $F_{x'}$, all three forces can be found.

In the third, but special case, where the O and A legs are parallel, the same two forces will be found at each end. In this case use of the equations (12) through (17) (two will always be applicable) will produce the third force.

It is evident that in the use of the above system there is in every case an abundance of information. Several methods are available for reducing such redundant information, but in the examples involved in this paper a simple arithmetic average was taken when the unknown was found twice in the same manner (e. g. measurement of same force at both ends, or use of two of equations (12) through (17) .)

We have thus far extensively covered methods of reducing the dis-

placement measurements to the nine important unknowns (three forces and three moments at each end, but the forces at one end are equal in magnitude to those at the other) of a piping flexibility problem. If any information is desired at any intermediate position on the model, simple modifications of equations (12) through (17) will produce this information.

The question now arises as to what kind of accuracy can be expected in the results obtained above. A glance at Appendix IV indicates that for cases of a generous L dimension, results are excellent; and a look at Appendix V shows that in cases of all but extremely small reactions the results are equally good.

Now let us consider the case where the dimensions of the problem dictate that we use a small L and another case where a normal discrepancy in a very small reaction will cause a large percentage error. In these cases a quantitative refinement can be made to the data based on past experiences and results of previous experiments and calibrations. Examples of such experiments are available in the form of Figs. 20 , 22 , and 23. Fig. 20 shows a curve of percent error in $M_{x'}$ versus L ; Fig. 22 , percent error in $F_{y'}$ versus L[1] ; and Fig. 23 , percent error of $M_{z'}$ versus L[1] . The ordinates of these curves show percent error between experimental results and theory; and they indicate errors in one direction only. In fact, the model test experiments indicate the model is systematically more flexibile than theoretical predictions. These curves were obtained as being representative of the three types of equations relating D's and F's . To use this information, it is desirable to take two complete readings at one end at different L distances. If a qualitative examination of the two sets of results

---

[1] See pages 87 through 97 for a discussion of the unexpected shape of these curves.

reveals a general agreement with curves mentioned above, then it is safe to go right to these curves, pick off an approximate percentage error for the L used, and simply reduce the reaction concerned by this amount.[1]

Now in results where a component is small and the percent error is therefore suspect, or where it is obvious that some of the static equations, (12) through (17) are not satisfied, the following procedure is recommended. Any increases or decreases in accordance with the above paragraph should be applied, and then one of the equations (12) through (17) may be solved for the questionable unknown. In many instances two of these equations can be used and their results averaged. In the two main cases where the lack of F_x, means solving for one of the forces in some manner, it is advantageous to apply all the above refinements before the equations are solved for the unknown force.

7. Results.

In an effort to test the capabilities of this system of model testing, four general systems were analyzed. The solutions are contained in the Appendix.

The first set-up was a simple cantilever with end weights applied. (See Appendix III)

The next model tested was for analysis of the two-dimensional Z-Bend recommended as a standard piping flexibility analysis problem by Crocker and McCutchan [4]. (See Appendix IV)

The first three-dimensional problem tested was the Hovgaard Bend, another standard problem recommended by Crocker and McCutchan. (See Appendix V)

Finally, in an effort to ascertain the versatility of the deflection

---

[1] Further suggestions for corrections to short-L data are discussed in Appendix IV .

model test system, a typical steam piping problem was created. In this system L was equal to 5.16 inches so that the refinements referred to in section 6 were made after measured results were obtained. The final results were recorded, and then the problem was solved by analytical means on a digital computer.[1] Appendix VI shows the good agreement between model and analytical analysis. This system was also analyzed by use of an identical model made from aluminum. The aluminum model, while not producing the accurate results obtained by the steel model, gave agreement with theory within 25% for all components and within 9% for resultants.

The table below is a brief compilation of percentage of error between resultants of reactions as measured by the deflection model test method and as solved by analytical methods on a digital computer. It is to be remembered that the analytical solutions with which we make these comparisons are for the problems given but with the bend flexibility factor set equal to one.

TABLE I

	Percent error obtained between deflection model test and theory			
	Z - Bend	Hovgaard Bend	Typical System	
Reaction			Steel	Aluminum
$\overline{F}$	3.6	3.7	1.8	0.2
$\overline{M}_O$	1.5	1.9	2.1	2.3
$\overline{M}_A$	2.7	1.3	2.4	8.1

[1] All analytical solutions were obtained on a National Cash Register Co. CRC 102 A general purpose electronic digital computer by use of the matrix method of piping flexibility analysis described by Professor John E. Brock [1].

It is true that the above picture does not tell the complete story. In the situation above an error as high as 7.1% for cantilever problems was found; maximum error for Z-bend was 3.8% for one component; for the Hovgaard Bend, the maximum error was 5.7%; and for the typical problem, example 3, the maximum component error was 10.3%. These, however, were not in major components as confirmed by the resultants above. These results are indeed gratifying. A comparison of the results of all major model test laboratories in Europe and in the United States was made by the Belgian I. R. S. I. A. Commission [8]; this report shows that the average model test error by other methods is of the order of 10 to 15 percent. One series of tests conducted by the Commission, however, has been made where every detail is accounted for as meticulously as possible, and in this case they report average errors in the vicinity of 1% for tube models of 13 mm outside diameter making up a three-dimension model consisting of three legs welded at right angles. Clearly bend flexibility was not involved in these tests. For this reason it is certainly permissible to compare the results as listed in the table above with those of the Belgian I. R. S. I. A. Commission.

8. Conclusions.

Model tests reported in this thesis confirm that results of adequate engineering accuracy can be obtained to piping flexibility problems for two anchor configurations using the "deflection method" described herein and employing simple equipment composed largely of commercially available components. If bend flexibility factors other than unity are required it is necessary to simulate this in the model; however, this was not done in the tests conducted for this report and has been left for subse-

quent investigators. In configurations for which the point of measurement can be approximately eight inches or more from the point of anchor, it can be expected that reasonable care with experimental techniques will produce values of resultant force and moment at the anchor substantially within 10% error and that individual components, unless they are quite small compared to the resultant, will also be of better than 10% accuracy. If the measuring leg must be less than approximately eight inches, systematic errors very similar to those reported by other investigators, are introduced, but if the measured leg is at least four inches long, to a reasonable extent they may be compensated by the use of correction curves. Possibilities for corrections for use with extremely short legs are discussed in Appendix IV. Since the heart of the deflection model method and its equipment is a set of displacement measuring devices, this model technique is particularly well adapted to the determination of deflections at various points in the configuration so as to provide information of value in specifying hangers and supports.

This model test system imposes no new difficulties in the preparation of models nor does it lessen any of those which pertain to other model procedures; the models used in this investigation were cold-bent by hand from commercial rod and provided adequately accurate simulation of the prototype piping system, subject to the limitation on bend flexibility factor mentioned above. While no tests were made on multi-anchor problems, it appears evident from the success which was achieved for two-anchor problems, that the more complicated problems can be treated with comparable success merely by introducing additional deformation assemblies.

As a result of encountering difficulties with less accurate design

and components, the measuring systems described in this report represent considerable evolution from the first attempts. However, it is not intended that the description of the apparatus which is given here be used as a blue-print for the construction of similar facilities, but rather that it provide a point of departure for others in exercising ingenuity and making use of local facilities so as to produce model testing equipment of particular utility and economy.

BIBLIOGRAPHY

1. J. E. Brock, A Matrix Method for Flexibility Analysis of Piping Systems, Journal of Applied Mechanics, pages 502 and 503, December 1952.

2. T. M. Charlton, Model Analysis of Structures, Wiley and Sons, page 75, 1954.

3. Code for Pressure Piping, ASA B31.1-1955, American Society of Mechanical Engineers, pages 90 to 97, 1955.

4. Sabin Crocker and Arthur McCutchan, Methods of Making Piping Flexibility Analyses, Heating, Piping, and Air Conditioning, June 1946.

5. J. P. Den Hartog, Advanced Strength of Materials, McGraw-Hill Book Company, Inc., pages 234 to 245, 1952.

6. H. H. George and E. C. Rodabaugh, Effect of Internal Pressure on the Flexibility and Stress Intensification Factors of Curved Pipe or Welding Elbows, paper number 56-SA-50 presented at the American Society of Mechanical Engineers Semi-annual meeting in Cleveland, Ohio, June 17 to 21, 1956, pages 22 and 23.

7. William Hovgaard, Stresses in Three Dimension Pipe Bends, Transactions of American Society of Mechanical Engineers, Vol 57, 1935.

8. Institute pour l'Encouragement de la Recherche Scientifique dans l'Industrie et l'Agriculture, (I. R. S. I. A.), Les Comptes Rendus de Recherches, Travaux de la Commission de Recherches Pour L'Etude des Tuyauteries a Vapeur (Premiere Partie), Number 16, pages 61 to 84, November 1955. (Published by the I. R. S. I. A., 53, rue de la Concorde, Brussels, Belgium)

9. M. W. Kellogg Company, Design of Piping Systems, Second Edition, John Wiley and Sons, Inc. pages 198 to 202, 1956.

10. S. Timoshenko and G. H. MacCullough, Elements of Strength of Materials, Second Edition, D. Van Nostrand Company, page 170, May 1940.

APPENDIX I

CALIBRATION OF OPTICS SYSTEM

In order to provide an accurate relation between displacements of the reflected point of light ($\Delta\xi$, $\Delta\eta$, and $\Delta\zeta$) and actual angular displacements, D_4 , D_5 , and D_6 , an optics experiment was conducted wherein the mirrors could be rotated to give a definite reflected-dot displacement while the true mirror rotation could be measured.

To accomplish this, the following apparatus was employed. The mirror mounting barrel was placed vertically in the center of the platform of a spectrometer. The lens from the model test apparatus was placed about 2.5 inches from one of the mirrors, and the point of light source together with the rotation-measuring scale (also from the model-testing apparatus) was placed 19.7 inches from the center plane of the lens. (Lens focal length = 500 mm = 19.7 inches)

Two experiments were then conducted. In the first, the rotation-measuring cross-section paper and point of light source were oriented with the light below the center of the graph paper mounting board. (See Fig. 16, Case 1) The mirror mounting barrel, secured to the spectrometer platform by wax, was tilted slightly to allow the point of light to be reflected to the center of the cross-section paper, approximately 25 mm above the light source bulb. The spectrometer was rotated until the reflected light dot rested directly on an even scale line at the center, and the platform angle was read and recorded. The vernier scale made possible a reading to the nearest one minute of arc, and a reading to one-half a minute could be estimated.

The spectrometer platform was then rotated in 10 mm of reflected-

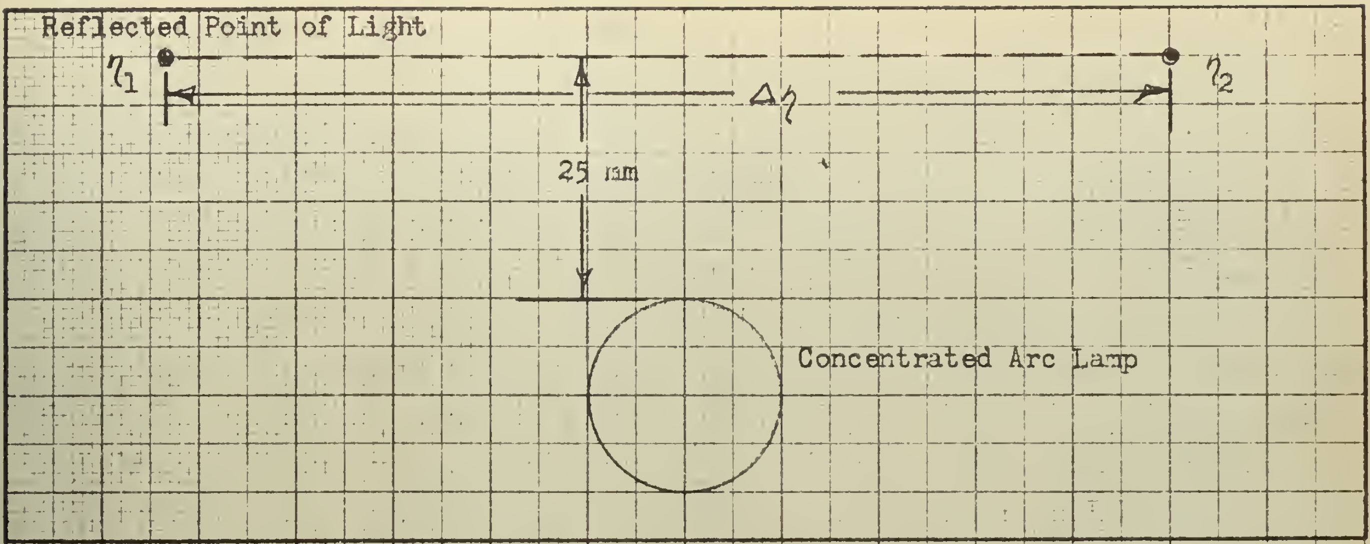

Case (1) Typical Path of Reflected Light for Measurement of D_5 or D_6

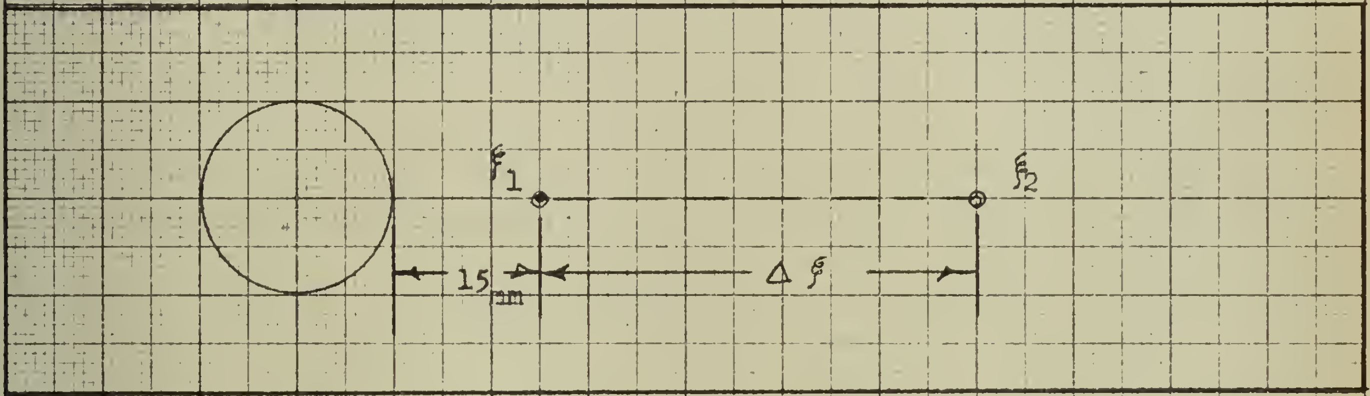

Case (2) Typical Path of Reflected Light for Measurement of D_4

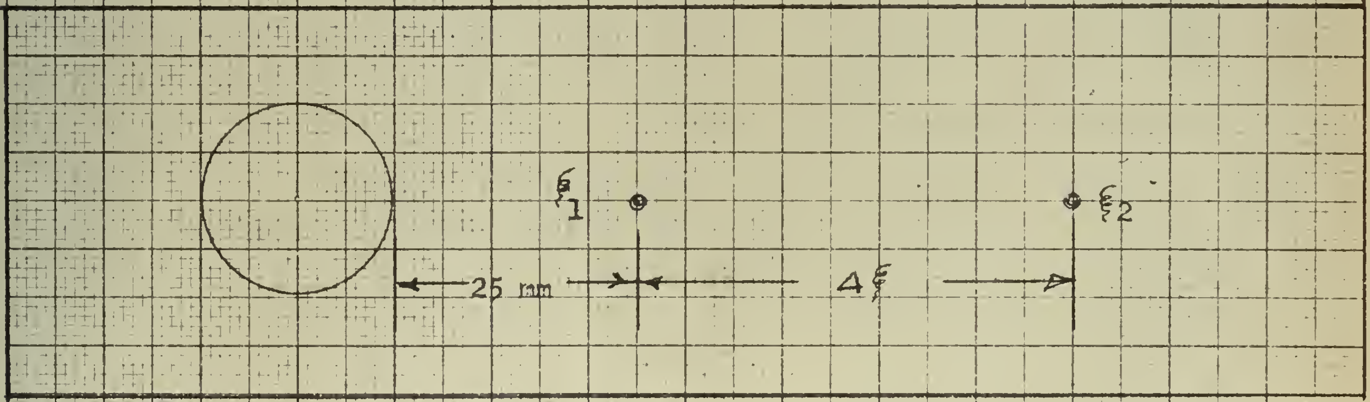

Case (3) Typical Path of Reflected Light for Measurement of D_4, With ξ_1 at Different Starting Point

Figure 16 Paths of Reflected Point of Light for Three Cases of Rotation Measurement

dot-displacement increments to 70 mm on both sides of the center scale line. Then for each 10 mm displacement, the spectrometer platform arc was recorded. The results tabulated in Table 2 were obtained. This type of reflected-dot motion would be typical of a rotation about either y'' or z'' axes and therefore gives D_5 or D_6. Thus, the millimeter scale displacements were $\Delta\eta$ or $\Delta\zeta$, respectively; hence, the symbol, η, is used for the reflected light in Case 1. Actual measurements of arc will be listed as θ, while $\Delta\theta$ converted to radians will be thought of as D_5 (representing D_5 or D_6). As just pointed out, the calibration thus obtained is valid for both η and ζ.

Now once the data of Table 2 were obtained it remained to transform this information to useful conversion data. Inasmuch as most configurations would involve η (or ζ) by producing η_1, one one side of the center and η_2 on the other side, $\Delta\eta$'s were computed to provide for this type of motion. (See column 3 of Table 3) The corresponding $\Delta\theta$'s were then found and recorded. From this the ratio $\frac{\Delta\theta}{\Delta\eta}$ was tabulated; and finally $\Delta\theta$ (minutes of arc) was converted to D_5 (rotation in radians), and the useful value $\frac{D_5}{\Delta\eta}$ resulted. By plotting this information, $\frac{D_5}{\Delta\eta}$ versus $\Delta\eta$, calibration curve (1) of Fig. 17 was produced.

Experiment number two consisted of using the same general procedure to arrive at data for $\frac{D_4}{\Delta\xi}$. This time the reflected point would move from a point near the center of the graph paper on a line going through this point and the center of the light source lamp. (See Fig. 16, Cases 2 and 3) Since it was realized that different results might pertain if the ξ_1 were not always at precisely the same spot, two manipulations of the data were effected, Case (2) for starting point 15 mm away from the edge of the concentrated arc lamp and Case (3) for ξ_1

25 mm away. (See Tables 4 and 5) Plotting these results produced curves (2) and (3) of Fig. 17.

TABLE 2

Data for Optics Calibration Experiment, Case 1

η	θ		$\Delta\theta$(for $\Delta\eta = 10$)
0	12°	36'	--
10	13°	11'	35'
20	13	46	35
30	14	21	35
40	14	55.5	34.5
50	15	30	34.5
60	16	04	34.0
70	16	38	34.0
-10	12	01	35
-20	11	26.5	34.5
-30	10	52.0	34.5
-40	10	18	34
-50	9	44	34
-60	9	10	34
-70	8	36	34

TABLE 3

Computation of Conversion Data for Optics Calibration, Case 1

η_1	η_2	$\Delta\eta$	$\Delta\theta$	$\frac{\Delta\theta}{\Delta\eta}$	$\frac{D_5}{\Delta\eta}$
0	10	10	35'	3.50	1.018×10^{-3}
-10	20	30	105	3.50	1.018
-20	30	50	174.5	3.49	1.015
-30	40	70	243.5	3.48	1.012
-40	50	90	312	3.47	1.010
-50	60	110	380	3.45	1.004
-60	70	130	448	3.45	1.002

TABLE 4

Data for Optics Calibration Experiment, Cases 2 and 3

ξ	θ		$\Delta\ \theta$(for $\Delta \xi = 10$)
0 (15 mm from edge of lampP	5°	56'	--
10	5	21	35
20	4	46	35
30	4	11.5	34.5
40	3	37	34.5
50	3	03	34

TABLE 5

Computation of Conversion Data for Optics Calibration, Cases 2 and 3

CASE 2 (original point 15 mm from edge of concentrated arc lamp)

ξ_2	$\frac{\Delta\theta}{\Delta\xi}$	$D_4/\Delta\xi$
10	3.5	1.17×10^{-3}
20	3.5	1.17×10^{-3}
30	3.49	1.13
40	3.47	1.08
50	3.46	1.05

CASE 3 (original point 25 mm away)

ξ_2	$\frac{\Delta\theta}{\Delta\xi}$	$D_4/\Delta\xi$
10	3.5	1.17×10^{-3}
20	3.47	1.09
30	3.47	1.08
40	3.45	1.02

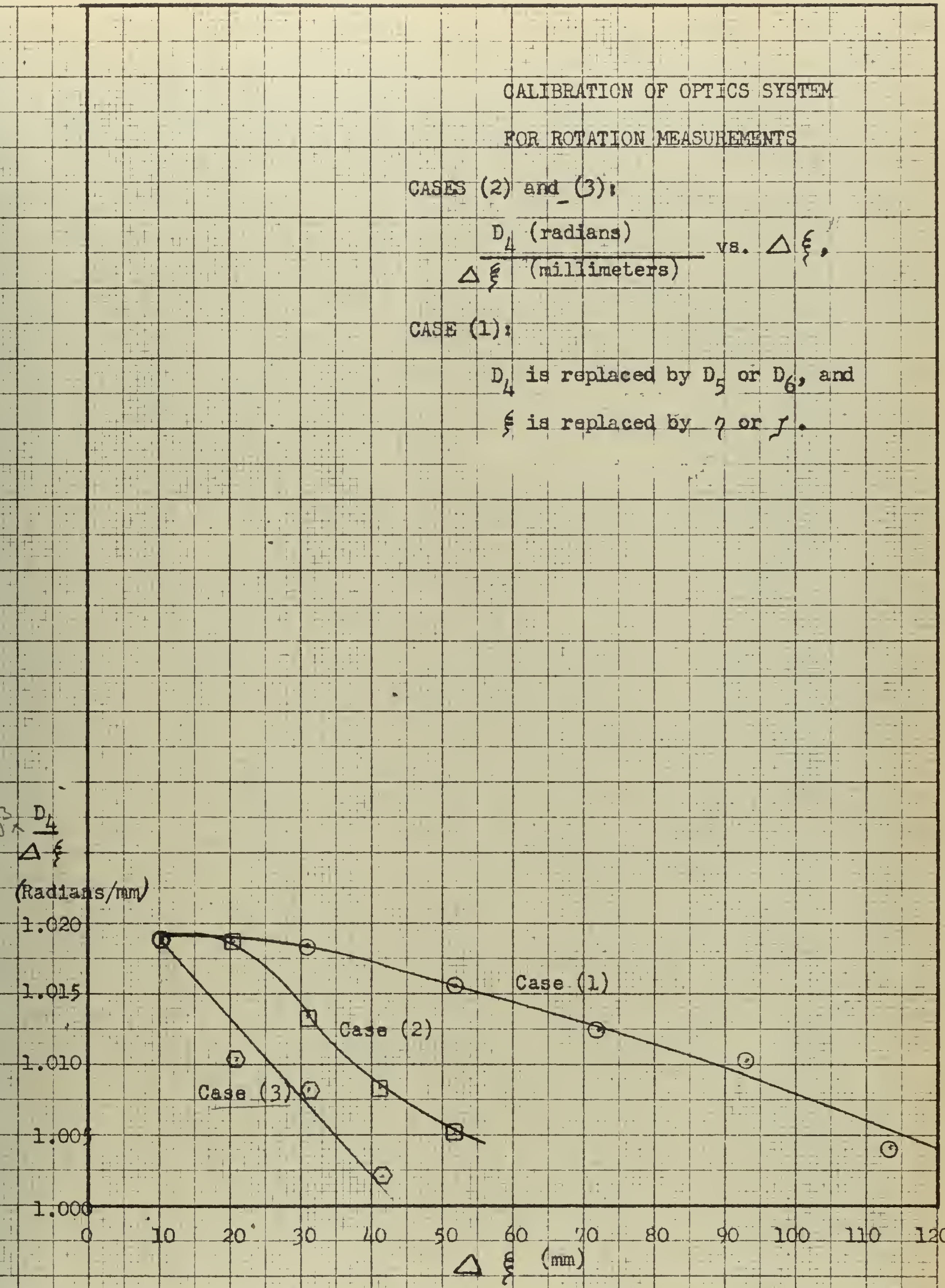

Figure 17 Calibration Curves for Rotation Measuring Apparatus for the Three Cases of Figure 16

APPENDIX II

DEVELOPMENT OF BASIC FORMULAS RELATING REACTIONS TO DEFLECTIONS

In order to present in an orderly fashion the development of the equations for reactions at point P as a function of linear and angular displacements, a matrix analysis will be used. Thus, it is necessary to define a few symbols not specifically listed in the Table of Symbols at the front of this paper.

(a) D' is a column matrix, $(D_1, D_2, D_3, D_4, D_5, D_6)$, where D_1, D_2 and D_3 are linear displacements at point P and D_4, D_5 and D_6 are rotations about axes x'', y'', and z'' respectively. See Fig. 1 for coordinates.

(b) F' is another column matrix (F_1 through F_6), where again F_1, F_2, and F_3 are forces in directions x'', y'', and z'', and F_4, F_5 and F_6 are moments about axes x'', y'', and z'', respectively.

(c) C' is a 6 X 6 matrix relating forces applied at point P to deflections, at the same point, produced by these forces.

Thus,

$$C' F' = D' , \tag{18}$$

where c'_{ij} is equal to the i-deflection due to a j-force. Therefore, by use of equations of article 57, (1) and (5) of Timoshenko and MacCullough [10] the matrix C' can be constructed as follows:

$$C' = \begin{bmatrix} 0 & 0 & 0 & 0 & 0 & 0 \\ 0 & L^3/3EI & 0 & 0 & 0 & -L^2/2EI \\ 0 & 0 & L^3/3EI & 0 & L^2/2EI & 0 \\ 0 & 0 & 0 & L/JG & 0 & 0 \\ 0 & 0 & L^2/2EI & 0 & L/EI & 0 \\ 0 & -L^2/2EI & 0 & 0 & 0 & L/EI \end{bmatrix} \qquad (19)$$

For simplification in manipulation, let

$$a = L^3/3EI, \qquad (20)$$

$$b = L^2/2EI, \qquad (21)$$

$$c = L/EI, \quad \text{and} \qquad (22)$$

$$d = L/JG \qquad (23)$$

It is clear from the zeros that appear in column one and row one that there will be no relation linking F_1 and D_1. Therefore, for further simplification we can eliminate these terms and utilize the following equation obtained by substituting equations (19) through (23) in (18) : (The 5 X 5 matrix shown below will be designated as C, and the two column matrices as F and D, respectively.)

$$\begin{bmatrix} a & 0 & 0 & 0 & -b \\ 0 & a & 0 & b & 0 \\ 0 & 0 & d & 0 & 0 \\ 0 & b & 0 & c & 0 \\ -b & 0 & 0 & 0 & c \end{bmatrix} \times \begin{bmatrix} F_2 \\ F_3 \\ F_4 \\ F_5 \\ F_6 \end{bmatrix} = \begin{bmatrix} D_2 \\ D_3 \\ D_4 \\ D_5 \\ D_6 \end{bmatrix} \qquad (24)$$

Now what we desire is F as a function of D. Thus, from (18),

$$F = C^{-1} D, \qquad (25)$$

where C^{-1} is the ~~reciprocal~~ inverse of C ; i.e. $C\,C^{-1} = C^{-1}\,C = I$. The ~~reciprocal~~ inverse of C is given by the formula

$$C^{-1} = \frac{1}{|C|}\,[C_{ji}] \,, \tag{26}$$

i.e. the ~~reciprocal~~ inverse of matrix C is equal to the product of the reciprocal of the determinant of C and the transpose of the adjoint of C. Solving for the determinant of C yields

$$\begin{aligned} |C| &= a^2c^2d - 2\,ab^2cd + b^4d \\ &= d(ac - b^2)^2 \end{aligned} \tag{27}$$

The adjoint of C is a matrix composed of the cofactors of each term, and is equal to

$$[C_{ij}] = \begin{bmatrix} (ac^2d - b^2cd) & 0 & 0 & 0 & (-abcd + b^3d) \\ 0 & (ac^2d - b^2cd) & 0 & (-abcd + b^3d) & 0 \\ 0 & 0 & (ac - b^2)^2 & 0 & 0 \\ 0 & (-abcd + b^3d) & 0 & (a^2cd - ab^2d) & 0 \\ (abcd - b^3d) & 0 & 0 & 0 & (a^2cd - ab^2d) \end{bmatrix}$$

Equation (28)

Then by substituting (27) and the transpose of (28) in equation (26) , we obtain the equation:

$$C^{-1} = \frac{1}{d(ac - b^2)^2} \begin{bmatrix} (ac^2d - b^2cd) & 0 & 0 & 0 & (+abcd - b^3d) \\ 0 & (ac^2d - b^2cd) & 0 & (-abcd + b^3d) & 0 \\ 0 & 0 & (ac - b^2)^2 & 0 & 0 \\ 0 & (-abcd + b^3d) & 0 & (a^2cd - ab^2d) & 0 \\ (abcd - b^3d) & 0 & 0 & 0 & (a^2cd - ab^2d) \end{bmatrix}$$

Equation (29)

Dividing the elements of the matrix by $d(ac - b^2)$, we get

$$C^{-1} = \frac{1}{(ac - b^2)} \begin{bmatrix} c & 0 & 0 & 0 & b \\ 0 & c & 0 & -b & 0 \\ 0 & 0 & 1/d & 0 & 0 \\ 0 & -b & 0 & a & 0 \\ b & 0 & 0 & 0 & a \end{bmatrix} \qquad (29a)$$

Thus, substituting equation (29a) into equation (25),

$$\begin{bmatrix} F_2 \\ F_3 \\ F_4 \\ F_5 \\ F_6 \end{bmatrix} = \frac{1}{(ac - b^2)} \begin{bmatrix} c & 0 & 0 & 0 & b \\ 0 & c & 0 & -b & 0 \\ 0 & 0 & 1/d & 0 & 0 \\ 0 & -b & 0 & a & 0 \\ b & 0 & 0 & 0 & a \end{bmatrix} \times \begin{bmatrix} D_2 \\ D_3 \\ D_4 \\ D_5 \\ D_6 \end{bmatrix}$$

Equation (30)

Now taking the various equalities implied by the above matrix equation and substituting the values from equations (20) , (21) , (22) , and (23) , we have the desired results:

$$F_2 = \frac{cD_2 + bD_6}{ac - b^2} = \frac{6EI}{L^2}\left(\frac{2D_2}{L} + D_6\right) \tag{31}$$

$$F_3 = \frac{cD_3 - bD_5}{ac - b^2} = \frac{6EI}{L^2}\left(\frac{2D_{\cancel{2}3}}{L} - D_5\right) \tag{32}$$

$$F_4 = \frac{1}{d} D_4 = \frac{JG\,D_4}{L} \tag{33}$$

$$F_5 = \frac{-bD_3 + aD_5}{ac - b^2} = \frac{6EI}{L^2}\left(\frac{2L\,D_5}{3} - D_3\right) \tag{34}$$

$$F_6 = \frac{bD_2 + aD_6}{ac - b^2} = \frac{6EI}{L^2}\left(\frac{2L\,D_6}{3} + D_2\right) \tag{35}$$

APPENDIX III

TESTS CONDUCTED ON SIMPLE CANTILEVERS WITH STANDARD WEIGHTS

Two experiments were conducted on simple cantilevers in order (1) to point out accuracy possible by the deflection measurement method and (2) to ascertain the effect of length L (distance from anchor to measuring point P) on the results obtained for a moment about the axis of the model, $M_{x'}$ [1].

In the first experiment four runs were made, utilizing weights of 50 gms, 100 gms, 200 gms, and 300 gms, respectively, as known force F_y (also $= F_{y''}$ in this case). (See Fig. 18) In each run the force was computed three different ways and in each case compared with the known force. First, the formula utilizing displacement, D_2 and distance S (from anchor to point of application of the weight) was used. This is given by Timoshenko and McCullough [10] as[2]

$$D_2 = \frac{F_2 L^2 (3S - L)}{6EI} \tag{36}$$

and therefore,

$$F_2 = \frac{6EI}{L^2} \frac{D_2}{(3S - L)} \tag{37}$$

The second computation is based on another equation [10] which employs the angular displacement D_6 and distance S ;

$$D_6 = \frac{-F_2 L (2S - L)}{2EI} \tag{38}$$

---

[1] For effect of L on results of other reactions, see Appendix IV.

[2] Symbols from Timoshenko and McCullough correspond to those used herein as follows: $D_2 = \delta$; $F_2 = P$; $L = x$; $S = \ell$; $D_6 = \theta$

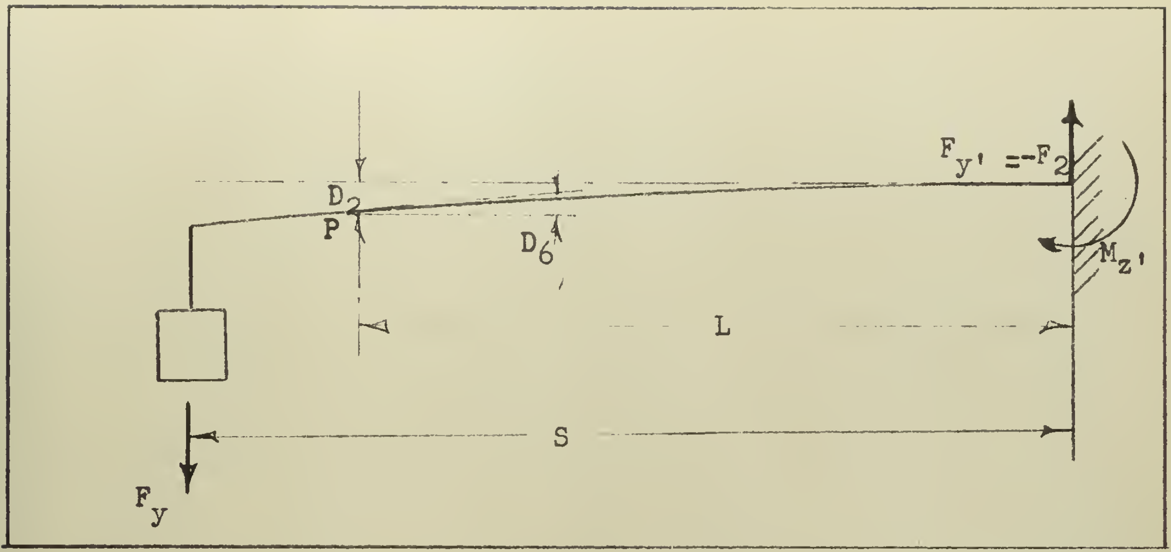

Figure 18 Drawing showing Displacement Measurements on Simple End-Loaded Cantilever

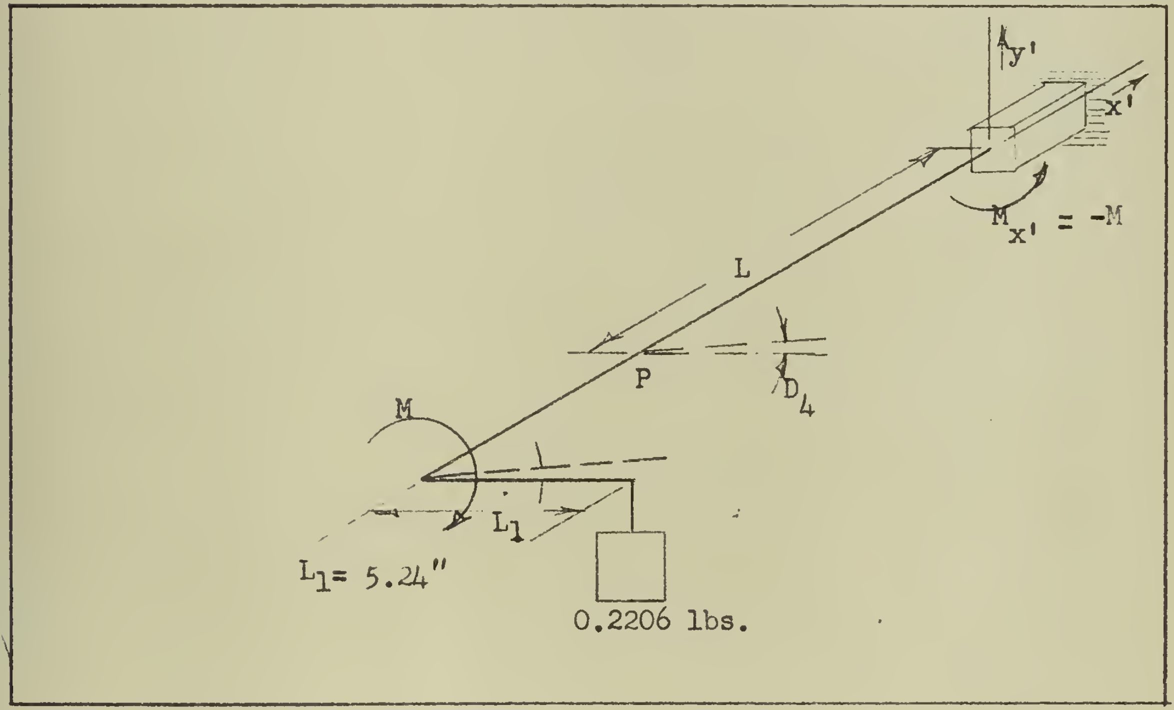

Figure 19 Drawing Showing Displacement Measurement for Simple Cantilever With End Moment About the Axis of the Model (Other moments and forces not considered)

or

$$F_2 = \frac{2EI\,D_6}{L\,(2S - L)}. \qquad (39)$$

And finally since S has no meaning in a continuous length of winding pipe as encountered in the problems of main interest, a third computation was made using equation (31). (It will be noted that equation (31) is merely a combination of equations (37) and (39) above with S eliminated). Equation (31) is repeated below:

$$F_2 = \frac{6EI}{L^2}\left(\frac{2D_2}{L} + D_6\right) \qquad (31)$$

For this experiment L = 8.56 inches, and S = 10.75 inches. The results are recorded below in Table 6 :

TABLE 6

Percentage Error in F_2 as Computed by Displacement Data and Utilizing Three Different Equations

Known Force (lbs.)	Percent Errors		
		Parameters	
	D_2 and S [Equation 37]	D_6 and S [Equation 39]	D_2 and D_6 [Equation 31]
0.1103	0.0	-1.4	3.9
0.2206	-0.2	0.5	-2.7
0.4412	0.9	0.2	6.6
0.6618	0.8	-0.7	7.1

This experiment was valuable inasmuch as it clearly indicated the increased error that could be expected when using the equations of Appendix II. The results obtained by equations (37) and (39) are

exceptionally good and serve as evidence that the methods of measuring D_2 and D_6 are verified. Nevertheless this knowledge was beneficial in demonstrating at an early point the accuracy needed in D_2 and D_6. Furthermore, early experiments of this type (not recorded here) were of great assistance in (1) showing where the main errors were and in (2) eventually leading to the improvement of both measuring systems to their present state.

Now in order to ascertain the influence of the distance, L, on the accuracy of the moment about the x' axis, an L-shaped wire was constructed as shown in Fig. 19 and anchored at one end so that both legs were in a horizontal plane. A known weight was then suspended from the end of the free leg to produce two known moments: M_z, which was not of interest in this experiment[1], and M_x. As the lever arm, $L_1 = 5.24$ inches, and the weight was 0.2206 pounds, the moment M_x was actually 1.156 pound inches.

Measurements of D_4 were made at various distances L for the configuration by taking readings of ξ_1 and ξ_2 with and without the weight, respectively. Results obtained from this experiment are tabulated below and are plotted to produce the curve of Fig. 20.

---

[1] See Appendix IV for variation of $M_{z'}$.

TABLE 7

Percent Error in Computing $M_{x'}$ Versus Length L Used

L inches	JG/L	D_4 radians	Computed $M_{x'}$ $(JG/L)D_4$	Error	Percent Error
4.45	64.7	.01855	1.200	.044	3.81
5.93	48.5	.0243	1.180	.024	2.08
7.60	37.87	.0311	1.179	.023	1.99
9.80	29.35	.0400	1.174	.018	1.56

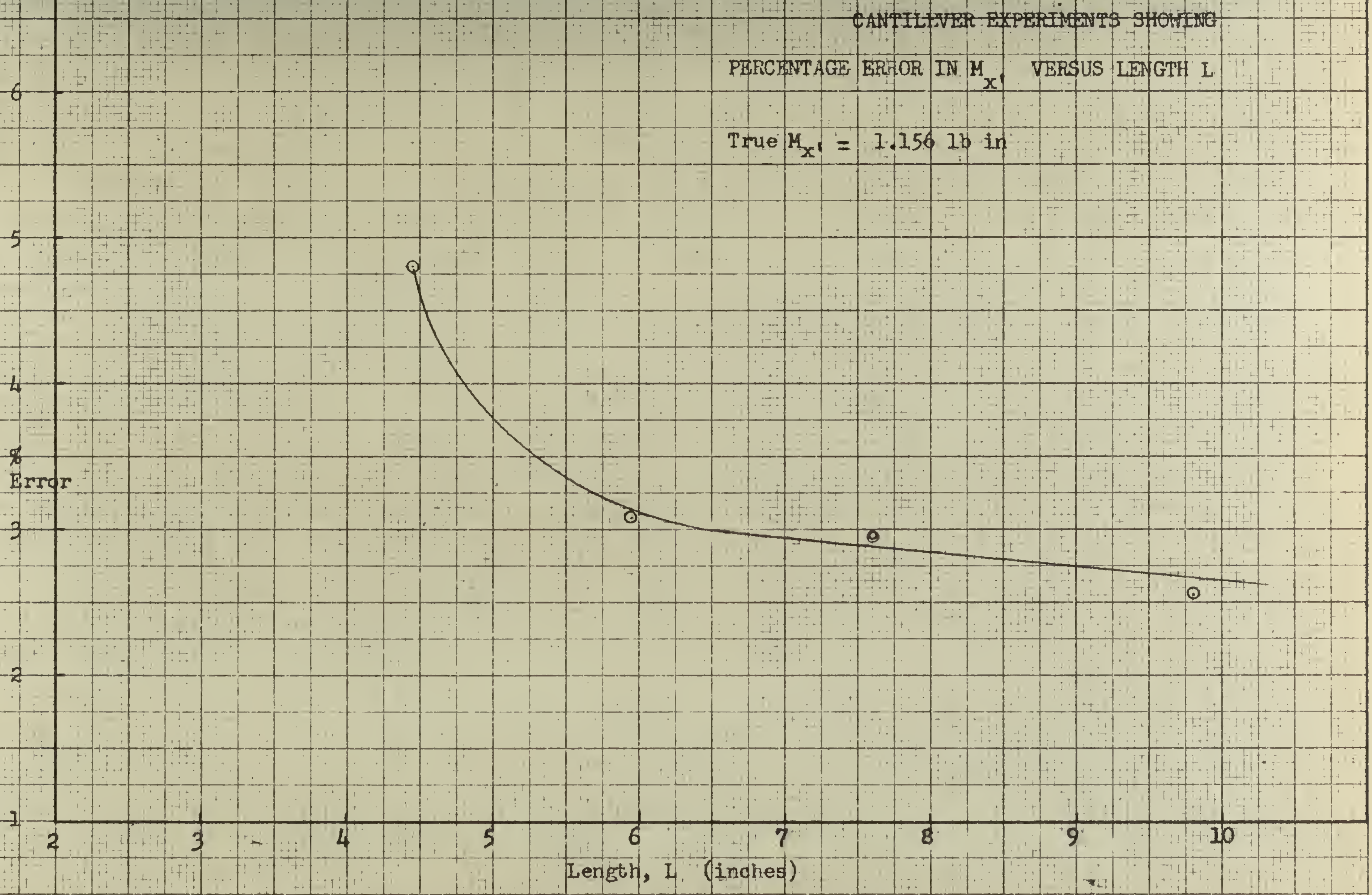

Figure 20 Curve Showing Percentage Error in $M_{x'}$ Versus Length L

APPENDIX IV

SOLUTION OF TWO DIMENSION Z-BEND PROBLEM, EXAMPLE 1

The problem shown in Fig. 21 is a two-dimensional pipe layout that was recommended by Crocker and McCutchan [4] as a standard problem to be attempted by various piping flexibility analysis methods.

The solution of the problem is carried out in the computation sheets of Tables 8, 9, and 10 of this Appendix. The model was constructed to a scale of $\frac{1}{40.7}$. The reactions at point A (less $F_{x'}$) were first determined; then the model was removed and inverted 180° about the z axis. After the model was reinstalled in this orientation, reactions at point O (also less $F_{x'}$) were found. Since. F_x was not yet obtained, the two values of F_y obtained were averaged, and F_x was computed by use of the static formula, equation (12) below:

$$F_{xA} = \frac{(M_{zO} + M_{zA}) + F_{yA}X}{Y} \tag{12}$$

$$F_{yO} = - F_{yA} = \frac{-(1496 + 1475)}{2} = -1486 \text{ pounds,}$$

$$M_{zO} = +34{,}700; \qquad M_{zA} = +16{,}160 \text{ pound feet,}$$

$$X = \frac{715 + 515}{12} = 102.5 \text{ feet;} \qquad Y = \frac{330}{12} = 27.5 \text{ feet ,}$$

Therefore,
$$F_{xA} = \frac{(34,700 + 16,160) - (1486)(102.5)}{27.5}$$
$$= -3690 \text{ pounds.}$$

Z-BEND,

from "Methods of Making Piping Flexibility Analyses," by Crocker and McCutchan, HEATING, PIPING, AND AIR CONDITIONING, June 1946

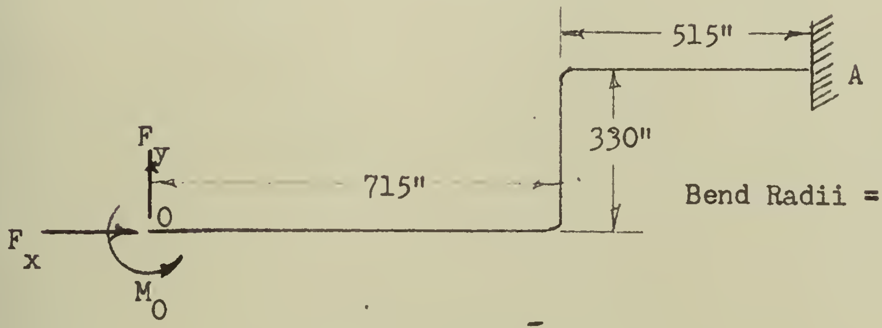

Bend Radii = 15"

Temperature Range = 60 - 785°F.

10.75" O.D. X 0.593" wall

$I = 244.8$; $E_H = 25 \times 10^6$

$\Delta x = 1230/12 \times 5.88/100 = 6.03$ inches

$\Delta y = 330/12 \times 5.88/100 = 1.62$ inches

welding elbows

Figure 21 Z-Bend Problem; Example 1

TABLE 8

DATA SHEET I - SCALING FACTORS

[1]

$$\frac{E_p}{E_m} = \frac{25\times 10^6}{30\times 10^6} = \frac{5}{6} \quad ; \qquad \frac{I_p}{I_m} = \frac{244.8}{\frac{\pi\left(\frac{1}{8}\right)^4}{64}} = 2.045\times 10^7 \quad ;$$

$$\frac{\Delta_p}{\Delta_m} = \frac{10}{1} = 10 \quad ; \qquad \frac{\lambda_m}{\lambda_p} = \frac{1}{40.7} = \frac{1}{40.7} \quad ;$$

$$\frac{\lambda_m^{\,2}}{\lambda_p^{\,2}} = \frac{1}{(40.7)^2} = \frac{1}{1658} \quad ; \qquad \frac{\lambda_m^{\,3}}{\lambda_p^{\,3}} = \frac{1}{(40.7)^3} = \frac{1}{67500} \quad ;$$

$$S_F = \frac{E_p I_p \Delta_p \lambda_m^{\,3}}{E_m I_m \Delta_m \lambda_p^{\,3}} = \frac{5\times 2.045\times 10^7\times 10}{6\times 6.75\times 10^4} = 2527 \quad ;$$

$$S_M = \frac{E_p I_p \Delta_p \lambda_m^{\,2}}{(12) E_m I_m \Delta_m \lambda_p^{\,2}} = \frac{5\times 2.045\times 10^7\times 10}{6\times 1658\times 12} = 8575 \quad .$$

[1] When this problem was first described in 1946, it was customary to use the hot value of the modulus of elasticity, E_H. Since most of the solutions to this problem have been made using this value, E_H was also used here.

TABLE 9 - DATA SHEET II

System: Example 1; Measurements at point A; L = 8.6; Δ_m/Δ_p = 0.100

2/L = .2327; (2/3)L = 5.73; L^2 = 73.95; $6EI/L^2 = 2155/L^2$ = 29.15; JG/L = 287.5/L= ____

TRANSLATION

y''_2 = .3730
y''_1 = .3943
D_2 = .0213 inches

z''_2 =
z''_1 = ____
D_3 = ____ inches

ROTATION

ξ_2= (distance of ξ_1 from light source: ____ mm)
ξ_1= ____
D_4= ____ mm X (____) X10^{-3} = ____ rad.

η_2=
η_1= ____
D_5= ____ mm X (____) X 10^{-3} = ____ rad.

ζ_2= 21.3
ζ_1= 6.5
D_6= 14.8 mm X (1.018) X 10^{-3} = .01506 rad.

$(2/L)D_2$ = .00495	$(2/L)D_3$ =	D_4 =	$(2/3)LD_5$ =	$(2/3)LD_6$ = .0863
D_6 = .01506	$-D_5$ = ____	(JG/L)= ____	$-D_3$ = ____	D_2 = .0213
alg. sum = .02001	alg. sum =	F_{4m}= ____	alg. sum=	alg. sum= .1076
$6EI/L^2$ = (29.15)	$6\ EI/L^2$ = ____		$(-6EI/L^2)$= ____	$(-6EI/L^2)$= (-29.15)
F_{2m} = .583	F_{3m} = ____		$-F_{5m}$= ____	$-F_{6m}$ = -3.135
			$-LF_{3m}$= ____	LF_{2m} = 5.020
			$M_{y'm}$ = ____	$M_{z'm}$= 1.885
$(-S_F)$ = (-2527)	$(-S_F)$ = ____	$(-S_M)$= ____	(S_M) = ____	(S_M)= (8575)
$F_{y'p}$ = -1475	$F_{z'p}$ = ____	$M_{x'p}$= ____	$M_{y'p}$ = ____	$M_{z'p}$= 16160
F_{YA} = -1475 lbs	F ____ = ____ lbs	M ____ = ____ lbft	M ____ = ____ lbft	M_{zA}= 16160 lbft

TABLE 10 - DATA SHEET II

System: Example 1 ; Measurements at point O ; L = 14.045; Δ_m/Δ_p = 0.100

2/L = .1424 ; (2/3)L = 9.36 ; L^2 = 73.95; $6EI/L^2 = 2155/L^2$ = 10.9 ; JG/L = 287.5/L =

TRANSLATION

y''_2 = .1655
y''_1 = .5160
D_2 = .3505 inches

z''_2 =
z''_1 =
D_3 = inches

ROTATION

ξ_2 = (distance of ξ_1 from light source: mm)
ξ_1 =
D_4 = mm X ( ) X10^{-3} = rad.

η_2 =
η_1 =
D_5 = mm X ( ) X 10^{-3} = rad.

ζ_2 = 49.3
ζ_1 = 45.05
D_6 = 4.25 mm X (1.018) X 10^{-3} = .00432 rad.

$(2/L)D_2$ = .04995	$(2/L)D_3$ =	D_4 =	$(2/3)LD_5$ =	$(2/3)LD_6$ = .0404
D_6 = .00432	$-D_5$ =	(JG/L)=	$-D_3$ =	D_2 = .3505
alg. sum = .05427	alg. sum =	F_{4m}=	alg. sum=	alg. sum= .3909
$6EI/L^2$ = (10.9)	$6EI/L^2$ =		$(-6EI/L^2)$=	$(-6EI/L^2)$= (−10.9)
F_{2m} = .591	F_{3m} =		$-F_{5m}$=	$-F_{6m}$ = −4.26
			$-LF_{3m}$=	LF_{2m} = 8.31
			$M_{y'm}$ =	$M_{z'm}$= 4.05
$(-S_F)$ = (−2527)	$(-S_F)$ =	$(-S_M)$=	(S_M) =	(S_M)= (8575)
$F_{y'p}$ = −1496	$F_{z'p}$ =	$M_{x'p}$=	$M_{y'p}$ =	$M_{z'p}$= 34700
F_{YO} = 1496 lbs	F = lbs	M = lbft	M = lbft	M_{zo} = 34700 lbft

$F_{xO} = -F_{xA} = 3690$ pounds. Solving for the resultant,

$$\bar{F} = \sqrt{(F_x)^2 + (F_y)^2} = 3980 \text{ pounds.}$$

Thus, all the reactions acting on the pipe at both extremities of the system were obtained. Table 11 is a compilation of the above results and a comparison with the solutions found by analytical means. The analytical results are shown for two problems: one simulating the results of the deflection model test method by using a flexibility factor of unity, and the other one showing the results when using the actual flexibility factor for the bends and pipe employed.[1]

Having found a solution to the Z-bend problem, it was decided to conduct two further experiments with this configuration. Since we had the theoretically calculated answers available, it seemed pertinent to ascertain the variations of the percent errors in forces found by deflection model test as a function of (1) distance L , and (2) deformation ratio Δ_m/Δ_p . To accomplish this measurements were made using combinations of seven different L's and four different values of Δ_m/Δ_p .

Reactions obtained by 28 tests utilizing combinations of the above set-ups were used to produce two graphs. Fig. 22 shows curves of F_{yO} versus L , for the four different values of Δ_m/Δ_p . A glance at the curve shows the values of $\Delta_m/\Delta_p = .050$ are rather erratic. This probably was caused by the inaccuracies resulting from the attempt to measure very small displacements. The other points were in excellent agreement, however; and as a result only the curve for $\Delta_m/\Delta_p = 0.100$ was plotted in the case of M_{zO} versus L . This second

---

[1] See pages 8 and 9 .

TABLE 11

RESULTS OF EXAMPLE 1 AND COMPARISON WITH THEORY

Reaction	Deflection Model Test Solution	Analytical k = 1	Difference	% Error	Analytical k included
F_{xO}	+3690	3556	134	3.8	2564
F_{yO}	+1486	1449	37	2.6	1063
$\overline{F}$	+3980	3840	140	3.6	2776
$\overline{M}_O$	34700	34200	500	1.5	25840
$\overline{M}_A$	16160	16600	440	2.7	12580

All forces in pounds and moments in pound feet.

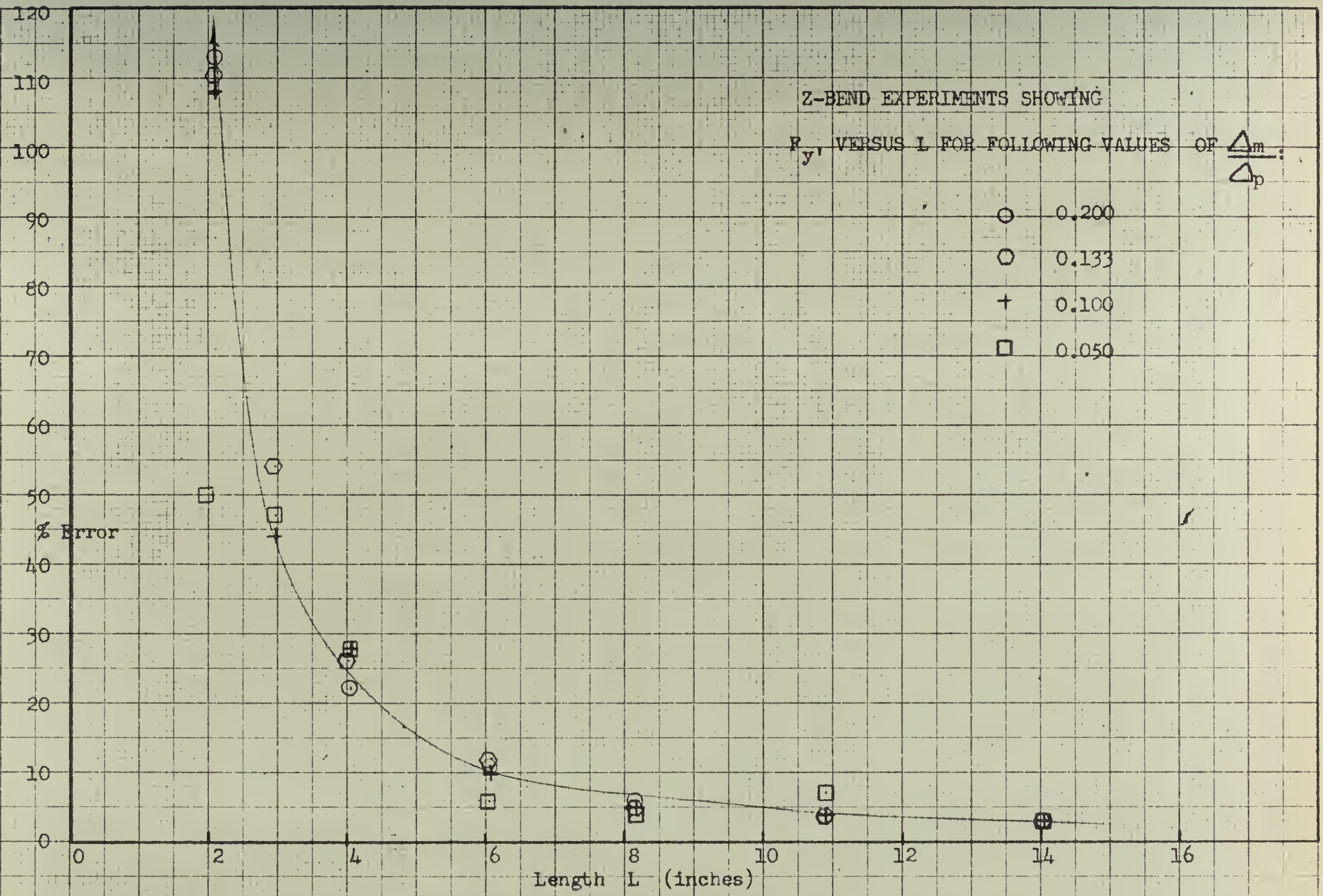

Figure 22 Curves Showing Percentage Error in $F_{y'}$ Versus Length L for Example 1.

curve is shown in Fig. 23.

The severity of the slope of these curves, especially the one for F_{yO}, was somewhat puzzling. Two possible reasons for it (error due to neglecting shear deflection and/or to neglecting possibility of a small motion of the anchor) were investigated, but only the latter produced a possible explanation. In order to test the effect of any anchor motion that might occur, the number II data sheets for all seven sets of data for the $\Delta_m/\Delta_p = 0.100$ runs were worked backwards starting with the analytical results for $F_{y'}$ and $M_{z'}$ (1449 pounds and 34,200 pound feet, respectively) as correct and solving for translation, D_2, needed to produce these results. Any error in rotation, D_6, was neglected momentarily. By doing the above, we obtained for each L, the error in D_2 that would cause the $F_{y'}$ errors found experimentally. From this information a curve was drawn with an abscissa of L and an ordinate of the D_2 error necessary to cause the $F_{y'}$ experimental error found. From the shape of this curve, it was possible to predict a translational and <u>also</u> a rotational motion of the point of anchor that may possibly cause the unexpected slope of the $F_{y'}$ versus L curve of Fig. 22. The resulting curve seemed to be composed of a constant D_2 error of .0014 inches plus a linearly increasing component of an approximate slope of .0003 radians.

Therefore, in order to test this theory, we assumed a motion of the point of anchor as follows:

$$(D_2)_{L=0} = .0014 \text{ inches, and } (D_6)_{L=0} = .0003 \text{ radians,}$$

and from these assumptions, we corrected measured displacements, D_2 and D_6, (corrected values called D_2' and D_6', respec-

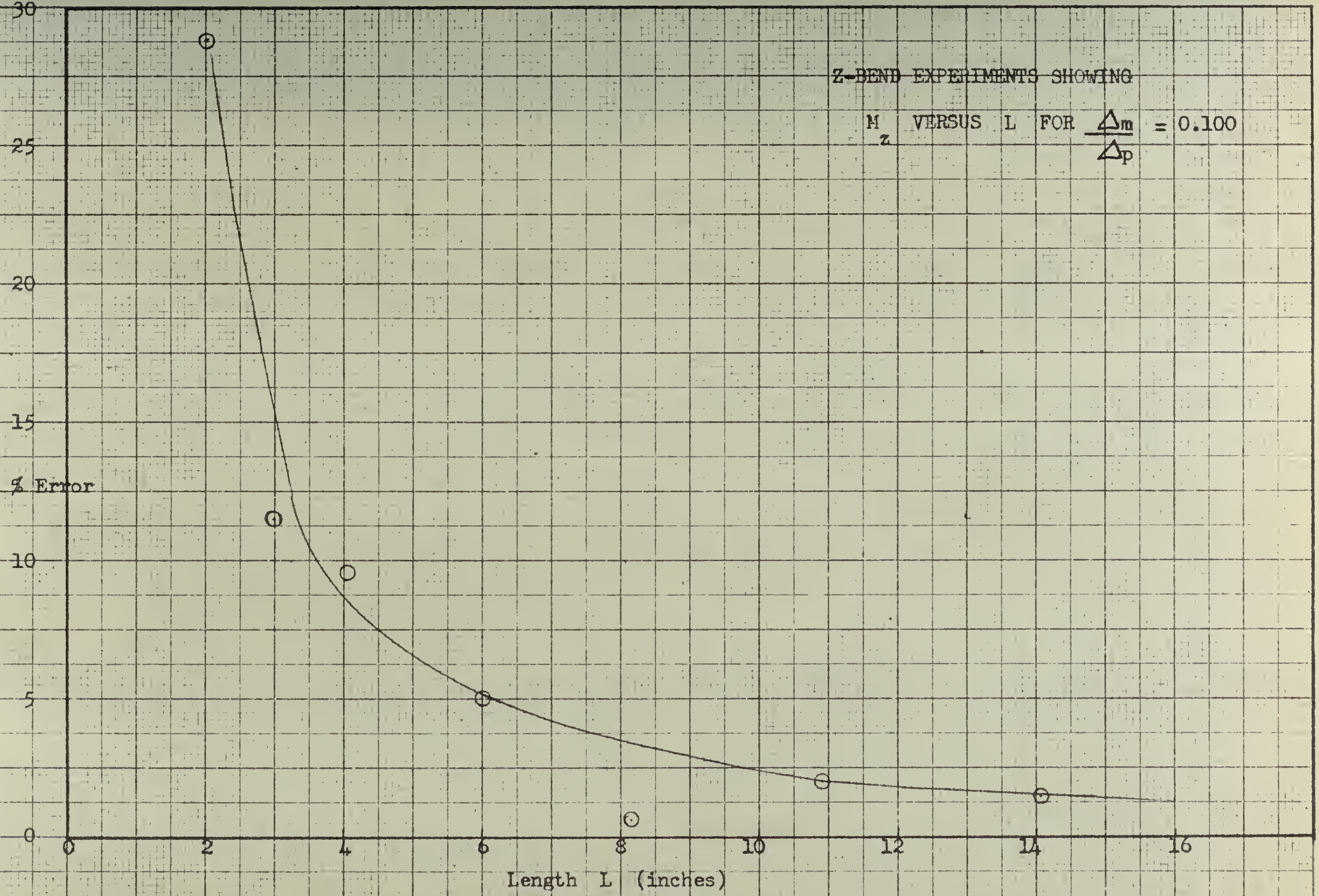

Figure 23 Curve Showing Percentage Error of M_z, Versus Length L for Example 1

tively) by the following formulas:

$$(D_2{}')_L = (D_2)_L - (.0014 + .0003L) \quad , \quad \text{and}$$

$$(D_6{}')_L = (D_6)_L - .0003.$$

By using these corrected deflections, $D_2{}'$ and $D_6{}'$, in place of D_2 and D_6 on the number II data sheets for the $\Delta_m/\Delta_p = 0.100$ runs, the results below were obtained:

L (approx.)	$F_{y'}$	$(F_{y'} - 1449)$	% Error	$M_{z'}$	$(M_{z'} - 34,200)$	% Error
2	1443	-6	-0.4	35100	900	2.6
3	1442	-7	-0.5	34750	550	1.6
4	1519	70	4.8	34800	600	1.8
6	1471	22	1.5	33750	-450	-1.3
8	1465	16	1.1	33400	-800	-2.3
11	1472	23	1.6	24120	-80	-0.2
14	1461	12	0.8	34050	-150	-0.4

These data show that due to loads imposed on the frame in this case there is in fact a motion of the anchor very similar to the above assumed displacements (anchor translation of .0014 inches, and anchor rotation of .0003 radians). Attempts at experimentally measuring such anchor motion were not productive, but this is understandable due to the difficulty of completely divorcing the measuring apparatus from the main structure.

Since larger deformation ratios, Δ_m/Δ_p, result in increases in anchor displacement proportional to the increase in model deflection measurements, a similar error curve should result for all four Δ_m/Δ_p runs, and this is indeed the case as is evidenced by the proximity of corresponding experimental points of Fig. 22. Therefore, the percent error data from the curve of Fig. 22 was used in subsequent problems as a method of arbitrarily correcting "measured" reactions. (See Appendix VI).

It may be noted, moreover, that the Belgian I. R. S. I. A. Commission [8] discovered a similar phenomenon of pronounced disagreement between experiment and theory for shorter length models. The nature of the problems in the two cases is somewhat different, in that the I. R. S. I. A. Commission found this variation with overall model length and in the experiments of this Appendix the error variation was with distance, L, to point of measurement. However, the two situations are indeed related; and, in fact, if a plot is made of log L versus percent disagreement with theory for this experiment, the slope is approximately the same as that of a graph obtained by the I. R. S. I. A. Commission by plotting log of total model length versus percent disagreement with theory. It is, therefore, suggested that a similar distortion of the framework of their model test equipment may possibly be the cause for the systematic disagreement between theory and experiment that they experienced.

Early in the development of this thesis a determination of the reason for the unusual shape of the $F_{y'}$ versus L curve (Fig. 22) was attempted, and the translations (D_2') necessary to produce the correct answer (obtained by analytical means) for each L of the Δ_m/Δ_p

= 0.100 runs were calculated. However, this information was abandoned at the time since it seemed to indicate possible displacements of the anchor, and that could not be corroborated experimentally. However, after the text of this thesis was completed, the further reduction of this data as presented above was completed.

Now having established that motion of the anchor itself is a plausible reason for the apparent disagreement between theory and experiment for short L-lengths, it was felt that a method of predicting this anchor displacement both could and should be found. In any one plane two unknowns exist; considering only the $x''y''$ plane for the moment they are translation in the y'' direction (δ) and rotation (γ) about the z'' axis. Two equations are therefore necessary, and they can be obtained by any one of three methods. The first of them will be discussed at some length below.

We know there exists a certain translation (D_2') and rotation (D_6') at point P that will produce the correct value of $F_{y'_m}$ by equation (31). Now assuming the measured translation at point P is accurate <u>with the exception of anchor displacement</u>, we can write the following equation for the corrected translation:

$$D_2' = D_2 - (\delta - \gamma L) \quad , \qquad (40)$$

and similarly we can correct the rotation measurement by

$$D_6' = D_6 - \gamma . \qquad (41)$$

Now substituting values of D_2' and D_6' from equations (40) and (41) for D_2 and D_6, respectively, in equation (31) we find the correct value of the y' force as follows:

$$F_{y'm}(\text{corr.}) = \frac{6EI}{L^2}\left(\frac{2(D_2 - \delta + \gamma L)}{L} + D_6 - \gamma\right) \qquad (42)$$

Since the above equation gives the <u>correct</u> answer, $F_{y'm}(\text{corr.})$ will be the same regardless of where the measurements are taken. Therefore, if we take two sets of data, D_{2a} and D_{6a} and D_{2b} and D_{6b} at two different measuring lengths, L_a and L_b, we can say that

$$F_{y'm}(\text{corr.}) = \frac{6EI}{L_a^2}\left(\frac{2(D_{2a} - \delta + \gamma L_a)}{L_a} + D_{6a} - \gamma\right)$$

$$= \frac{6EI}{L_b^2}\left(\frac{2(D_{2b} - \delta + \gamma L_b)}{L_b} + D_{6b} - \gamma\right) \qquad (43)$$

From this we can cancel $6EI$ on both sides of the equation and collect terms to produce

$$2(L_a^{-3} - L_b^{-3})\,\delta - (L_a^{-2} - L_b^{-2})\,\gamma$$
$$= 2D_{2a}L_a^{-3} - 2D_{2b}L_b^{-3} + D_{6a}L_a^{-2} - D_{6b}L_b^{-2}.$$

Equation (44)

This is one of our equations, and we can easily obtain another in the same manner by taking a third set of data (D_{2c} and D_{6c}) at a measuring length L_c. Then,

$$2(L_a^{-3} - L_c^{-3})\,\delta - (L_a^{-2} - L_c^{-2})\,\gamma$$
$$= 2D_{2a}L_a^{-3} - 2D_{2c}L_c^{-3} + D_{6a}L_a^{-2} \quad D_{6c}L_c^{-2}.$$

Equation (45)

If the moment equations (35) and (9) are used as the basis instead of the force equation (31) , by a similar procudure, the following will result:

$$-(L_a^{-2} - L_b^{-2})\,\delta + \tfrac{2}{3}(L_a^{-1} - L_b^{-1})\,\gamma$$

$$= \tfrac{1}{3} D_{6b} L_b^{-1} + D_{2b} L_b^{-2} - \tfrac{1}{3} D_{6a} L_a^{-1} - D_{2a} L_a^{-2} ,$$

Equation (46)

and

$$-(L_a^{-2} - L_c^{-2})\,\delta + \tfrac{2}{3}(L_a^{-1} - L_c^{-1})\,\gamma$$

$$= \tfrac{1}{3} D_{6c} L_c^{-1} + D_{2c} L_c^{-2} - \tfrac{1}{3} D_{6a} L_a^{-1} - D_{2a} L_a^{-2} .$$

Equation (47)

This is another set of equations that can be solved for the anchor motion δ and γ. A THIRD possibility is to use equations (44) and (46) ; this appears to have a decided advantage inasmuch as measurements at two points only are required.

To test the above theory, all three possible sets of equations were used with data obtained from the $\Delta_m / \Delta_p = 0.100$ runs. Then with the δ and γ values thus found corrected displacements D_2' and D_6' were computed. These in turn were substituted for D_2 and D_6 in equations (31) and (35) to produce corrected values of $F_{y'}$ and $M_{z'}$. The results of these various correction equations are tabulated on page 94 . It is evident from checking these various methods that we can expect the most favorable agreement with theory if we utilize

RESULTS OF ANCHOR DISPLACEMENT CORRECTIONS

Method of Obtaining		Anchor Displacement		% Errors after Corrections Made				
Anchor Displacement	Note	δ(in.)	γ(rad.)	Reaction	L=2"	L=2.98"	L=4.04"	L=6.015"
Force Eq.(44) and (45) with Data from L=2, 2.98, and 4.04 inches	(a)	.00208	.00056	$F_{y'}$	16.3	16.5	16.6	
				$M_{z'}$			6.9	
Force Fq.(44) and (45) with data from L=2, 2.98, and 6.015 inches		.00155	-.00012	$F_{y'}$	2.6	2.7		2.7
				$M_{z'}$	3.6			0.6
Moment Eq.(46) and (47) with data from L=2, 2.98, and 6.015 inches		.00138	-.00053	$F_{y'}$	20.2			-0.8
				$M_{z'}$	-1.5			-1.3
Force Eq.(44) and Moment Eq(46) with data from L=2 and 2.98 inches	(b)		-.01533					
Force Eq.(44) and Moment Eq.(46) with data from L=2 and 6.015 inches	(c)	-.00129	-.00319	$F_{y'}$	-20.1			-19.3
				$M_{z'}$				-13.5
Percent error in measured reactions with data not corrected for anchor displacement				$F_{y'}$	174	52	31	12.5
				$M_{z'}$	27.6	11.4	9.6	5.0

NOTES: (a) A positive γ is unrealistic in that it indicates anchor rotation opposite to the rotation of the model attached to it.

(b) With γ = .01533 radians, an anchor rotation of 0.9 degrees is indicated; this is excessive.

(c) A negative δ is unrealistic in that it means translation of anchor opposite to the translation of the model attached to it.

three points of measurements together with equations (44) and (45), which were based on the force equation (31). In fact, it will be noted that with an end leg so small that a measurement is necessary with L no greater than six inches, by measurements at two inches, three inches, and six inches, and use of equations (44) and (45), an accuracy of 2.7% error will result. This is exceedingly better than the 12.5% error obtained with uncorrected data.

Now having found the desired correction equation for the x''y'' plane, by a similar procedure for the x''z'' plane we find:

$$2(L_a^{-3} - L_b^{-3})\mathcal{T} + (L_a^{-2} - L_b^{-2})\beta$$
$$= 2D_{3a}L_a^{-3} - 2D_{3b}L_b^{-3} - D_{5a}L_a^{-2} + D_{5b}L_b^{-2} ,$$

Equation (48)

and

$$2(L_a^{-3} - L_c^{-3})\mathcal{T} + (L_a^{-2} - L_c^{-2})\beta$$
$$= 2D_{3a}L_a^{-3} - 2D_{3c}L_c^{-3} - D_{5a}L_a^{-2} + D_{5c}L_c^{-2} .$$

Equation (49)

where $\mathcal{T}$ = anchor translation in the z''-direction and β = anchor rotation about the y'' axis.

Going through a similar procudure for the y''z'' plane, where we have only $M_{x'}$ to find, we can derive the equation as follows:

$$M_{x'm} = \frac{JG}{L_a}(D_{4a} - \alpha) = \frac{JG}{L_b}(D_{4b} - \alpha) ; \qquad (50)$$

and, therefore,

$$(L_a^{-1} - L_b^{-1})\alpha = D_{4a}L_a^{-1} - D_{4b}L_b^{-1} ; \qquad (51)$$

thus equation (51) gives us α, the twist of the anchor point about the x'' axis.

With all the above equations at our disposal, we can therefore proceed with an orderly analysis of data. If the end leg is over eight inches, accuracy well within 10% can be anticipated for most reactions by using the measured data as it is. However, if any of these results are suspect, or if the length, L, is less than eight inches, we should correct our data before proceeding further. If it is feasible to take three measurements at least an inch apart with the minimum being at two inches, then we should find the anchor displacement by using equations (44) and (45) for δ and γ, equations (48) and (49) for τ and β, and equation (51) for α. Thus, in lieu of using correction curves of Figs. 20, 22, and 23, we can take the above anchor displacements to correct the measured deflections, D_2 through D_6; then with these more accurate displacements (now called D_2' and D_6' after being corrected) we can substitute in the data sheet II forms and solve for all the reactions.

We are reasonably sure that these results will fall within an accuracy of less than 10% error. However, it is still advisable to utilize the statics relationships available, equations (12) through (17), as checks. And as pointed out in section 6 of the text of this thesis, all these corrections should be made before solving for the unknown force when that is necessary.

One more comment seems pertinent; by measuring at three points we really have redundant data since we have two unknowns and the possibility of four equations(although we presently plan to use only two of

them, (44) and (45)). Therefore, a more exhaustive treatment of this phase of the analysis might well lead to a method of using statistics or employing weighted averages to reduce such a multiplicity of data.

Another possible solution to the anchor displacement problem is simply to make the entire apparatus more rigid. Due to the adjustability required, this does not seem feasible for all configurations. However, where short-leg measurements are necessary, it may be desirable to take exceptional precautions to increase the rigidity of the entire apparatus. With scaffold fittings and extra lengths of pipe, several diagonals and other strength members may be conveniently installed.

APPENDIX V

SOLUTION OF THREE-DIMENSIONAL HOVGAARD BEND PROBLEM, EXAMPLE 2

Another problem suggested as a standard by Crocker and McCutchan [4] was the three-dimensional bend problem depicted in Fig. 24 and first treated by Professor William Hovgaard [5]. In order to solve this problem by deflection model test methods, a scale model was constructed to a scale of 1 to 5 . In this problem as before reactions at point A were found (less $F_{x'}$), but it must be pointed out that coordinates at the measured end were dependent on the orientation of the anchor and measuring equipment. Their relation to the basic coordinates of the problem can be seen by an examination of Fig. 24. Thus, at point A we had F_y , F_x , and all A-moments.

As before, the configuration was inverted but this time for ease in fitting the model to the framework, it was rotated 90° about the x axis and then 180° about the z axis. Fig. 25 shows the coordinates of the two systems with the model in this configuration . Again, reactions at point O were obtained, and again it was necessary to shift to the coordinates of the problem. In this case, though, actual forces F_z and F_x plus all O-moments were obtained.

It will be noted, therefore, in this problem where the two end legs are not parallel but axes of one coordinate system are parallel to the axes of the other (not necessarily the same axes), it was possible to arrive at all three forces and all six moments by direct measurement. In addition F_x was found by two different methods; and therefore, an average of the two was taken as the recorded value of this component.

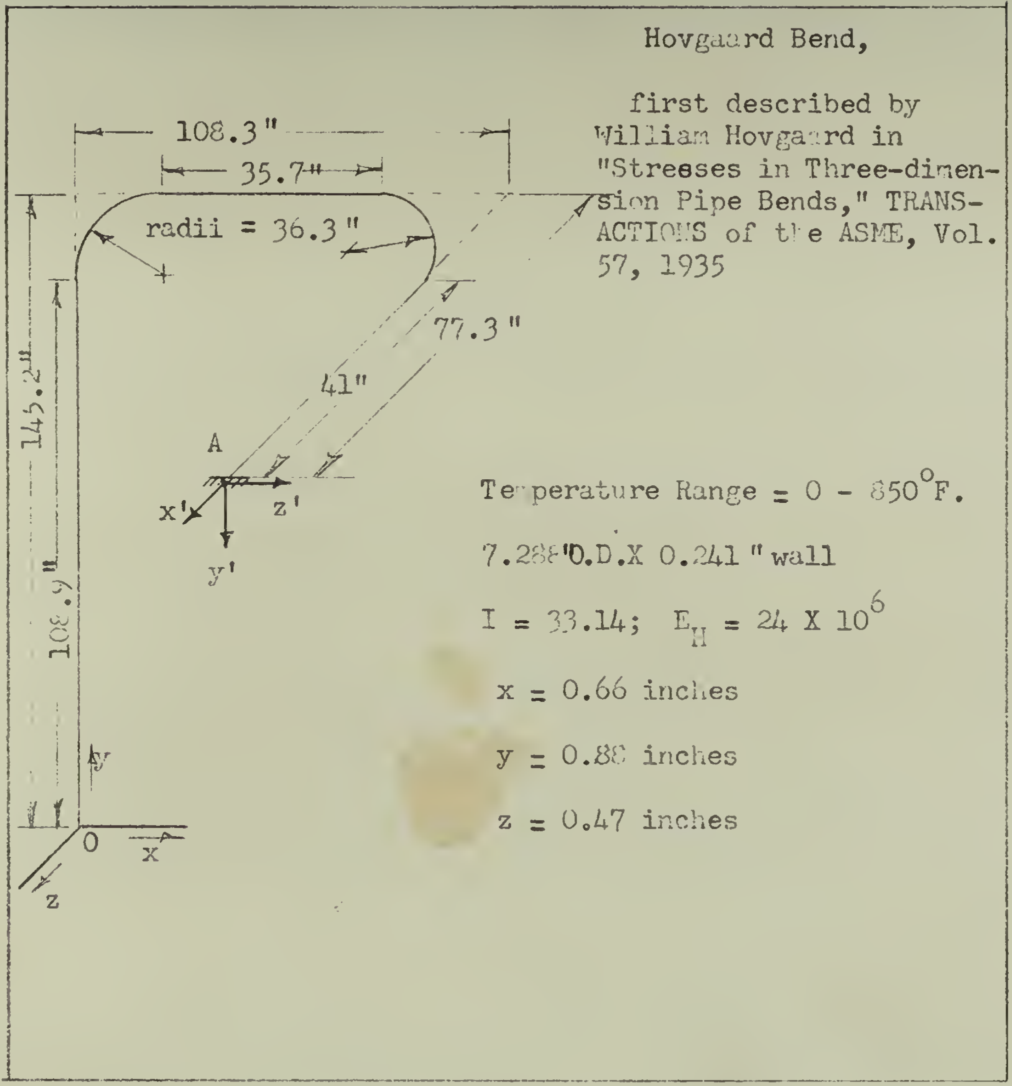

Hovgaard Bend,

first described by William Hovgaard in "Stresses in Three-dimension Pipe Bends," TRANSACTIONS of the ASME, Vol. 57, 1935

Temperature Range = 0 - 850°F.

7.288"O.D.X 0.241 " wall

I = 33.14; $E_H = 24 \times 10^6$

x = 0.66 inches

y = 0.88 inches

z = 0.47 inches

Figure 24 Hovgaard Bend Problem; Example 2

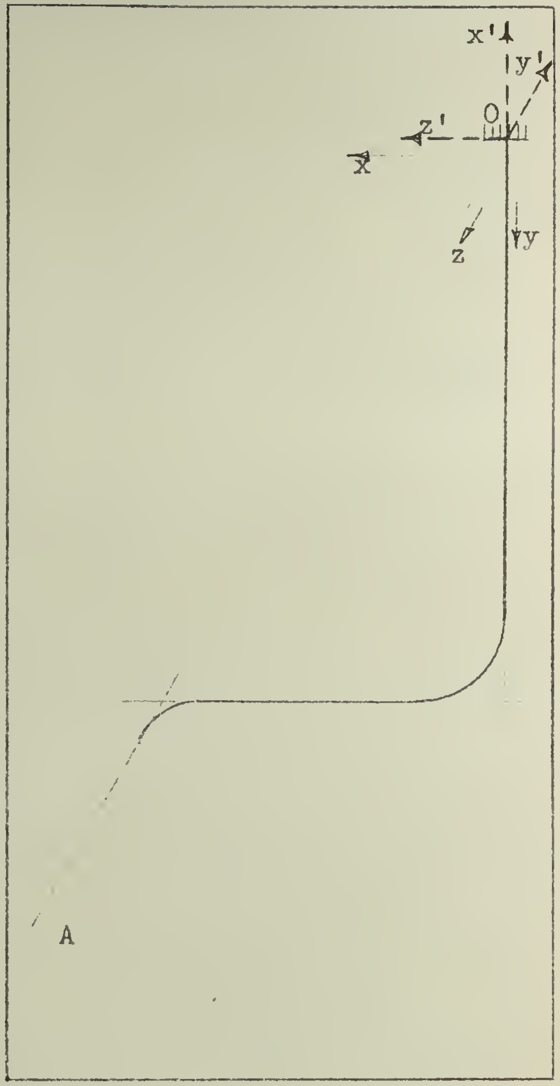

Figure 25 Orientation of Coordinates of Example 2 With Model Inverted

$$F_{xO} = \frac{(2140 + 2510)}{2} = \frac{4650}{2} = 2325 \text{ pounds}$$

In Table 15, the results of this experiment are compared with the analytical results for the problem with flexibility factor not included and also with the values that should obtain with bend flexibilities considered. As before, errors shown are a result of comparison with the problem with $k = 1$ inasmuch as this investigation is concerned solely with this problem.[1]

It will be noted that to this point in the problem, no use was made of the static equations relating the two ends. Moreover, it was possible to take advantage of these equations to check any reaction desired. The greatest percentage error occurs usually in small components. There were two in this problem, M_{yO} and F_z. However, since M_{yO} was a result of an F_4 measurement, the greatest error we could expect here was one of a few percent. (See Fig. 20) Thus, we could solve for F_z in two ways and average the results:

$$F_{zA} = \frac{F_{yA}Z - (M_{xO} + M_{xA})}{Y} = \frac{(M_{yO} + M_{yA}) + F_{xA}Z}{X},$$

Equations (16) and (17)

where $X = 108.3$ inches $= 9.04$ feet; $Y = 145.2$ inches $= 12.1$ feet; and $Z = 77.3$ inches $= 6.44$ feet.

By (16): $$F_{zA} = \frac{-(2600)(6.44) - (-11620 + 5610)}{12.1} = -888 \text{ lbs.},$$

and by (17): $$F_{zA} = \frac{(8250 - 774) + (-2325)(6.44)}{9.04} = -829 \text{ lbs.}$$

---

[1] See page 8 .

Therefore, $F_{zA} = \frac{(888 + 829)}{2} = 859$ lbs.,

which is in error by only 3.5 %.

TABLE 12

DATA SHEET I - SCALING FACTORS

[1]

$$\frac{E_p}{E_m} = \frac{24\times10^6}{30\times10^6} = \frac{4}{5} \quad ; \qquad \frac{I_p}{I_m} = \frac{33.14}{\frac{\pi(\frac{1}{8})^4}{64}} = 2.765\times10^6 \;;$$

$$\frac{\Delta_p}{\Delta_m} = \frac{1}{2} = \frac{1}{2} \quad ; \qquad \frac{\lambda_m}{\lambda_p} = \frac{1}{5} = \frac{1}{5} \;;$$

$$\frac{\lambda_m^2}{\lambda_p^2} = \frac{1}{(5)^2} = \frac{1}{25} \quad ; \qquad \frac{\lambda_m^3}{\lambda_p^3} = \frac{1}{(5)^3} = \frac{1}{125}$$

$$S_F = \frac{E_p I_p \Delta_p \lambda_m^3}{E_m I_m \Delta_m \lambda_p^3} = \frac{4\times2.765\times10^6}{5\times125\times2} = 8850$$

$$S_M = \frac{E_p I_p \Delta_p \lambda_m^2}{(12)E_m I_m \Delta_m \lambda_p^2} = \frac{4\times2.765\times10^6}{5\times25\times2\times12} = 3690$$

---

[1] For the reason noted in the footnote on Table 8, E_H was also used in the computation of this problem.

TABLE 13 - DATA SHEET II

System: Example 2; Measurements at point A; L = 7.71; Δ_m/Δ_p = 1

2/L = .2595; (2/3)L = 5.145; L^2 = 59.45; $6EI/L^2 = 2155/L^2$ = 36.25; JG/L = 287.5/L = 37.3

TRANSLATION

y''_2 = .5250
y''_1 = .3260
D_2 = -.1990 inches

z''_2 = .4208
z''_1 = .2870
D_3 = .1338 inches

ROTATION

ξ_2 = 43.2 46.1
ξ_1 = 0.3 3.2
42.9 42.9
D_4 = -42.9 mm X (1.004) X10^{-3} = -.0431 rad.
(distance of ξ_1 from light source: 20 mm)

η_2 = 37.1
η_1 = 9.5
D_5 = 27.6 mm X (1.018) X 10^{-3} = .02085 rad.

ζ_2 = 49.1
ζ_1 = 6.3
D_6 = 42.8 mm X (1.018) X 10^{-3} = .0435 rad.

$(2/L)D_2$ = -.05160
D_6 = .04350
alg. sum = -.00810
$6EI/L^2$ = (36.25)
F_{2m} = -.2934
$(-S_F)$ = (-8850)
$F_{y'p}$ = 2600
F_{YA} = -2600 lbs

$(2/L)D_3$ = .03472
$-D_5$ = -.02805
alg. sum_2 = .00607
$6EI/L^2$ = (36.25)
F_{3m} = .2415
$(-S_F)$ = (-8850)
$F_{z'p}$ = -2140
F_{xA} = -2140 lbs

D_4 = -.0431
(JG/L) = (37.3)
F_{4m} = -1.600
$(-S_M)$ = (-3690)
$M_{x'p}$ = 5900
M_{zA} = 5900 lbft

$(2/3)LD_5$ = .1442
$-D_3$ = .1338
alg. sum = .0104
$(-6EI/L^2)$ = (-36.25)
$-F_{5m}$ = -.377
$-LF_{3m}$ = -1.860
$M_{y'm}$ = -2.237
(S_M) = (3690)
$M_{y'p}$ = -8250
M_{YA} = 8250 lbft

$(2/3)LD_6$ = .2236
D_2 = -.1990
alg. sum = .0246
$(-6EI/L^2)$ = (-36.25)
$-F_{6m}$ = -.893
LF_{2m} = -2.260
$M_{z'm}$ = -3.153
(S_M) = (3690)
$M_{z'p}$ = -11620
M_{xA} = -11620 lbft

TABLE 14 - DATA SHEET II

System: Example 2 ; Measurements at point O ; L = 10.34; Δ_m/Δ_p = 2

2/L = .1935 ; (2/3)L = 6.90 ; L^2 = 47.68; 6EI/L^2 = 2155/L^2 = 20.13 ; JG/L = 287.5/L= 27.8

TRANSLATION

y_2'' = .2203
y_1'' = .4101
D_2 = .1898 inches

z_2'' = .8075
z_1'' = .4285
D_3 = -.3790 inches

ROTATION

ξ_2= 8.2 11.9
ξ_1= 0.4 4.4
-7.6 -7.5
D_4= -7.55 mm X (1.000) X10^{-3} = -.00755 rad.
(distance of ξ_1 from light source: 30 mm)

η_2= 60.7
η_1= 2.2
D_5= -58.5 mm X (1.014) X 10^{-3} = -.0593 rad.

ζ_2= 40.35
ζ_1= 7.65
D_6= 32.70 mm X (1.017) X 10^{-3} = -.0332 rad.

(2/L)D_2 = .03670	(2/L)D_3 = -.07340	D_4= -.00755	(2/3)LD_5 = -.409	(2/3)LD_6 = -.2290
D_6 = -.03320	- D_5 = .05930	(JG/L)= (27.8)	- D_3 = .379	D_2 = .1898
alg. sum = .00350	alg. sum_2 = -.01410	F_{4m}= -.2097	alg. sum= -.030	alg. sum= -.0392
6EI/L^2 = (20.13)	6 EI/L^2 = (20.13)		(-6EI/L^2)= (-20.13)	(-6EI/L^2)= (-20.13)
F_{2m} = .0705	F_{3m} = -.284		- F_{5m}= +.603	- F_{6m} = .789
			- LF_{3m}= +2.940	LF_{2m} = .729
			$M_{y'm}$ = 3.543	$M_{z'm}$= 1.518
($-S_F$) = (-8850)	($-S_F$) = (-8850)	($-S_M$)= (-3690)	(S_M) = (3690)	(S_M)= (3690)
$F_{y'p}$ = -624	$F_{z'p}$ = 2510	$M_{x'p}$= 774	$M_{y'p}$ = 13080	$M_{z'p}$ = 5610
F_{zO} = 624 lbs	F_{xO} = 2510 lbs	M_{yO}= -774 lbft	M_{zO} = -13080 lbft	M_{xO} = 5610 lbft

TABLE 15

Results of Hovgaard Bend Problem and Comparison with Analytical Values

Reaction		Deflection Model Test Solution	Analytical, k = 1	Difference	% Error	Analytical, k included
F_{xO}		2325	2340	15	0.9	1740
F_{yO}		2600	2369	231	9.8	1690
F_{zO}		624	830	206	24.8	637
F_{zO}	Computed from (eq. 16 and 17)	859	830	29	3.5	637
$\bar{F}$		3560	3432	128	3.7	2508
A: M_x		-11620	-11190	430	3.9	-7810
M_y		8250	8330	80	1.0	6660
M_z		5900	5800	100	1.7	5240
$\bar{M}_A$		15390	15100	290	1.9	11530
O: M_x		5610	5950	340	5.7	4630
M_y		-774	-740	34	4.6	-1208
M_z		-13080	-12730	350	2.8	-11060
$\bar{M}_O$		14240	14060	180	1.3	12050

All forces in pounds and moments in pound feet.

APPENDIX VI

ANALYSIS OF TYPICAL PIPING SYSTEM, EXAMPLE 3

The two standard problems suggested by Crocker and McCutchan [4] being completed, it seemed appropriate to put the acquired technique to work on a typical piping system that may be actually encountered in a steam plant. The system as described in Fig. 26 was constructed as being such a problem.

The model was formed to a scale of 1 to 30 and mounted according to the lay-out of Fig. 26 . However, before starting this problem it was necessary to compute the deformations; here they included both the reverse of the expansion of the pipe, as before, and the expansion of the anchoring equipment. Table 16 was a convenience in arriving at the various deformations.

With this information established, the displacements near the A-end were measured and the reactions at A (less $F_{xA'} = F_{zA}$) were found. See Table 19. The model was then rotated 180° about the z axis and reinserted for measurements near O . (See Fig. 27) At point O two complete sets of data were found: (1) reactions at O (less $F_{x'O} = F_{zO}$) due to measurements with $L = 5.16$ inches, and (2) the same reactions with $L = 5.97$ inches. Two results were taken to get a qualitative variation of reactions with increasing L so that a quantitative correction based on previous experiments could be applied in the proper direction. However, data of the L-equal-5.16 experiment was used to be consistent with data from point A .

Due to the dimensions of the problem we were forced to take displacement measurements relatively close to the anchor (i.e., L =

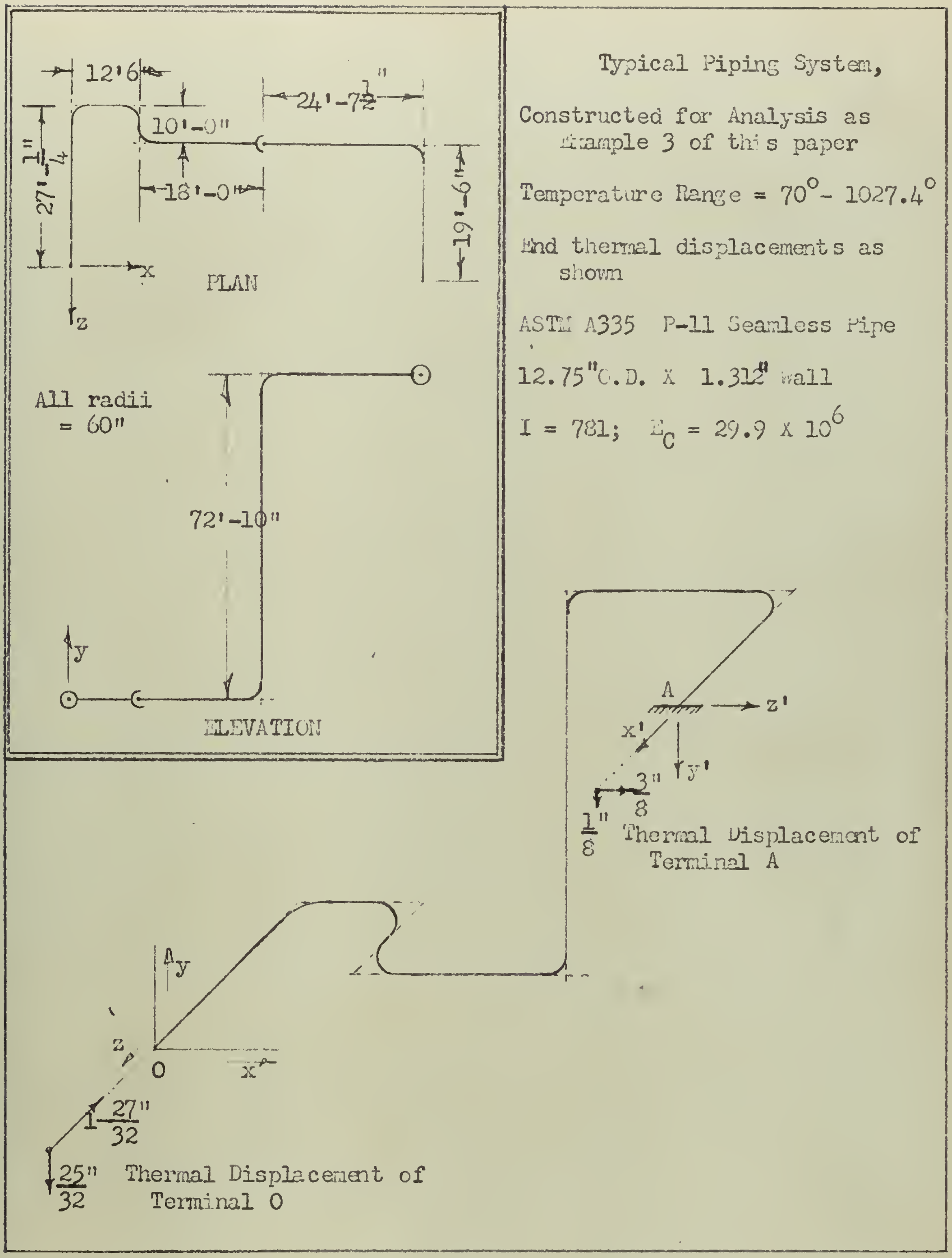

Typical Piping System,

Constructed for Analysis as Example 3 of this paper

Temperature Range = $70^\circ - 1027.4^\circ$

End thermal displacements as shown

ASTM A335 P-11 Seamless Pipe

12.75" O.D. X 1.312" wall

$I = 781; \quad E_c = 29.9 \times 10^6$

Figure 26 Typical Piping System; Example 3

TABLE 16

CALCULATION OF DEFORMATIONS

	Pipe Expansion Alone	Equipment Expansion Alone		Total	Model Deformation
	(O stationary; motion of A with A unrestrained)	Motion of point O	Reverse of motion of point A		$(\Delta_m/\Delta_p = \frac{1}{4})$
Δ_x	$+(12.5+18.0+24.625)\frac{9.205}{100}$ $= 5.075''$	0	$-.375''$	$+4.700''$	1.175 inches
Δ_y	$72.833 \times \frac{9.205}{100} = 6.700''$	$-\frac{25}{32}'' = -.782''$	$+\frac{1}{8}'' = +0.125''$	$+6.043''$	1.511 inches
Δ_z	$(-27.021+10+19.5)\frac{9.205}{100}$ $= +0.228''$	$-1\frac{27}{32}'' = -1.844''$	0	$-1.616''$	$-.404$ inches

5.16 inches). As a result, based on previous experiments, reactions thus obtained were held to be somewhat suspect. Therefore, several refinements were made based on the generous supply of data and information at our disposal. Table 17 shows the various methods used to modify our data to more realistic values. This table was laid out chronologically to show the order of steps taken. It is significant to note that the final results shown in Table 17 were obtained before the problem was solved analytically on the computer. These refinements were straightforward and were made because of the relatively short L used

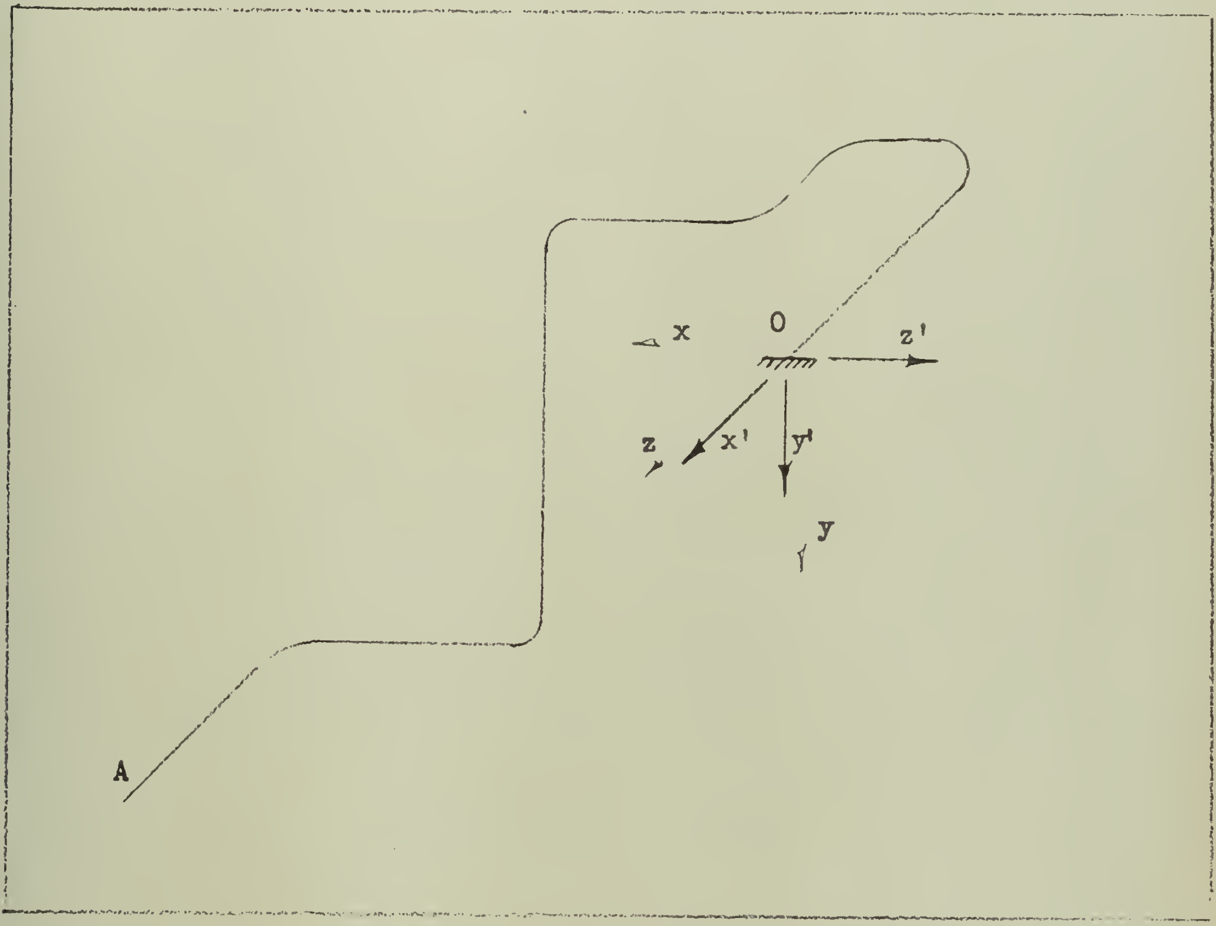

Figure 27 Orientation of Coordinates for Example 3 with Model Inverted

in the measurements. F_{yA} and all moments were increased or decreased by an approximate factor arrived at by looking at curves obtained for variations of reactions with L. A glance at the static formulas showed the values thus far obtained were not statically consistent. It was therefore decided that since F_x was exceptionally small and since it was produced by $F_{z''}$, about which we had no specific F-versus-L curve, F_x was most likely to be in error. Thus, we solved for F_x in terms of the other information. And then with what were felt to be fairly accurate results, F_z was found by the two static equations shown and the results averaged.

Having arrived at the underlined reactions as our answers (Table 17) we then turned to the digital computer for an analytical solution. For this problem, the bend flexibility factor, k, turned out to be unity so in this case only one analytical solution was made. Table 22 is a comparison of results obtained by deflection model testing and those found by analytical means.

In addition to solving the problem by the described model test method, another solution was made exactly as the one outlined above but with 1/8-inch aluminum rod used for the model instead of steel. Results of this solution are recorded in Table 22 also.

TABLE 17

MODIFICATIONS TO SOLUTION OF EXAMPLE 3

Step	Reaction	Measured	How modified	Basis	Formulae	Corrected Reaction
1.	F_{yA}	$\begin{vmatrix}6000\\5960\end{vmatrix}$ and	average the two	-	$\frac{-(6000 + 5960)}{2}$	-5980 lbs.
2.	F_{yA}	-5980 from 1	dec. magnitude 20 %	Fig. 22	$-(5980)(.8)$	-4780 lbs.
3.	M_{xO}	95000	decrease 6 %	Fig. 23	$(95000)(.94)$	89300 lb. ft.
4.	M_{yO}	-40800	increase 3 %	Estimate from two O measurements	$(-40800)(1.03)$	-42000 lb. ft.
5.	M_{zO}	49200	decrease 2 %	Fig. 20	$(49200)(.98)$	48200 lb. ft.
6.	M_{xA}	-93400	decrease 6 %	Fig. 23	$(-93400)(.94)$	-87800 lb. ft.
7.	M_{yA}	38200	increase 3 %	Same as 4.	$(38200)(1.03)$	39300 lb. ft.
8.	M_{zA}	34600	decrease 2 %	Fig. 20	$(34600)(.98)$	33900 lb. ft.
9.	F_{xA}	$\begin{vmatrix}996\\899\end{vmatrix}$ and	Equation (12)	Being small it was uncertain	$\frac{M_{zO} + M_{zA} + F_{yA}X}{Y}$	-2490 lbs.
10.	F_{zA}	unknown	Static equations	Equation (16)	$\frac{M_{yO} + M_{yA} + F_{xA}Z}{X}$	- 161 lbs.
11.	F_{zA}	unknown	Static equations	Equation (17)	$\frac{F_{yA}Z - (M_{xO} + M_{xA})}{Y}$	- 184 lbs.
12.	F_{zA}	161 and 184 from 10 and 11	average the two	-	$\frac{-(161 + 184)}{2}$	- 173 lbs.

TABLE 18

DATA SHEET I - SCALING FACTORS

$$\frac{E_p}{E_m}^{1} = \frac{29.9 \times 10^6}{30.0 \times 10^6} = \frac{29.9}{30.0} \quad ; \qquad \frac{I_p}{I_m} = \frac{781}{\frac{\pi(\frac{1}{8})^4}{64}} = \frac{781\,(64)^3}{\pi} \quad ;$$

$$\frac{\Delta_p}{\Delta_m} = \frac{4}{1} = 4 \quad ; \qquad \frac{\lambda_m}{\lambda_p} = \frac{1}{30} = \frac{1}{30} \quad ;$$

$$\frac{\lambda_m^2}{\lambda_p^2} = \frac{1}{(30)^2} = \frac{1}{900} \quad ; \qquad \frac{\lambda_m^3}{\lambda_p^3} = \frac{1}{(30)^3} = \frac{1}{27{,}000} \quad ;$$

$$S_F = \frac{E_p I_p \Delta_p \lambda_m^3}{E_m I_m \Delta_m \lambda_p^3} = \frac{29.9 \times 781 \times (64)^3 \times 4}{30.0 \times \pi \times 2.7 \times 10^4} = 9615 \quad ;$$

$$S_M = \frac{E_p I_p \Delta_p \lambda_m^2}{(12) E_m I_m \Delta_m \lambda_p^2} = \frac{29.9 \times 781 \times (64)^3 \times 4}{30.0 \times \pi \times 900 \times 12} = 24{,}040 \quad .$$

---

[1] For this problem the presently accepted method of using $E_p = E_C$ was used. This is recommended in the Code for Pressure Piping [3].

TABLE 19 - DATA SHEET II

System: *Example 3*; Measurements at point *A*; L = *5.16*; Δ_m / Δ_p = *1/4*

$2/L$ = *.388*; $(2/3)L$ = *3.44*; L^2 = *26.6*; $6EI/L^2 = 2155/L^2$ = *81.0*; $JG/L = 287.5/L$ = *55.7*

TRANSLATION

y''_2 = *.7364*
y''_1 = *.6316*
D_2 = *-.1048* inches

z''_2 = *.5781*
z''_1 = *.5263*
D_3 = *.0518* inches

ROTATION

ξ_2 = *30.3* *27.8*
ξ_1 = *4.8* *2.4*
25.5 *25.4*
D_4 = *-25.45* mm X (*1.016*) X10^{-3} = *-.02585* rad.

(distance of ξ_1 from light source: *15* mm)

η_2 = *20.7*
η_1 = *2.2*
D_5 = *18.5* mm X (*1.018*) X 10^{-3} = *.01882* rad.

ζ_2 = *40.2*
ζ_1 = *7.8*
D_6 = *32.4* mm X (*1.018*) X 10^{-3} = *.03295* rad.

$(2/L)D_2$ = *-.04060*	$(2/L)D_3$ = *.02010*	D_4 = *-.02585*	$(2/3)LD_5$ = *.06480*	$(2/3)LD_6$ = *.1132*
D_6 = *.03295*	$-D_5$ = *.01882*	(JG/L) = *(55.7)*	$-D_3$ = *.05180*	D_2 = *-.1048*
alg. sum = *-.00765*	alg. sum$_2$ = *.00128*	F_{4m} = *-1.440*	alg. sum = *.01300*	alg. sum = *.0084*
$6EI/L^2$ = *(81.0)*	$6EI/L^2$ = *(81.0)*		$(-6EI/L^2)$ = *(-81.0)*	$(-6EI/L^2)$ = *(-81.0)*
F_{2m} = *-.620*	F_{3m} = *.1035*		$-F_{5m}$ = *-1.054*	$-F_{6m}$ = *-.680*
			$-LF_{3m}$ = *-.534*	LF_{2m} = *-3.200*
			$M_{y'm}$ = *-1.588*	$M_{z'm}$ = *-3.880*
$(-S_F)$ = *(-9615)*	$(-S_F)$ = *(-9615)*	$(-S_M)$ = *(-24040)*	(S_M) = *(24040)*	(S_M) = *(24040)*
$F_{y'p}$ = *5960*	$F_{z'p}$ = *-996*	$M_{x'p}$ = *34600*	$M_{y'p}$ = *-38200*	$M_{z'p}$ = *-93400*
F_{YA} = *-5960* lbs	F_{XA} = *-996* lbs	M_{ZA} = *34600* lbft	M_{YA} = *38200* lbft	M_{XA} *-93400* lbft

TABLE 20 - DATA SHEET II

System: Example 3 ; Measurements at point O ; L = 5.16 ; Δ_m/Δ_p = ¼

2/L = .388 ; (2/3)L = 3.44 ; L^2 = 26.6 ; $6EI/L^2 = 2155/L^2$ = 81.0 ; JG/L = 287.5/L = 55.7

TRANSLATION

y''_2 = .7261
y''_1 = .6199
D_2 = −.1062 inches

z''_2 = .5780
z''_1 = .5214
D_3 = .0566 inches

ROTATION

ξ_2 = 50.7 47.8
ξ_1 = 14.2 11.2
(distance of ξ_1 from light source: 25 mm)
D_4 = 36.5 36.6 −36.55 mm X (1.004) X10^{-3} = −.0367 rad.

η_2 = 24.9
η_1 = 4.3
D_5 = 20.6 mm X (1.018) X 10^{-3} = .02080 rad.

ζ_2 = 40.0
ζ_1 = 7.1
D_6 = 32.9 mm X (1.018) X 10^{-3} = .0335 rad.

(2/L)D_2 = −.0412
D_6 = .0335
alg. sum = −.0077
$6EI/L^2$ = (81.0)
F_{2m} = −.624
($-S_F$) = (−9615)
$F_{y'p}$ = 6000
F_{YO} = 6000 lbs

(2/L)D_3 = .02195
− D_5 = .02080
alg. sum = .00115
6 EI/L^2 = (81)
F_{3m} = .093
($-S_F$) = (−9615)
$F_{z'p}$ = −899
F_{XO} = 899 lbs

D_4 = −.0367
(JG/L) = (55.7)
F_{4m} = −2.044
($-S_M$) = (−24040)
$M_{x'p}$ = 49200
M_{ZO} = 49200 lbft

(2/3)LD_5 = .0716
− D_3 = −.0566
alg. sum = .0150
($-6EI/L^2$) = (−81.0)
− F_{5m} = −1.217
− LF_{3m} = −.480
$M_{y'm}$ = −1.697
(S_M) = (24040)
$M_{y'p}$ = 40800
M_{YO} = −40800 lbft

(2/3)LD_6 = .1152
D_2 = −.1062
alg. sum = .0090
($-6EI/L^2$) = (−81.0)
− F_{6m} = −.729
LF_{2m} = −3.220
$M_{z'm}$ = −3.949
(S_M) = (24040)
$M_{z'p}$ = −95000
M_{XO} = 95000 lbft

TABLE 21 - DATA SHEET II

System: *Example 3* ; Measurements at point *O* ; L = *5.97* ; Δ_m/Δ_p = *1/4*

2/L = *.335* ; (2/3)L = *3.98* ; L^2 = *35.7* ; $6EI/L^2 = 2155/L^2$ = *60.4* ; JG/L = 287.5/L = *48.15*

TRANSLATION

y''_2 = *.7113*
y''_1 = *.5773*
D_2 = *−.1340* inches

z''_2 = *.6016*
z''_1 = *.5300*
D_3 = *.0716* inches

ROTATION

ξ_2 = *52.7* *49.6*
ξ_1 = *10.7* *7.8*
42.0 *41.8*
D_4 = *−41.9* mm X (*1.005*) $X10^{-3}$ = *−.0421* rad.
(distance of ξ_1 from light source: *20* mm)

η_2 = *25.2*
η_1 = *3.8*
D_5 = *21.4* mm X (*1.018*) X 10^{-3} = *.02175* rad.

ζ_2 = *39.2*
ζ_1 = *4.6*
D_6 = *34.6* mm X (*1.017*) X 10^{-3} = *.03516* rad.

$(2/L)D_2$ = *−.04490*
D_6 = *.03516*
alg. sum = *−.00974*
$6EI/L^2$ = *(60.4)*
F_{2m} = *−.589*
$(-S_F)$ = *(−9615)*
$F_{y'p}$ = *5660*
F_{yO} = *5660* lbs

$(2/L)D_3$ = *.02400*
$-D_5$ = *−.02173*
alg. sum = *.00227*
$6EI/L^2$ = *(60.4)*
F_{3m} = *.1371*
$(-S_F)$ = *(−9615)*
$F_{z'p}$ = *−1319*
F_{xO} = *1319* lbs

D_4 = *−.0421*
(JG/L) = *(48.15)*
F_{4m} = *−2.027*
$(-S_M)$ = *(−24040)*
$M_{x'p}$ = *48700*
M_{zO} = *48700* lbft

$(2/3)LD_5$ = *.0866*
$-D_3$ = *−.0716*
alg. sum = *.0150*
$(-6EI/L^2)$ = *(−60.4)*
$-F_{5m}$ = *−.906*
$-LF_{3m}$ = *−.819*
$M_{y'm}$ = *−1.725*
(S_M) = *(24040)*
$M_{y'p}$ = *−41500*
M_{yO} = *−41500* lbft

$(2/3)LD_6$ = *.1397*
D_2 = *−.1340*
alg. sum = *.0057*
$(-6EI/L^2)$ = *(−60.4)*
$-F_{6m}$ = *−.344*
LF_{2m} = *−3.520*
$M_{z'm}$ = *−3.864*
(S_M) = *(24040)*
$M_{z'p}$ = *−93000*
M_{xO} - *93000* lbft

TABLE 22

Results of Example Three and Comparison with Analytical Solution

	Reaction	Deflection Model Test	Analytical	Difference	% Error	Deflection Model Test (Aluminum)	% Error (Aluminum)
	F_x	2490	2609	119	4.5	2450	6.1
	F_y	4780	4837	57	1.2	4950	2.3
	F_z	173	178	5	2.8	218	16.8
	$\overline{F}$	5400	5499	99	1.8	5510	0.2
A:	M_x	-87800	-84100	3700	4.4	-87000	3.5
	M_y	39300	43800	4500	10.3	37600	14.1
	M_z	33900	31100	2800	9.0	37900	21.9
	$\overline{M}_A$	102000	99900	2100	2.1	102150	2.3
O:	M_x	89300	85300	4000	4.7	91800	7.6
	M_y	-42000	-46800	4800	10.3	42700	8.8
	M_z	48200	45450	2750	6.1	57100	25.7
	$\overline{M}_O$	110000	107400	2600	2.4	116100	8.1

All forces in pounds and moments in pound feet.

APPENDIX VII

LIST OF COMMERCIALLY AVAILABLE EQUIPMENT USED IN MODEL TEST APPARATUS

	Description of Equipment Used	Model Test Sub Assembly	Approx. cost
1.	Compound feed for Delta Wood Lathe, ranges 4-1/2" and 5"	Deformation Assembly	$40.00
2.	No. 7525 Clausing Lathe Milling Attachment for 12-inch lathe	Deformation Assembly	36.50
3.	Two each, .001-inch graduation, 1-inch range, dial indicators with tell tale hands, double dials, and plain bearings; Starrett No. 25-C-1"	Translation Measuring Assembly	34.00 each
4.	Bausch and Lomb Mechanical Stage (31-59-62) for microscopes	Translation Measuring Assembly	72.00
5.	Two each, double convex, 500 mm focal length, 4-inch diameter lenses; Central Scientific Co. No. 8645-11	Rotation Measuring Assembly	4.00 each
6.	Two each, Two-watt Concentrated Arc Lamps and 25 watt, 60 cycle, 115 volt Power Supply; Central Scientific Co.	Rotation Measuring Assembly	43.00 each
7.	12 each, Standard right angle 2" x 2" Tube-Lox couplers; The Patent Scaffolding Co. Inc.	Main framework and accessories	3.45 each